Isolation and characterization of anti-SLP single domain antibodies for the therapy of C. difficile infection

Kandalaft, Hiba

Isolation and characterization of anti-SLP single domain antibodies for the therapy of *C. difficile* infection

By
Hiba Kandalaft

Thesis submitted to the Department of Biochemistry, Microbiology and Immunology in partial fulfillment of the requirements for the degree of Master of Science.

Department of Biochemistry, Microbiology and Immunology (BMI)
Faculty of Medicine
University of Ottawa
Ottawa, Ontario, CANADA

Abstract

Clostridium difficile is the leading cause of death from gastrointestinal infections in Canada. Current antiobiotic treatment is non-ideal due to the high incidence of relapse and the rise in hyper-virulent antibiotic-resistant strains. Surface layer proteins (SLPs) cover the entire bacterial surface and mediate adherence to host cells. Passive and active immunization against SLPs greatly enhances survival in hamsters, suggesting that antibody-mediated bacterial neutralization may be an effective alternative therapeutic strategy. Using a recombinant-antibody phage display library, and SLPs from strain QCD 32g58 as bait antigen, we isolated and extensively characterized 11 SLP-specific recombinant single-domain antibodies (sdAbs), in terms of affinity and specificity, intrinsic stability, and ability to inhibit cell motility. Several sdAbs exhibit promising characteristics for a potential oral therapeutic based on their high affinity, high thermal stability, and resistance to pepsin digestion. Our study provides the basis of a proof-of-principle model with which to develop specific, broadly neutralizing and intrinsically stable antibodies for the oral therapy of *C. difficile* infections, as an alternative to conventional antibiotic treatment.

ACKNOWLEDGMENTS

I cannot begin to fully express my appreciation and gratitude to my supervisor Dr. Jamshid Tanha for whole heartedly welcoming me to his lab, for his continued support and faith in my abilities, and for pushing me to see and think of things in a different perspective. His extent of knowledge and experience will never cease to amaze me, and I am truly grateful for the opportunity to have worked and trained under him.

I would also like to sincerely thank Henk van Fassen and Dr. Roger MacKenzie, not only for all the hard work and thought that went into the acquisition of the SPR data, but also for having the patience to spend lengths of time with me meticulously reviewing this data afterwards.

I would like to thank all those who contributed to this project both in theory and in practice. Dr. MacKenzie, Dr. Susan Logan, and Dr. Thienn-Fah Mah, thank you for taking the time to be on my advisory committee, for your guidance, and expert advice, and for bringing fresh perspective into the project. Thank you to all my lab mates and friends in the Antibody and Protein Engineering group at the National Research Council of Canada, each of whom has helped me in this journey one way or another. Special thanks to Drs. Dae Young Kim and Jyothi Kumaran, as well as to Gabrielle Richard, Robert Gene, and Greg Hussack for your constant support, advice, and for taking the time to help make revisions to this thesis. Thank you Jyothi for helping me understand protein modeling and electrostatics; you have taught me so much and you are truly a great addition to any team!

This thesis is dedicated to my family, and my high school sweetheart and fiancé, Peter Keriakos—I couldn't have made it this far by myself. Thank you mom and dad especially, for sacrificing so much to give me this opportunity; I will spend the rest of my life happily indebted

to you, and by your sides. Thank you also to my little brother Iyad for just being you; I want you to always know that I look up to, and that your gentle nature and breadth of knowledge constantly humbles me. Last but most of all, I would like to thank you God, for without him nothing is possible.

TABLE OF CONTENTS

LIST OF FIGURES

LIST OF TABLES

LIST OF ABBREVIATIONS

Ab	Antibody
Ag	Antigen
Amp	Ampicillin
AP	Alkaline phosphatase
BSA	Bovine serum albumin
cDNA	Complementary Deoxyribonucleic acid
CDR	Complementarity determining region
CFU	Colony forming unit
CH	Constant domain from heavy chain of antibody
CL	Constant domain from light chain of antibody
Da	Daltons
DNA	Deoxyribonucleic acid
EDTA	Ethylenediaminetetraacetic Acid
ELISA	Enzyme-linked immunosorbent assay
Fab	Antigen binding fragment
Fd	Type of filamentous phage
FPLC	Fast protein liquid chromatography
FR	Framework region
Fv	Variable Fragment
HCAb	Heavy chain antibodies
HEPES	N-2-Hydroxyethylpiperazine-N'-2-Ethanesulfonic Acid
HRP	Horseradish peroxidase
IgA	Immunoglobin A
IgG	Immunoglobin G
IgM	Immunoglobin M
IMAC	Immobilized metal affinity chromatography
IPTG	Isopropyl-Beta-d-Thiogalactopyranoside
K_D	Affinity constant
k_{off}	Association rate constant

k_{on}	Dissociation rate constant
M13	Type of filamentous phage
mAb	Monoclonal antibody
mRNA	Messenger ribonucleic acid
MW	Molecular weight
OD	Optical density
PAGE	Polyacrylamide gel electrophoresis
PBL	Peripheral blood lymphocytes
PBS	Phosphate buffered saline
PCR	Polymerase chain reaction
PEG	Polyethylene glycol
PFU	Plaque forming unit
pI	Isoelectric point
PMSF	Phenylmethanesulfonyl Fluoride
PVDF	Polyvinylidene difluoride
rAb	Recombinant antibody
R_{max}	Maximum response defined as saturation of surface plasmon resonance
RNA	Ribonucleic acid
RU	Response unit
scFV	Single-chain variable fragment
sdAb	Single-domain antibody
SDS	Sodium Dodecyl Sulfate
SLPs	Surface layer proteins
SOC Media	Super optimal catabolic repression medium
SPR	Surface plasmon resonance
VH	Variable domain from heavy chain of antibody
VHH	Variable domain from HCAb in camelids
VL	Variable domain from light chain of antibody

1. GENERAL OVERVIEW, OBJECTIVES, AND HYPOTHESIS

Clostridium difficile is a Gram-positive, anaerobic, gastrointestinal pathogen that is transferred by the fecal-oral route. It is the leading cause of hospital acquired infections in developed countries. A recent study reports that the United States spends an estimated $3.2 billion USD per annum for the treatment of *C. difficile* associated disease (CDAD) (O'Brien et al., 2007) – a three fold increase of the previously modest estimate of $1.1 billion USD per annum. Several outbreaks occurred in over 30 hospitals in the province of Quebec, Canada, in a span of 4 years. From 2003-2005, *C. difficile* has been linked to the death of an estimated 2000 people in the province of Quebec alone (Jean-Benoit Legault, 2008). In Canada, *C. difficile* is the leading cause of deaths due to gastrointestinal (GI) infections (Statistics Canada; Canadian Vital Statistics, Death Database). Antibiotics are the predisposing agents to *C. difficile* infections as they eliminate competition from the normal flora, allowing this opportunistic pathogen to flourish. Ironically, *C. difficile* infections are treated with vancomycin, or metranidazole, however, there is increased pressure to develop alternative therapeutic methods to treat *C. difficle* infections with the recent emergence of hypervirulent strains in combination with the continued rise in antibiotic resistance.

C. difficile produces two major toxins, toxin A and toxin B, and the majority of research is focused on these toxins as they are the primary virulence factors (Lyerly et al., 1988; Giannasca and Warny, 2004; Hussack and Tanha, 2010). However, other virulence factors such as cell wall proteins, SLPs, and flagellar components have been identified as additional potential therapeutic targets. SLPs in particular are attractive targets for this purpose due to their abundance on the cell surface and their requirement for adherence to host cells (takumi et al., 1991; Drudy et al., 2001; Calabi et al., 2002). Moreover, several

studies have demonstrated the efficacy of anti-SLP antibody therapy in hamster models of *C. difficile* infections (O'Brien et al., 2005; Torres et al., 1995; Pechine et al., 2007).

Currently, toxin-neutralizing monoclonal antibodies are undergoing clinical trials (Taylor et al., 2008), but, little effort is focused on alternative strategies for reducing the bacterial burden and promoting bacterial clearance. However, while antibody therapy is an attractive alternative for treating *C. difficile* infections, developing monoclonal antibodies is labor intensive. A cost effective alternative is the selection, using phage display technologies, of single-domain antibody fragments which retain the full binding capabilities of full size IgGs. A single-domain antibody (sdAb) is the variable domain (i.e. antigen binding site) of a full size antibody. Camelid sdAbs are particularly attractive therapeutic reagents due to their high affinity, low immunogenicity, high expression yields, increased stability, and high solubility (Holliger and Hudson, 2005; Arbabi-Ghahroudi et al., 2005; Hussack and Tanha, 2010). The work presented in this thesis is based on the hypothesis that llama SLP-specific sdAbs are potential alternative oral therapeutics for treating *C. difficile* infection. To investigate this, we set out to accomplish the following main objectives:

i. To isolate llama VH/VHH antibodies with high affinity and specificity to purified *C. difficile* SLPs, using phage display technology,
ii. To demonstrate the ability of the isolated antiSLP antibodies to bind *C. difficile* cells *in vitro,* and
iii. To assess their therapeutic potential by determining their solubility, thermal stability, resistance to pepsin digestion, and ability to inhibit cell motility.

2. LITERATURE REVIEW

2.1 *C. difficile* and its targets for antibody therapy

C. difficile causes a gastrointestinal infection with symptoms ranging from mild diarrhea to fatal pseudomembranous colitis (PMC). Symptoms are collectively termed CDAD. As an opportunistic pathogen, it awaits a disturbance in the gut microflora in order to establish infection. The primary predisposing agent to PMC and CDAD is prolonged treatment with broad-spectrum antibiotics, which eliminate competition from the commensal bacterial flora of the bowel. This lack of competition allows *C. difficile* spores to germinate and colonize the gastrointestinal tract. 1-3% of all healthy adults are asymptomatic carriers, but this rate increases to 20% upon antibiotic treatment (McFarland et al., 1989). In humans, *C. difficile* colonizes the distal colon (Lyerly et al., 1988; Borriello, 1998). Surface layer proteins (SLPs) then play a critical role in adherence to the intestinal epithelium in order to establish infection (Calabi et al., 2002; Drudy et al., 2001). Upon colonization, the bacterial cells begin secreting toxins that result in an inflammatory reaction at the epithelial lining of the GI tract, leading to diarrhea (Lyerly et al., 1988). Toxin production has been linked to the activity of quorum sensing molecules (Lee and Song, 2005), suggesting that the process may be cell-density dependent within the GI tract. Inflammatory cells, fibrin, bacterial and cellular components begin to accumulate after prolonged inflammation, leading to the formation of pseudomembranes at the mucosal wall. Perforation and degradation of the intestinal mucosa leads to mortality. Ironically the most common method to treat *C. difficile* infections is through the administration of antibiotics, namely vancomycin, bacitracin or metronidazole. However, there is a 20% chance of relapse even after prolonged antibiotic treatment, and a further 30-50% will experience a third relapsing episode (Kyne et al., 2001;

Barbut et al., 2000). Interestingly, patients with relapse incidences were found to exhibit a low antibody response to the bacterial toxins (Aronsson et al., 1985; Leung et al., 1991; Warny et al., 1994), and low immunoglobin M (IgM) antibodies to SLPs (Drudy et al., 2004). It is clear that treatment of an antibiotic-'associated' disease using an antibiotic is not ideal.

2.1.1. Strains and toxigencity: the evolution of hypervirulent strains

There are a number of *C. difficile* strains isolated, each with its own level of toxigenicity; however, not all strains are toxigenic. The *C. difficile* genome contains a 19.6 Kb pathogenicity locus (PaLoc) which encodes the toxin genes *tcdA* and *tcdB*, as well as the positive and negative regulators TcdR and TcdC, respectively (Voth and Ballard, 2005). Mutations in the regulatory genes greatly affect toxin production.

Hypervirulent strains have emerged over the last two decades. For example, a non epidemic strain isolated in 1985, and belonging to the PCR ribotype 027, became epidemic through the accumulation of genetic elements (Stabler et al., 2009). Ribotype 027 strains have evolved to produce higher levels of toxins due to deletions within *tcdC*, and they have also acquired motility, additional response regulators and transcription factors, additional antibiotic resistance cassettes and have shown enhanced sporulation ability, all of which contribute to their hyper virulence. The most prominent of the hypervirulent strains belong to this PCR ribotype. These strains are classified as North American pulsed field gel electrophoresis type 1 (NAP1), toxinotype III, and restriction endonuclease analysis group BI. A binary toxin gene is also typically found in ribotype 027 strains (Cartman et al., 2010). Quebec strain QCD-32g58 is one such hypervirulent strain belonging to this group. It was undetected in 2000 and 2001, but was responsible for the 2003 outbreak, in which its

prevalence was estimated at 75.2% of all PCR-ribotyped strains. It possess the signature 18-bp deletion within the *tcdC* gene, as well as a single nucleotide deletion at position 117 – both of which were identified in a United Kingdom reference strain – leading to the severe disruption of TcdC function (MacCannell et al., 2006).

2.1.2. *C. difficile* toxins

C. difficile produces two potent toxins that are the primary virulence factors. Toxin A (TcdA), and toxin B (TcdB) are cytotoxins (reviewed in (Lyerly et al., 1988; Giannasca and Warny, 2004; Hussack and Tanha, 2010)). Both toxins target the Rho/Ras family of GTPases which are essential for cellular function since their permanent inactivation leads to disruption of many critical pathways that are necessary to maintain cellular integrity and thus cell-barrier function of the epithelium (Jank and Aktories, 2008; Voth and Ballard, 2005; Jank et al., 2007; Pothoulakis, 2000). Administration of TcdA intragastrically was shown to be lethal in animal studies, while administration of TcdB alone was not; however, they appear to act synergistically when co-administered (Lyerly et al., 1985). Interestingly, after mechanically compromising the intestinal wall, administration of TcdB leads to death, therefore suggesting that TcdA initially affects the epithelial integrity, paving the way for the more potent cytotoxin, TcdB.

Some strains also produce the binary *C. difficile* transferase (CDT) toxin. This toxin was shown to inhibit actin polymerization (Goncalves et al., 2004). Interestingly, this toxin was also shown to induce the formation of microtubule protrusions that form a dense meshwork at the surface of the epithelial cell (Schwan et al., 2009). This meshwork enhanced bacterial adherence by wrapping and embedding bacterial cells. Quebec strain

QCD-32g58 produces and secretes CDT as well as comparatively higher levels of toxin A and toxin B.

2.1.2.1. Structure and function of toxins A and B

TcdA and TcdB are exotoxins with molecular weights of 308 kDa and 269 kDa, respectively. They are single polypeptide chains possessing multiple domains with distinct functions (reviewed in (Hussack and Tanha, 2010)). The C-terminal end of both toxins is a cell receptor binding domain that is thought to interact with host cell surface receptors, through multivalent interactions. Binding to the host cell surface receptors, which are thought to be glycoproteins, induces endocytosis. Endosomal pH changes then induce a conformational change in the toxin which frees the N-terminal glucosyltransferase (GT) domain into the cytosol, where it proceeds to transfer glucose to Rho-GTPases rendering the enzyme permanently inactive, leading to disruption of structural integrity and increased permeability of cells (Jank and Aktories, 2008).

These toxins have been studied extensively, and efforts are now focused on developing therapeutic alternatives to mainstream antibiotic treatment. It was demonstrated that antibodies to toxins are effective at preventing disease (Salcedo et al., 1997; Babcock et al., 2006; Hussack and Tanha, 2010). Recently, Hussack *et al.* (2011a) isolated anti-toxin antibodies that were highly potent at toxin neutralization *in vitro*, and when used in combination were in fact super-potent.

Understanding the structure and function of each toxin is crucial for designing effective therapeutic agents. The majority of research on *C. difficile* therapeutics is focused on its toxins as they are well characterized and are the major virulence factors; however,

other virulence factors such as cell wall proteins, SLPs, and flagellar components warrant further investigation as possible targets for therapeutic intervention.

2.1.3. *C. difficile* surface layer proteins

SLPs are common to almost all Archaea, and can be found in almost every phylogenetic group within Eubacteria (Sleytr and Beveridge, 1999). In *C. difficile*, the surface layer is composed of SLPs with other minor cell wall proteins arranged in a para-crystalline array (Sara and Sleytr, 2000; Kawata et al., 1984; Takumi et al., 1991; Cerquetti et al., 2000). SLPs are encoded by the *slpA* gene (Calabi et al., 2001). Studies suggest that the cell wall proteins identified may play a role in *C. difficile* pathogenicity. Cwp66 was identified in a gene cluster located near the *slpA* gene (Calabi et al., 2001) and was later demonstrated to possess adhesive properties (Karjalainen et al., 2001; Waligora et al., 2001). More recently Cwp84 was identified as a protease required for SLP maturation (Kirby et al., 2009).

SLPs are the most abundant proteins in the S-layer of *C. difficile*. The SLP protein precursor is cleaved to generate what is generally termed as the high- and low-molecular weight (MW) subunits, or P47 and P36, respectively (Figure 1) (Calabi et al., 2001). The two subunits associate to form a mature protein that covers the entire surface of the bacterium. It remains unclear if the post translational processing occurs in the cytoplasm or periplasm. Based on their outer surface localization and abundance, it is speculated that SLPs play a critical role in host-pathogen interactions.

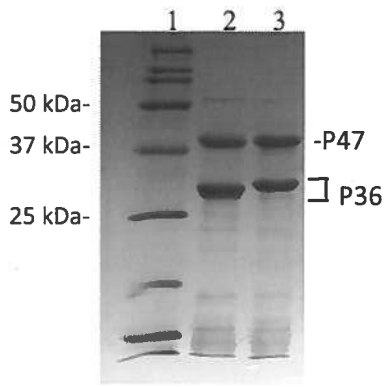

Figure 1: SDS-PAGE profiles of SLPs extracted from *C. difficile* strain 630 (CD630) and QCD-32g58 (QCD). The two major bands are the subunits of SLPs, P47 and P36. SLPs comprise the majority of the S-layer. Minor proteins can also be released during SLP extraction by low pH. The array of bands present in the preparations could also be breakdown products of SLPs. Lane 1: MW markers; lane 2: CD630 SLPs; lane 3: QCD SLPs.

2.1.3.1. Patterns of sequence conservation of *slpA*

The SlpA precursor protein, encoded by *slpA*, contains a signal sequence which targets it for translocation across the cytoplasmic membrane (Calabi et al., 2001; Karjalainen et al., 2001). Cleavage of the precursor by Cwp84 results in the two subunits, P36 and P47, that combine to form the mature protein (Kirby et al., 2009). The SlpA cleavage site, the P36 C-terminal and the P47 N-terminal are relatively well conserved (Calabi et al., 2001; Calabi and Fairweather, 2002; Fagan et al., 2009).

P36 is encoded by the 5' terminus of the *slpA* gene (Karjalainen et al., 2001; Drudy et al., 2004), and is the most consistently recognized subunit by anti-sera raised against the immunizing strain (Pantosti et al., 1989). P47 is encoded by the 3' end of the *slpA* gene. P36 is conserved in length, yet it exhibits low interstrain identity among the different PCR-ribotypes (Calabi and Fairweather, 2002; Spigaglia et al., 2011). The high variability observed could be due to either the lack of functional constraints, or the evolutionary need to evade the hosts' immune response. In contrast, P47 varies in length but displays higher inter-

strain identity. Studies have demonstrated the cross-reactivity of antisera to P47 from different strains, and across the different groups albeit to a less-consistent degree, while P36 is only recognized by antisera to SLPs from the immunizing strain or members of the same group, with very low cross-reactivity among the different groups (Calabi et al., 2001; Cerquetti et al., 2000). P47 is ~45% homologous to a *Bacillus subtilis* N-acetylmuramoyl-L-alanine amidase, and shows amidase activity (Calabi et al., 2001). The homology domain is thought to mediate anchoring to the cell wall and may play a role in cell wall turn-over.

2.1.3.2. SLP structure

Recently Fagan et al. (2009) reported structural insights into the organization of SLPs in *C. difficile*. Low resolution Small Angle X-ray Scattering (SAXS) data collected of the Low-MW SLP and the High/Low (H/L) complex demonstrates the presence of interaction domains within the high- and Low-MW subunits of SLPs, and that the two SLPs are oriented to form an elongated structure. By generating deletion mutants, they were able to map the essential residues of the interaction domains to residues 260-321 and 1-40 on the low- and High-MW subunits, respectively (Figure 2). Moreover, deletion of residues 211-259 in the Low-MW subunit reduced affinity to the High-MW subunit by 10-fold. Consistent with these results, an alignment of six representative *C. difficile* stains reveals a 70-74% sequence identity for C-terminal residues 245-274 and 304-321, confirming their relevance in subunit interactions.

The first crystal structure of a surface layer protein from a pathogen came when Fagan *et al.* (2009) reported the structure of a truncated version of the Low-MW SLP (residues 1-262). Their crystal structure revealed two domains within the Low-MW SLP, where domain 1 forms a two-layer sandwich architecture and contains both N- and C-

terminals of the subunit. Domain 2 contains a loop rich region that is mapped to the end of the H/L complex, and is most probably exposed to the environment. The remaining conserved residues lie in the center of domain 2 and extend towards the loop rich region. Fagan *et al.* hypothesize that the loop rich region is a key feature that enables the structure to tolerate residue variability while maintaining the overall fold. Their model supports the hypothesis that the high variability observed in the Low-MW SLP is a function of environmental pressure to evade the host immune response by altering receptor specificity. Moreover, since the two domains within the Low-MW SLP are oriented towards the environment, the conserved residues could represent a necessary functional motif.

The High-MW subunit contains two cell wall binding domains with the C-terminus protruding away from the bacterial surface. The N-terminus is only slightly accessible to the environment. Since it plays a role in host-pathogen interactions, it is probable that either termini mediate the host-cell interaction, and not the inner region of the High-MW SLP, as an array of SLPs may leave the inner region of the protein inaccessible to host receptors.

A

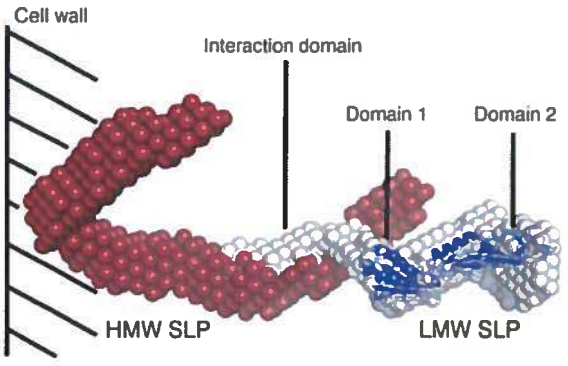

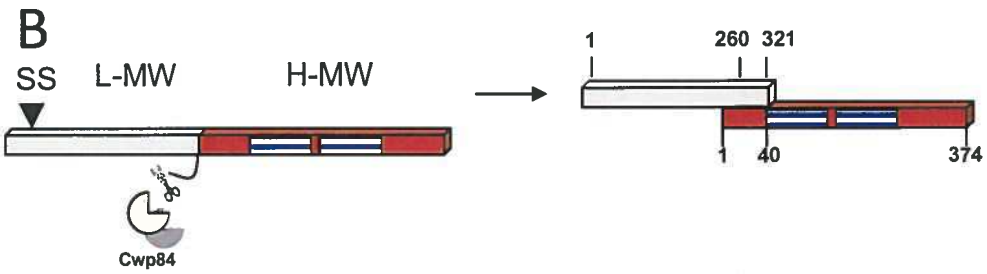

Figure 2: *C. difficile* SLPs. A) Structural representation of the Low-MW subunit (silver) of SLPs in complex with the High-MW subunit (red), anchored to the cell wall of *C. difficile*. The Low-MW subunit crystal structure was solved, and two domains were identified. B) The respective orientation of each subunit in the SlpA precursor protein. The positions of the signal sequence (SS) and the Cwp84 cleavage sites, as well as the two domains within the High-MW subunit are indicated. The residues essential for subunit association are also indicated. (Fagan et al., 2009)

2.1.3.3. SLPs in host-cell interactions and disease

SLPs have been hypothesized to play an important role in bacterial adherence to host tissue, and many studies using tissue sections and immortalized cell lines have demonstrated so. The first observation came when Takumi *et al.* (1991) assayed the adherence of *C. difficile* cells to HeLa cells *in vitro*. They found that intact *C. difficile* cells adhered to HeLa cells at a ratio of 34.4:1, while gluteraldehyde fixed bacterial cells lacking their S-layer adhered at a ratio of 2.2:1. Furthermore, antibody fragments (Fab, fragment antigen binding) from anti-sera to either P36, P47, or to both subunits, reduced *C. difficile* adherence to HeLa cells to levels of 63%, 55% and 83%, respectively.

Although P36 was studied more intensively than P47, several studies have demonstrated the role of both SLPs in cell-host attachment. Drudy et al. (2001) used human biopsy specimens of primary colonic and intestinal epithelial cells to demonstrate that toxigenic and non-toxigenic *C. difficile* adhere to human tissue, indicating that adherence is

independent of toxin production. They also demonstrated that adherence to immortalized human ileocaecal and colonic cell lines (Caco-2 and HT29) is possible, albeit to a lesser extent than to human tissue. The observed differences in adherence maybe due to an altered or less differentiated *C. difficile* receptor(s) on the cell lines' surface. Moreover, pre-incubation of *C. difficile* cells with immune sera significantly decreased bacterial adherence to these cell lines when compared to controls. Calabi et al. (2002) have demonstrated binding of native and recombinant SLPs, as well as labeled whole *C. difficile* cells, to mouse and human gut tissue sections, and to the human epithelial cell-line HEp-2. Binding was observed by both recombinant High-MW (rP47), and recombinant Low-MW (rP36) by ELISA to HEp-2 cells. However, rP36 binding was significantly lower than that of rP47. Fluorescence activated cell sorting (FACS) analysis revealed that anti-sera to rP47 preincubated with fluorescently labeled *C. difficile* reduced binding to HEp-2 cells by 20-30%. A similar study reported the reduction of *C. difficile* adherence to Caco-2 cells when bacteria were pre-incubated with P36 specific antisera (Karjalainen et al., 2001). Examination of *C. difficile* binding to human intestinal biopsy tissue sections revealed a distinct intensity and binding pattern to the various segments and cell subpopulation of the intestinal tract (Calabi et al., 2002). Interestingly, the rP47 binding pattern replicates the pattern seen with whole *C. difficle* cells, while rP36 shows only weak and punctuated binding to certain sections and cell sub-populations. Collectively, this suggests that while both SLPs play a role in cell-host interaction, P47 primarily mediates binding of *C. difficile* to intestinal tissue.

2.1.4. Current and potential therapies for *C. difficile* infections

The current choice of treatment for *C. difficile* infection is administration of vancomycin or metronidazole. However, vancomycin is rather expensive, and resistance to both antibiotics has been observed (Pelaez et al., 2002). Alternative therapies such as novel *C. difficile*-specific antibiotics (Rea et al., 2010), fecal-transplantation therapy to re-establish normal flora, toxin binding resins, toxin-based and cell-wall antigen-based vaccines, and toxin specific antibodies have been explored (reviewed in (Hussack and Tanha, 2010)). There is a focus on neutralizing toxins in order to reduce disease severity, with little effort focused on reducing infection and promoting bacterial clearance. By identifying other virulence factors, new treatment options can be developed to target whole cells in addition to toxin neutralization. Cell surface proteins are excellent candidates for this approach, and SLPs in particular are ideal targets for new therapeutic strategies due to their abundance and drug accessibility, and their implication in adhesion to host cells.

The Syrian hamster *Mesocricetus auratus* is widely accepted as the animal model for *C. difficile* infection; however, CDAD is more severe in hamsters than in humans, therefore making this a very stringent model. Recently, a study by O'Brien *et al.* (2005) demonstrated that passive immunization of hamsters using anti-SLP sera results in significantly prolonged survival of individuals. The anti-serum also readily agglutinated *C. difficile* cells and promoted phagocytosis *in vitro*. In another study, hamsters were actively immunized using toxoids A and B and *C. difficile* whole cell antigens (Torres et al., 1995). Significantly higher anti-toxin antibody levels, as well as sera with high bacterial agglutination activity, were observed in hamsters that were protected against *C. difficile* challenge. This suggests that the ability to mount an antibacterial antibody response may significantly enhance survival. In parallel studies, mucosal immunization of hamsters with FliD and cell wall

extracts, followed by challenge with *C. difficile,* proved most successful in reducing bacterial colonization for the duration of the study (100-fold reduction in CFUs) with respect to a control group receiving adjuvant only, and when compared to immunization with FliD with flaggellar extracts (10-fold reduction in CFUs), or FliD with Cwp84 (also a 10-fold reduction in CFUs) (Pechine et al., 2007). These studies provide support for the development of *C. difficile* SLP antibody therapeutics that aim to alleviate bacterial burden, by acting as mechanical obstacles which prevent bacterial adherence to the host's gastrointestinal epithelium and therefore promote bacterial clearance.

Currently, human monoclonal antibodies to *C. difficile* toxins are undergoing clinical trials (Taylor et al., 2008), however, there is no known report of antibodies to SLPs developed as therapeutic agents. Antibody fragments offer an alternative to the full size mAb molecules.

2.2. Antibody engineering and biotechnology

The immune systems of vertebrates produce several different gamma globulin proteins of large molecular weight that target foreign antigens. These immunoglobins, also known as antibodies (Ab), are produced by B cells as part of the humoral immune response. There are five classes of vertebrate antibodies: IgG, IgM, IgA, IgD, and IgE, with IgG being the most abundant (Joosten et al., 2003). IgGs have been exploited as therapeutic agents and clinical diagnostic tools, and have become invaluable within biotechnology fields.

Over the last 20-30 years, technologies and protocols have been developed to dissect and fragment, increase affinity, display, and even multimerize antibodies (Hudson, 1998). Efforts for the *in vitro* production of antigen-specific Abs have resulted in the establishment of hybridoma technology in 1975. In hybridoma technology an antigen is used to stimulate

B-cells which are immortalized by fusion to myloma cells. Hybridoma cells are capable of large-scale antigen-specific monoclonal antibody (mAb) production (Köhler and Milstein, 1975). Since then, efforts to develop, isolate, and modify recombinant Abs (rAb) (Figure 3) gave rise to a wide array of rAb technologies for a broad range of applications. Phage-display is routinely used to screen rAb libraries (reviewed in (Winter et al., 1994; Hoogenboom, 2005)). Optimization of expression systems and hosts now offers the possibility to produce rAb fragments on a larger scale while improving cost efficiency. In this chapter, established and emerging technologies for the isolation and production of antigen specific rAb fragments as alternatives to mAb technology or polyclonal serum are reviewed.

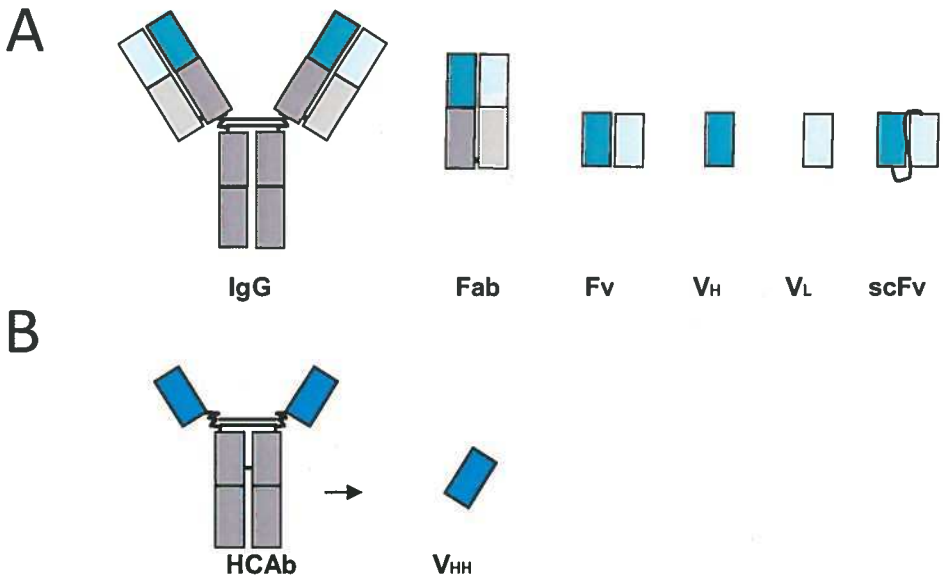

Figure 3: Naturally occurring antibodies and their recombinant counterparts. A) Whole IgG and rAb fragments. Fabs (~55 kDa), Fv (~30 kDa), VH and VL (~15 kDa), and scFvs (~32 kDa). B) Camelids produce heavy chain antibodies (HCAb) lacking the light chains. The variable domain of the heavy chain antibody is termed VHH. Adapted from Yau et al. 2003.

2.2.1. Whole IgG

An IgG is composed of two identical long polypeptide chains (heavy chains, ~50 kDa each), and two identical short polypeptide chains (light chains, ~25 kDa each), with a collective molecular weight of approximately 150 kDa. The heavy chains are composed of three constant domains (CH1, CH2, CH3) and one variable domain (VH), while the light chains each are composed of one constant domain (CL) and one variable domain (VL). The variable domains confer antigen specificity while constant domains (CH2 and CH3), or Fc portion, bind other cell surface targets or proteins of the complement system to recruit effector function (Joosten et al., 2003).

An IgG exhibits a tetrameric "Y" shaped quaternary structure with bilateral symmetry, where the heavy and light chains are linked to one another through hydrophobic interactions, and disulfide bridges at the CH1 and CL domains (Padlan, 1994; Maynard and Georgiou, 2000). A hinge connects the VH and CH1 to the Fc region. Disulfide bridges at these hinges connect the two heavy chains together. The hinge allows the VH-CH1 arm of the IgG to bend and rotate. Antigen binding sites are located at each end of the fork. The antigen binding sites, of which there are two per IgG molecule, consist of six complimentarity determining regions (CDRs) or hypervariable loops in the variable domains. Three of the six loops are within the VH domain and the other three within the VL domain (Holt et al., 2003). The genetic diversity of the hypervariable loops, and therefore the CDRs, theoretically results in a binding partner for all possible antigens.

Currently 26 mAb (or mAb-derived fragments) have been approved by the United States Food and Drug Administration for clinical use in treating diseases such as rheumatoid arthritis, non-Hodgkin's lymphoma, and respiratory syncytial virus infections (Mehdiratta

and Saberwal, 2007; The Immunology Link, 2011). mAbs are extremely potent and well tolerated by patients. However, they require mammalian expression systems, and as a relatively large molecule they are prone to degradation, aggregation and poor solubility, as well as limited tissue penetration and bio-distribution (Holt et al., 2003). While there are ways to improve the biophysical properties and pharmacokinetics of mAbs (Wu et al., 2010), antibody fragments represent an alternative to mAbs. Antibody fragments can offer improved physico-chemical properties while retaining the antigen affinities of the parental protein without the need for time consuming manipulations needed to improve functionality.

2.2.2. Recombinant antibody fragments

Proteolysis and genetic engineering have given rise to many antibody fragments (Figure 3). Size reduction, fragment dissection, and multivalent formats are only a few of the designs of antigen-binding antibodies developed over the last three decades. Whole IgGs can be digested with papain to produce Fab fragments (Fragment antigen binding) which are the variable domains with the CH1 and CL domains, linked by a disulfide bond to enhance stability (Maynard and Georgiou, 2000). They are of relatively large molecular weight (~55 kDa), however they are still amendable to protein engineering techniques in order to enhance their biological and biophysical properties (reviewed in (Filpula, 2007; Holliger and Hudson, 2005; Maynard and Georgiou, 2000)). A variable region fragment (Fv) molecule retains the monovalent affinity of its parent antibody and is composed of paired VH and VL domains (Hudson, 1998). However, the fragment is not easily generated by proteolysis of an IgG and must be engineered as a single chain variable fragment (scFv; ~27 kDa) that is composed of the VH and VL domain of the parent antibody linked by polypeptide chains.

Much like full size IgGs, the VL and VH combination within a Fab or scFv offers high affinity and specificity to antigens since there are six CDRs involved in binding an antigen. These antibody fragments retain the binding affinity of the parental antibody yet confer advantages over a full size antibody such as enhanced tissue penetration, higher expression yields, and are defective in complement activation that is mediated by the Fc region (Hudson, 1998; Holliger and Hudson, 2005). Both fragments have their advantages and disadvantages and selection between either will heavily depend on the purpose to be served by the rAb fragment. For example if tissue penetration is required, selecting an scFv would be more desirable. However, if stability and resistance to proteolytic digestion is more favorable, then one might consider a Fab fragment.

2.2.3. Heavy chain antibodies

Conventional antibodies are composed of two heavy chains and two light chains, however, their variable domains have been known to occur naturally as part of a single isolated chain in some human diseases such as heavy-chain disease (Hendershot et al., 1987), or Bence-Jones proteins (light chains) in patients with multiple myeloma (Hilschmann and Craig, 1965). Camelids produce heavy-chain-only antibodies (HCAb) devoid of light chains, in addition to conventional IgGs. These antibodies also lack the CH1 domains (Figure 3.B) (Hamers-Casterman et al., 1993). Sharks also produce antibodies lacking a light chain. The antigen binding site of these antibodies is composed of only one domain, termed VHH for camelids and VNAR for sharks. HCAbs represent 25-45% of antibodies in *Llama glama* serum and 75% of camel serum (van der Linden et al., 2000). Their molecular weight is approximately 80-92 kDa (Hamers-Casterman et al., 1993). The hydrophobic interface between the heavy chains and light chains in a conventional IgG is lost in HCAbs via the

substitution of hydrophobic residues with hydrophilic ones (discussed below) (Wesolowski et al., 2009).

2.2.4. Single domain antibodies: Special focus on VHHs

Studies have described the isolation of antigen specific VHH fragments with affinities comparable to Fab and scFv fragments isolated using the same antigen (Arbabi Ghahroudi et al., 1997). The engineering of single domain antibodies (sdAb) offer several advantages over the Fab and scFv format. A sdAb is the variable domain of a whole IgG, in a stand-alone format; these include VH, VHH, VL, and VNARs (Figure 3A). sdAbs are four times smaller than a Fab fragment, and half the size of an scFv fragment, with a molecular weight of ~15 kDa. The isolation of these small antigen-binding fragments was first described by Greg Winter's group in 1989 when lysozyme-binding murine VHs were selected from a cloned sdAb repertoire (Ward et al., 1989). Since then, VHs and VHHs have been studied extensively (reviewed in (Holliger and Hudson, 2005; Harmsen and De Haard, 2007)). The size of sdAbs makes them attractive candidates as functional biological molecules. They are superior at penetrating poorly vascularized tissue such as tumors (Carter, 2001); however they have a short serum half-life (Harmsen et al., 2005a; Cortez Retamozo and Lauwereys, 2002) and are rapidly cleared from the body.

Initially, isolated VHs were prone to aggregation in solution at concentrations higher than 1 mg/mL due to the absence of their domain partner. In contrast, VHHs exhibit higher solubility relative to their VH siblings due in part to a key tetrad of specific amino acid substitutions at the VL-interface (Muyldermans et al., 1994); and reviewed in (Muyldermans and Lauwereys, 1999). When compared to conventional VHs, residues normally conserved at positions 37, 44, 45 and 47 (Kabat number system (Kabat et al., 1992)) are substituted to

hydrophilic amino acids. The most common substitutions include but are not exclusive to Val37Phe or Val37Tyr, Gly44Glu, Leu45Arg or Leu45Cys and Trp47Gly. Moreover, studies have demonstrated that "camelization" of human VHs through the substitution of key amino acids with the camelid tetrad can enhance solubility and reduce aggregation (Davies and Riechmann, 1996; Tanha et al., 2001). Similarly, VHH molecules with attractive biophysical properties can be "humanized" in order to avoid eliciting an immune response when used as a therapeutic.

VHHs tend to have increased antigen-binding surface area due to their relatively long CDRs 1 and 3, which has a higher rate of somatic mutations, compared to conventional VHs (Vu et al., 1997; Muyldermans, 2001). An average VHH CDR3 is 16 residues long whereas a human VH CDR3 averages 12 residues and a mouse VH CDR3 averages 9 residues (Te Wu et al., 1993; Muyldermans et al., 1994). There are several advantages to this. First, this results in an increased antigen-binding surface with which to compensate for the lack of a VL binding partner. Secondly, this imparts the ability to form long finger-like protrusions that can fit into small cavities and enzymatic active sites which may not be accessible with conventional rAbs. Indeed the crystal structure of VHHs in complex with lysozyme demonstrated that the VHHs were able to bind the active sites of these enzymes which are not typically recognized by larger rAb fragments (Desmyter et al., 2002; Desmyter et al., 1996; De Genst et al., 2006). Finally, crystal structures demonstrate the folding of the CDR3 over the VL interface which presumably stabilizes the structure and prevents aggregation (Desmyter et al., 1996; Desmyter et al., 2002; Decanniere et al., 1999).

Camelid sdAbs are recognized as structurally stable and highly soluble (Holliger and Hudson, 2005; Arbabi-Ghahroudi et al., 2005; Hussack and Tanha, 2010). Van der Linden *et*

al. (1999) have experimentally demonstrated that VHHs retain their functionality at temperatures up to 90°C. Besides the canonical disulfide bond between positions 22 and 92 that attributes the immunoglobin fold to VHs and VHHs, VHHs possess a cysteine residue (~80 % of cases) in the CDR3, which forms an additional disulfide bond with either a cysteine in CDR1, position 45 in FR2, or CDR2 (Muyldermans et al., 1994; Davies and Riechmann, 1996; Vu et al., 1997; Harmsen et al., 2000). This additional disulfide bond acts to restrict the degrees of freedom of a long CDR3 which results in entropically favorable binding energetics and an overall stable molecule. Furthermore, the positions of the Cys residues in the CDRs are not fixed, which generates a geometrical diversity in the paratope resulting in an increase of the antigen-binding repertoire (Conrath et al., 2003). These domains can be further enhanced by the introduction of an artificial disulfide bond at the hydrophobic core which allows for greater structural stability (Arbabi-Ghahroudi et al., 2005; Chan et al., 2008; Hagihara et al., 2007; Saerens et al., 2008a), with which to withstand the highly acidic and protease rich environment of the GI tract. Highly soluble non-aggregating antibodies are especially desirable in therapeutic formulations because they retain their functionality under a wide range of conditions (Van der Linden et al., 1999; Goldman et al., 2006). Additionally, aggregating proteins are known to increase immunogenicity (Hermeling et al., 2004) thus necessitating the selection of small-sized protein therapeutics with non-aggregating properties.

2.2.4.1. Advantages and limitations of sdAbs

sdAbs, and more specifically VHHs, offer several advantages over larger and more complex mAbs, scFvs and Fabs; they exhibit higher expression yields, thermal and chemical stability, and solubility, as well as increased protease resistance and thus make excellent

candidates as therapeutic agents (Holt et al., 2003). The lack of the VL domain allows for greater structural flexibility when binding antigen, leading to higher affinities, with dissociation constants (K_Ds) in the nanomolar and sub-nanomolar range (Muyldermans, 2001; Spinelli et al., 2000). HCAb DNA can be readily isolated from peripheral blood leukocytes (PBLs) based on the distinct size of HCAbs (Arbabi Ghahroudi et al., 1997); library generation is efficient and camelids can be exploited in that immunization yields *in vivo* matured VHHs thereby negating the need for *in vitro* manipulation and affinity maturation. Moreover, only a single gene segment (i.e. VHH *vs.* VH and VL as in scFv) is required in order to recover the whole antigen-binding repertoire. In comparison to human or mouse sdAbs, where several VH or VL families exist, there is only one family of VHHs, therefore, only a single polymerase chain reaction (PCR) primer set is required to isolate the entire repertoire. In addition, VHH scaffolds with desirable biophysical properties can be used to construct libraries through the randomization of the CDRs, thus bypassing animal immunization (Muyldermans, 2001). Finally, It is estimated that the cost of producing proteins in a bacterial host under industrial scale fermentation conditions is approximately 1$ per gram of protein (Estell, 2006). With the relatively high yields obtained from bacterial expression of sdAbs it is obvious that they offer a cost-efficient alternative to the production of larger protein therapeutics.

However, there are limitations to sdAb fragments. In a VH or VL, affinity maturation during immunization occurs in the presence of the partnering variable domain; when the VH or VL are isolated individually, it results in lower affinity for the antigen relative to its parent antibody. In the case of VHHs, long loop length can render the CDR3 more flexible allowing it to adopt multiple conformations, resulting in a negative impact on binding

energetics (Muyldermans and Lauwereys, 1999). The latter short-coming is often countered in VHHs through the presence of a disulfide bond in CDR3 as mentioned above. Rapid blood clearance may be advantageous and disadvantageous depending on the purpose to be served by the antibody fragment. It is disadvantageous in a setting where an antibody is used for neutralization of an antigen, thus requiring a longer serum half-life. However, in cancer therapeutics (Cortez Retamozo and Lauwereys, 2002), it is advantageous to rapidly clear the tumor-targeting antibody in cases where it is coupled to an anti-tumor drug or a radio-isotope label for imaging and diagnostics, considering that longer residence times results in toxic effects on healthy cells.

2.2.5. Antibody libraries

sdAbs, like Fabs and scFvs can be displayed on a range of different platforms. Once the mechanism of creating immunoglobin genetic diversity was understood in 1983 (Tonegawa, 1983) , the concept of "antibody display" was established. Antibody display libraries are a collection of an Ab repertoire with direct linkage of the expressed antibody (i.e., phenotype) to the encoding gene (i.e., genotype). This link allows for high throughput screening of large repertoire libraries for antigen-specific antibody retrieval, wherein the genetic material is also available for further manipulation and engineering. There are several classifications of rAb libraries: immunized, naïve, semi-synthetic, or synthetic, depending on the source of genetic material used for library construction.

2.2.5.1. Immunized libraries *vs.* naïve libraries

Immune libraries are constructed from RNA isolated from PBLs of an immunized host. Genes that encode variable domains are amplified and cloned into vectors for expression of different antibody fragments such as VHH (Arbabi Ghahroudi et al., 1997;

Goldman et al., 2006), scFv (McCafferty et al., 1990), and Fab (Huse et al., 1989; Orum et al., 1993; Persson et al., 1991). Antibodies isolated from these libraries have already undergone affinity maturation *in vivo* (Hoogenboom et al., 1998); however, antibody library size is often limited when compared to non-biased (naïve) library formats (Burton et al., 1991; Clackson et al., 1991; Hoogenboom, 1997; Willats, 2002). Moreover, the immunization process is complicated at times when antigens are toxic, not readily available, or chemically unstable.

In contrast, naïve libraries are prepared in the same manner but without previous immunization of the host with the antigen of interest. The first naïve VHH library was created in 2002 (Tanha et al., 2002). Sources of mRNA for library construction could be peripheral blood lymphocytes, bone marrow, and spleen cells. For this type of library IgM is preferred because it has not been previously subjected to antigen selection and thus the repertoire remains unbiased (Dörsam et al., 1997; Griffiths et al., 1993; Little et al., 1993; Marks et al., 1991). In order to successfully retrieve antigen-specific rAb, library size must be large (Marks et al., 1991). Naïve libraries with diversity of 10^{10} are likely to yield Abs with nanomolar (nM) affinities (Vaughan et al., 1996). These findings demonstrate that size and therefore heterogeneity of naïve libraries are critical for isolating antibodies with high affinities without host immunization, and can serve as a universal source of antibodies.

2.2.5.2. Synthetic and semi-synthetic libraries

Synthetic and semi synthetic libraries offer the combined advantages of the structural diversity and universality of naïve libraries, as well as rAb structural and functional knowledge. These libraries can offer a level of control over aspects such as expression, immunogenicity, structural heterogeneity, solubility, stability, and affinity of an antibody

(Fellouse et al., 2007; Knappik and Pluckthun, 1995; Knappik et al., 2000; Winter and Milstein, 1991; Arbabi-Ghahroudi et al., 2008; Tanha et al., 2001). They evolved from the development of antibody scaffolds with desirable biophysical properties combined with synthetic CDR constructs in order to introduce diversity.

2.2.6. Antibody display platforms

Different display platforms can be used in order to facilitate antibody selection and isolation (Yau et al., 2003; Li, 2000). Peptides can be displayed on the surface of bacteria (Georgiou et al., 1993; Fuchs et al., 1991; Gunneriusson et al., 1996; Francisco et al., 1993) or yeast (Georgiou et al., 1997). The peptide can be expressed within the cell without the need for gene subcloning post-isolation. Cells displaying a desired antibody can be isolated either by FACS, or by continuous affinity-based selection (Patel et al., 2001). Yeast has a rigid and thick cell wall which allows for stable maintenance of the displayed peptide even under harsh conditions. Yeast cells can express large quantities of the protein, with proper post-translational modifications and folding which may not occur in bacterial display. Increased avidity is a disadvantage of these display system since 50,000 – 100,000 Abs can be displayed on the surface (Francisco et al., 1993b), thereby resulting in the isolation of 'false-positive' binders.

Ribosome display systems are an alternative to the expression of Ab on living cells, or phage. The phenotype-genotype link is maintained where the expressed Ab remains attached to the ribosome with its mRNA (He and Taussig, 1997; Schaffitzel et al., 1999; Yau et al., 2003). Ribosome display occurs entirely *in vitro* and is a completely cell-free system where transformation efficiency is not limiting library size; libraries with diversities of 10^{15} can be created (Roberts and Ja, 1999). Affinity maturation can occur at the selection stages

by using a polymerase with a high error rate. Moreover, expression of peptides that are toxic to yeast or bacteria is possible in this display system, therefore avoiding under-representation of the library. mRNA instability (Schaffitzel et al., 1999) and the availability of materials are disadvantages to using ribosome-display.

2.2.6.1. Phage display

Phage display is the first described display system when Smith (1985) reported the expression of a peptide fusion with the pIII coat protein of filamentous phage, providing the direct link of phenotype to genotype. Soon after, McCafferty et al. (1990) developed the first scFv phage display library, and since then, phage display technology became a widely adopted technique for the retrieval of antigen-specific antibodies, with improved binding affinities and biophysical characteristics. Phage display systems are built on filamentous phage. Their genome is well studied, and they are amenable to laboratory manipulations.

2.2.6.1.1. Filamentous bacteriophages

Filamentous bacteriophages such as M13 and fd infect and replicate within Gram-negative bacteria without lysing the host cell. They are ideal for rAb engineering due to their relatively small genome size which tolerates insertions into non-essential areas without affecting bacterial infectivity (Barbass III et al., 2004). Proteins are expressed as fusions to a phage coat protein and their DNA is packaged with the phage viral genome within the nascent phage particles. Once a bacterial cell is infected, other phage particles are prevented from entering the cell which ensures that all phage produced within the cell are identical clones (Paschke, 2006).

Filamentous phage (reviewed in (Hoogenboom et al., 1998; Yau et al., 2003)) contain a circular single stranded DNA genome of ~6.4 Kbp, coated with a long flexible protein tube that contains 2700 copies of the major coat protein pVIII. Minor coat proteins pIII, pVI, pVII, and pIX are located at the tips. pIII is the most commonly used protein for fusion peptides since it is most amendable to insertions without affecting phage infectivity. Different systems of phage display exist but most are based on a pIII-protein fusion and can differ in the display orientation and number of displayed peptides. These phage are stable under harsh condition which allows for selection of stable species under chemical or heat denaturation.

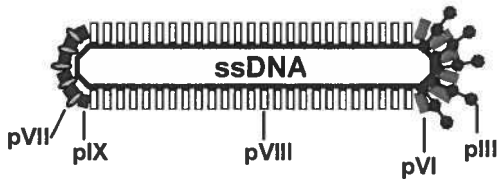

Figure 4: Filamentous bacteriophage. The single stranded DNA in a filamentous bacteriophage is encapsulated by a proteinacious coat. The five major coat proteins are indicated.

2.2.6.1.2. Vector type: phage *vs.* phagemid

Phage display libraries are constructed by cloning a repe toire of PCR-amplified Ab genes into either a phage or phagemid vector (Hoogenboom et al., 1991; Winter et al., 1994). Both vectors can be designed such that the rAb gene is inserted between a signal sequence and coat protein pIII. Both vectors contain antibiotic resistance genes for selection and a phage origin of replication in order to package foreign DNA into single stranded DNA (ssDNA) within the nascent phage particle. The phage vector contains all the necessary genetic information to produce full phage particles. However, the phagemid vector lacks

some of the genes required to form mature phage, and requires the addition of helper phage, in a process called 'phage rescue'. Helper phage supply the machinery necessary for phage replication and packaging, which is missing in the phagemid vector. Using a helper phage with a defective origin of replication can reduce the number of unwanted helper phage progeny in phage rescue (helper phage are not useful in phage display because although they may display the fusion protein, they do not contain the genetic code required for further isolation). The phage system produces particles displaying only the fusion protein in a multivalent display format, whereas the phagemid system produces phage displaying wild type pIII and pIII-Ab fusion in a monovalent display format thereby avoiding avidity effects.

2.2.6.2. Panning

Isolation of antigen-specific Abs from a phage display library is referred to as 'panning' (Figure 5). It is a step-wise procedure in which phage is isolated and amplified (Smith, 1985; McCafferty et al., 1990; Georgiou et al., 1997). Briefly, an antigen is immobilized on a solid support (or in solution, on beads, etc), and the full repertoire of Ab displayed in a library is exposed to the target. This is followed by several washing steps to remove non-specific binders. Those that remain bound to the target can be eluted by either: competitive elution, extreme pH, or protease cleavage, and then amplified in a bacterial host. After each round of panning, phage are subjected to increased selection pressure such as lowering the antigen concentrations, adding proteases, using pH denaturants, or increasing temperatures, in order to continue enrichment of phage displaying Ag-binding Abs with desirable biophysical properties. Three to five rounds of panning are usually necessary to

isolate high affinity Abs. After panning, the genes encoding the antibodies are retrieved by PCR, subcloned into an expression vector, and expressed in the system of choice.

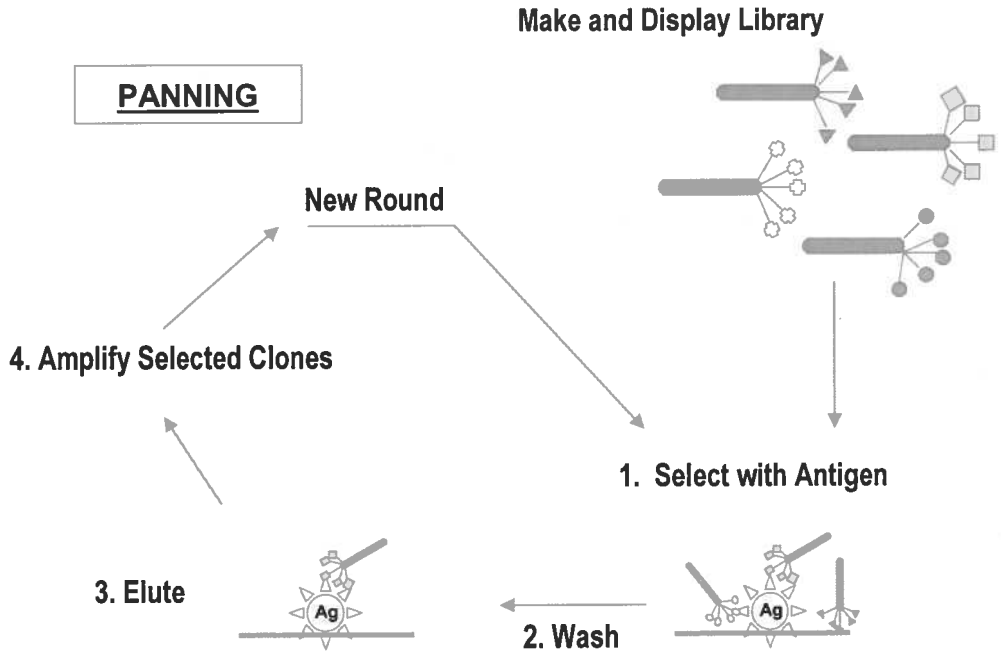

Figure 5: Panning of antibody phage-display libraries. The antibody repertoire is displayed on the surface of phage. Antigen is then immobilized on a solid support, and the library is applied for selection, where phage displaying antigen-specific antibodies will bind the antigen (1). Washing removes non-specific binding phage (2). The phage displaying antigen-specific antibodies will survive the washing step and are eluted (3), amplified (4), and used to start the subsequent panning round.

2.2.7. Expression and purification of single domain antibodies from phage display

With the growing demand for rAbs for the treatment of human diseases, there is an urgent need to develop cost effective and efficient production and purification methods. Abs retrieved from a phage or phagemid vector must be subcloned into an expression vector and transformed into an expression host. Currently, expression is based largely on bacterial

systems (reviewed in (Arbabi-Ghahroudi et al., 2005)) , however, alternative expression systems such as yeast (Ridder et al., 1995), mammalian cells (Riechmann et al., 1988), baculovirus (Carayannopoulos et al., 1994), and plants (Peeters et al., 2001) have been described (Joosten et al., 2003). It is important to note that there is no universal expression system that can guarantee yield, as each Ab sequence is unique and can pose unique challenges.

The choice of expression vector determines whether a monomer, dimer, or multimer is expressed. The expression vector often incorporates an affinity purification tag such as the hexa-His epitope tag. Large scale expression of sdAb can yield quantities in the tens of milligrams range. In a bacterial expression system, Ab can be extracted through either sucrose shock or total cell lysis. Sucrose shock is a method in which the Ab is released from the periplasm of the cells without cell lysis, and usually results in more pure Ab preparations with low levels of contaminating proteins. The simplest way to purify a rAb is by making use of an affinity tag.

The cytoplasm of *E. coli* is a reducing environment that does not allow for proper folding of expressed rAb, and thus leads to the formation of insoluble inclusion bodies that must be refolded *in vitro* in order to regain functionality (Gräslund et al., 2008). Periplasmic expression is a more promising route for producing functional rAb, but presents limitations for expressing full length Ab molecules. Periplasmic expression is very similar to eukaryotic expression where the expressed protein must travel through the endoplasmic reticulum and Golgi apparatus. Leader sequence peptides allow for the transport of rAb to the periplasm of *E. coli.* Proper folding can occur in the oxidative protease-free environment of the periplasm

(Plückthun, 1991). This environment is suitable for the proper folding of sdAb as a non-reducing environment is necessary for the formation of the canonical disulfide bond.

2.2.8. Current applications of sdAbs as therapeutics

The chemical and thermal stability, as well as monomeric behavior of sdAb makes them attractive protein therapeutic molecules. For example sdAbs can be used as toxin-neutralizing therapeutics (Hmila et al., 2008; Hussack et al., 2011a). They have also been used in a mouse model to treat rotavirus through oral administration and by administration of *Lactobacillus paracasei* expressing rotavirus-specific sdAbs (Van der Vaart et al., 2006; Pant et al., 2006). In cancer therapy, a sdAb antagonist of EGF receptor effectively inhibits growth of A-431-derived tumors (Roovers et al., 2007). The multimerization (reviewed in (Saerens et al., 2008b)) of a sdAb can greatly enhance the therapeutic functionality. For example, in frame cloning of two sdAb in a bivalent monospecific construct spaced with a short linker can increase specificity through avidity effects. Alternatively, targeting two epitopes on the same antigen by bivalent bispecific constructs can confer higher neutralizing activity, or enhance the specificity of two sdAbs with low affinity to the antigen. Bispecific constructs can also be employed to enhance serum half-life when necessary. For example, VHH-anti-IgG or a VHH-anti-serum albumin fusion can enhance blood residence by 100-fold (Harmsen et al., 2005a; Coppieters et al., 2006). Controlling half-life of antibodies is important in clinical settings and doses.

The design of man-made sdAb bispecific constructs or sdAb-effector molecule fusions is now being developed for immunotherapy of tumors and fatal infections. This approach is safer than the conventional non-specific chemotherapeutics. In a bispecific construct where one sdAb targets a cancer cell, the second sdAb can be used to recruit an

effector molecule, a cytotoxic T-cell, or natural killer cell for enhanced tumor clearance. Behar *et al.* isolated two antibodies specific to activating-receptor FcγRIII on NK cells which can be coupled to a tumor-specific sdAb for enhanced cancer therapy (Behar et al., 2007). Alternatively, cancer therapeutics or antimicrobials can be coupled to a sdAb for a higher-specificity drug delivery system (Miao et al., 2007; Cortez-Retamozo et al., 2004; Szynol et al., 2006).

Multimerization can greatly enhance the efficacy of neutralizing antibodies. Pentamerizing antibodies can be achieved by fusion to bacterial verotoxin B (VTB), a natural homopentamer (Figure 6). Pentamerization of low affinity sdAbs increased their affinity to an immobilized target through avidity effects (Zhang et al., 2004). This can be applicable in a setting where the target antigen is found in high copy numbers on the cell surface, as is the case with SLPs in *C. difficile*. Fusion can occur at either terminus of VTB, or at both to yield multivalent pentamers, or either monospecific or bispecific-multivalent decamers.

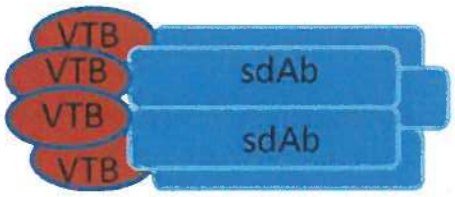

Figure 6: Pentamerization of sdAbs using the B-subunit of *E. coli* verotoxin. The verotoxin B subunit (VTB) is a natural homopentamer. Fusion of a sdAb to a VTB results in the pentamerization of the sdAb molecule. Courtesy of Dr. Tanha.

Neutralizing efficacy is often enhanced using a cocktail of different therapeutic antibodies (Babcock et al., 2006; Demarest et al., 2010; Nowakowski et al., 2002). In treating CDAD, using a combination of toxin-specific neutralizing mAb results in reduced mortality and enhanced protection (Babcock et al., 2006; Demarest et al., 2010). Hussack *et al.* (Hussack et al., 2011a) demonstrated that sdAbs to *C. difficile* toxin A were effective in neutralizing toxins *in vitro*, and in certain instances their efficacy was enhanced when administered in combinations.

2.3. Conclusion

The use of antibodies as neutralizing therapeutics in addition to studies implicating *C. difficile* SLPs as mediators for cell-host interactions (Calabi et al., 2002; Drudy et al., 2001) inspired the current study. SLP-specific llama sdAbs were isolated and characterized for the potential use as oral therapeutics by means of bacterial neutralization. The antibodies were analyzed for *in vitro* functionality, specificity and affinity, chemical stability under acid pressure and sensitivity to the GI protease pepsin, and for physical stability as indicated by the melting temperature. The sdAb is the smallest and simplest variant of antigen binding fragments of immunoglobins, yet it still retains full antigen binding capabilities and is very stable in solutions of different ionic strengths such as salts or high or low pH conditions, as well as under high temperature stress– features that make it an ideal oral therapeutic for treating *C. difficile* infection.

3. ISOLATION AND CHARACTERIZATION OF LLAMA SINGLE DOMAIN ANTIBODIES AGAINST *C. difficile* SLPs

3.1 Introduction

sdAbs to strain QCD-32g58 SLPs were selected from two phage display libraries—one naïve and one immune library. The antibodies were then functionally and biochemically characterized with respect to affinity, specificity, aggregation states, stability, resistance to pepsin digestion, and abilities to bind whole cells and inhibit motility were experimentally determined.

3.2. Materials and methods

3.2.1. Antigen extraction and purification

C. difficile SLPs (Appendix I) from strains QCD-32g58 (termed QCD for short), and CD630 were extracted using the low pH glycine extraction method (Calabi et al., 2001), and were obtained from Susan Logan's lab (National Research Council, Institute for Biological Science, Ottawa, Canada). Size exclusion chromatography was used to further purify the isolated SLP proteins after extraction. A Superdex^{TM} 200 10/30 GL column (GE Healthcare, Baie-d'Urfé, QC, Canada) was equilibrated with running buffer (10 mM HEPES buffer pH 7.5, 150 mM NaCl), and 500 µL of SLP extracts was loaded and eluted over one column volume as previously described in Fagan *et al.* (2009). Eluted fractions were then analyzed on SDS-PAGE for content. All fractions were stored at 4°C for later use.

3.2.2. sdAb display libraries and antibody selection

Two phage display libraries were used for the isolation of SLP-specific llama single domain antibodies. The first is a naïve llama VHH phage display library described in Tanha et al. (2002). For the immune phage display library, a llama was immunized with strains QCD and CD630 SLPs. The immune phagemid library was subsequently constructed in Arbabi-Gahroudi's lab according to previously published methods (Doyle et al., 2008).

3.2.2.1. Library panning

The naïve llama phage-display library was panned using whole QCD SLP preparation prior to gel filtration. The library was subjected to four rounds of panning; for each round of panning, 100 µL of 100 µg/mL antigen in PBS were coated on Immuno Maxisorp wells (Nalge Nunc Inc., Naperville, IL). Wells were blocked with 1% w/v casein in PBS for 2 h, and washed once with PBS prior to the addition of 10^{12} plaque forming units (PFUs) in 100 µL volume. Phage were incubated for 1.5 h at 37°C and washed 10 times with 0.1% v/v Tween 20-PBS, followed by 10 washes with PBS. Bound phage were eluted by high pH through the addition of 200 µL of freshly prepared 100 mM triethylamine solution for 10 min, transferred to a new 1.5 mL eppendorf tube and neutralized with 100 µL of 1.0 M Tris-HCl pH 7.4. The eluted phage were subsequently amplified as follows: 150 µL of phage were used to infect a 10 mL exponentially growing TG1 culture for 30 min at room temperature without shaking. 100-fold serial dilutions were used to determine eluted phage titer as described in Tanha et al. (2002) and phage titer was progressively tracked for the subsequent panning rounds to ensure enrichment. Fifty small plaques were picked from the titer plates of each panning round and the clones were stored in 10 µL H_2O for sequence analysis. Infected cells were then pelleted and resuspended in 900 µL 2YT (16 g Bacto-trypton, 5 g Bacto-yeast extract, 5 g NaCl per liter) , mixed in 300 µL aliquots with 3 mL

0.7% agar top, and plated on 2YT plates overnight at 37°C for phage propagation. The following day, the agar plates were incubated with 5 mL PBS each for 3 h with gentle shaking at 4°C to retrieve the amplified phage. An additional 5 mL PBS was used to rinse the plates. The two washes were combined and centrifuged at 6,000 rpm (Beckman J2-21M/E centrifuge, Beckman Coulter Inc., Brea, CA; J-10 rotor), at 4°C, for 20 min to remove debris. Phage purification was carried out as follows: to the phage-containing supernatant, 6 mL PEG/NaCl (20% PEG 8000-2.5 M NaCl) was added and incubated on ice for 1 h. The phage were pelleted at 10,800 g for 30 min at 4°C and the pellet was resuspended in 3.75 mL sterile water with 750 µL PEG/NaCl and incubated on ice for 30 min. The phage were pelleted once again as above, resuspended in 500 µL sterile PBS. Ten microliters of 10^6, 10^8, and 10^{10} serial dilutions in PBS were added to 200 µL of exponentially growing TG1 *E. coli* and incubated at 37°C for 30 min without shaking. The infected cells were then mixed with 3 mL of pre-warmed 0.7% agar top and poured over 2YT plates, allowed to solidfy, and incubated at 37°C overnight. The resulting plaques were counted to determine the phage titre, and 10^{11} PFUs were used to start the subsequent panning rounds.

The immune llama phagemid library was panned using QCD SLPs as the antigen. The library was subjected to four rounds of panning; for each round of panning, 100 µL of 100 µg/mL antigen in PBS were coated on Immuno Maxisorp wells. Wells were blocked with 1% w/v casein in PBS for 2 h, and washed once with PBS prior to the addition of 10^{12} (100 µL) colony forming units (CFUs) from the phagemid library. Phage were incubated for 1.5 h at 37°C and washed 10 times with 0.1% v/v Tween 20-PBS. Bound phage were eluted by adding 200 µL of freshly prepared 100 mM triethylamine solution for 10 min, transferred to a new tube and neutralized with 100 µL of 1.0 M Tris-HCl pH 7.4. The eluted phage were

subsequently amplified and rescued as follows: 150 µL of phage were used to infect a 2 mL exponentially growing TG1 culture for 15 min at room temperature without shaking. A 100-fold dilution of infected TG1 was plated on LB- agar plates (10 g Bacto-trypton, 5 g Bacto-yeast extract, 10 g NaCl, 12 g agar per 1 L), supplemented with 100 µg/mL of ampicillin, and used to determine the eluted phage titer and later for clonal analysis. Glucose was then added to a 2% final concentration, followed by 2 µL of 100 µg/mL ampicillin. The culture was incubated in a shaker incubator for 1 h at 37°C followed by infection with 10^{11} CFUs of M13KO7 helper phage (New England Biolabs, Pickering, ON, Canada) for 15 min without shaking at room temperature. The culture volume was adjusted to 10 mL using 2YT supplemented with 100 µg/mL of ampicillin, and grown for 1 h at 37°C, 250 rpm. Kanamycin was added to 75 µg/mL prior to overnight culture under the same conditions. The following day, cells were pelleted at 5,000 rpm (Beckman J2-21M/E centrifuge, J-10 rotor) and the supernatant filtered in a Millipore Stericup filter apparatus (Millipore). A 200 µL aliquot was used in a serial dilution in order to determine phage titer on LB-agar plates supplemented with 100 µg/mL ampicillin, prior to purification. Phage purification was carried out as described above. The titer was determined as follows: 10 µL of 10^6, 10^8, and 10^{10} serial dilutions were added to 90 µL of exponentially growing TG1 *E. coli* and incubated at room temperature for 5 min without shaking. The infected cells were plated on LB-agar plates supplemented with 100 µg/mL ampicillin, and the resulting colonies were counted to determine the phage titer, and 10^{11} CFUs were used to start the subsequent panning rounds.

3.2.2.2. Colony-PCR and clonal sequencing analysis

Primers fdT-GIIID (5'-GTGAAAAAATTATTATTCGCAATTCCT-3') and –96 gIII (5'-CCCTCATAGTTAGCGTAACG-3') (Stewart et al., 2007) were used to amplify the antibody fragments from the individual phage clones isolated from the naïve library, while primers MJ13RP (5'-CAGGAAACAGCTATGACC-3') and PN2 (5'-CCCTCATAGTTAAGCGTAACGATCT-3') were used to amplify the VHH fragments from individual phage clones of the immune library, by standard PCR. Positive clones were then sequenced as described in Doyle et al. (2008). Sequences were numbered and aligned using the LaserGene MegAlign software (DNASTAR Inc, Madison, WI) using the ClustalW method.

3.2.2.3. Phage enzyme-linked immunosorbent assay (ELISA) screening

Eluted phage clones were screened for SLP binding in a phage ELISA prior to cloning into expression vectors. The monoclonal phage from the naïve library were first amplified as follows: single plaques that were selected for clonal analysis were used to infect 2 mL of exponentially growing TG1 cells in 2YT for 30 min and 37°C, followed by overnight culture at 250 rpm, 37°C. The following day, the cells were pelleted and the phage-containing supernatant was subsequently used in the phage ELISA. The cells were resuspended in 15% glycerol-2YT and stored at -80°C. Single colonies carrying a sdAb insert were amplified for monoclonal phage ELISA as follows: each colony was cultured in 1 mL 2YT supplemented with 100 μg/mL ampicillin (2YT-Amp), and 2% glucose, for 1 h at 37°C. The cells were pelleted and the supernatant was replaced with 2 mL fresh 2YT-Amp for phage rescue. The culture was then infected with 10^{11} CFUs of M13K07 helper phage for 15 min at room temperature as standing culture, followed by incubation at 37°C for 1 h, 250 rpm. Kanamycin was added to 75 μg/mL and the phage were amplified overnight at 37°C,

250 rpm. The cells were pelleted and the phage-containing supernatant was subsequently used in the phage ELISA. The cells were resuspended in 15% glycerol-2YT and stored at -80°C.

For the phage ELISA, a microtiter ELISA plate was coated overnight at 4°C with 100 µL of 5 µg/mL SLPs or BSA for negative controls and blocked with 2% casein-PBS for 2 h at 37°C. Blank wells were coated with SLPs and blocked as before but did not receive phage treatment. Hundred µL of phage supernatant was added to each well and incubated at room temperature for 1.5 h. The plate was washed 5x with 0.05% Tween 20-PBS. Hundred µL of 1:5,000 antiM13-Horseradish peroxidase (HRP) conjugated antibody in blocking solution was added to each well and the plates incubated for 1 h at room temperature, followed by 5 washes as before. Bound phage were detected by the addition of 100 µL HRP colorimetric substrate (KPL, Gaithersburg, MD), followed by 100 µL 1 M phosphoric acid per well to stop the reaction. The optical density was determined at 450 nm on a standard ELISA plate reader (Dynatech MR5000).

3.2.3. Cloning, expression and purification of antiSLP sdAbs

3.2.3.1. Subcloning, expression, and purification of sdAbs in *E. coli*

VH or VHH gene-specific primers VH-BbsI (5'-TATGAAGACACCAGGCCGATGTGCAGCTGCAGGCGTCTG -3'), VHH-BbsI1 (5'-TATGAAGACACCAGGCCCAGGTGCAGCTGGTGGAGTCT -3'), or VHH-BbsI2 (5'-TATGAAGACACCAGGCCCAGGTAAAGCTGGAGGAGTCT-3') and VHH-BamHI (5'-TTGTTCGGATCCTGAGGAGACGGTGACCTG-3') were used to introduce BbsI and BamHI restriction sites into the ends of the VH/VHH DNA fragment via standard PCR. The

amplified DNA was purified using the QIAquick™ PCR Purification kit (QIAGEN, Mississauga, ON, Canada), and digested with Bbs1 and BamHI restriction enzymes, then ligated into pSJF2H vector (Arbabi-Ghahroudi et al., 2008) using standard techniques to produce His-tagged recombinant antibodies. By the same method, a mutant VH3, referred to as VH3-6E was constructed using the mutagenic primer VHBbsI-6E-Ext (5'-TATGAAGACACCAGGCCGATGTGCAGCTGCAGGAGTCTGGG-3'), and VHH-BamHI primer. Competent TG1 *E.coli* cells were transformed by electroporation (Tanha et al., 2001) and screened for antibody inserts by standard PCR techniques using the primers M13R and M13F. Clones positive for VH or VHH inserts were expressed using the M9 minimal salts method (Arbabi-Ghahroudi et al., 2009). Briefly, bacteria were subcultured in 25 mL LB broth supplemented with 100 µg/mL ampicillin, and used to start a 1 L M9 salts culture (0.2% glucose, 0.6% Na_2HPO_4, 0.3% KH_2PO_4, 0.1% NH_4Cl, 0.05% NaCl, 1 mM $MgCl_2$, 0.1 mM $CaCl_2$, supplemented with 0.4% casamino acids, 5 mg/L of vitamin B1 and 100 µg/mL of ampicillin). Bacteria were grown for 36 h at 28°C, 200 rpm, and then induced with 0.1-0.15 mM IPTG and 100 mL 10x TB nutrients (12% Bacto-trypton, 24% Bacto-yeast extracts, 4% glycerol), and allowed to grow for an additional 2.5 days. Cells were then harvested by centrifugation at 5,000 rpm (Beckman J2-21M/E centrifuge, J-10 rotor) for 20 min and the supernatant discarded. The pellet was resuspended in 20 mL TES buffer (0.2 M Tris, 0.5 mM EDTA, 20% Sucrose). After a 1 h incubation on ice, 30 mL 1/8 ice cold TES buffer was added and the cells were incubated for an additional hour with occasional stirring. Cells were pelleted at 7,000 rpm (Beckman J2-21M/E centrifuge, J-10 rotor), 4°C for 30 min. The supernatant containing the antibody was dialyzed overnight against immobilized metal affinity chromatography (IMAC) buffer A (10 mM HEPES buffer, 500 mM NaCl, pH

7.4), and the antibody was purified by IMAC (Porath and Olin, 1983; MacKenzie et al. 1994; Arbabi-Ghahroudi et al., 2009) using an ÄKTA FPLC (GE Healthcare). The aggregation status was determined by size exclusion chromatography on Superdex^{TM} 75 10/300 GL (GE Healthcare). The column was equilibrated with PBS buffer pH 7.4 as the running buffer, and the antibodies were eluted over one column volume.

3.2.3.2. Pentamerization of VH3

Pentamerization of antiSLP VH3 was carried out by introducing restriction sites BbsI and ApaI to the 5' and 3' ends of the VHH gene fragment using the VHH gene-specific primers VT-BbsI (5'-TAATAAGAAGACACCAGGCCGATGTGCAGCTGCAGGCGTC TG-3') and VT-ApaI (5'-ATTATTATGGGCCCTGAGGAGACGGTGACCTGGGTC-3') using standard PCR as before. The amplified DNA was first purified using the QIAquick^{TM} PCR Purification kit (Qiagen), digested with BbsI and ApaI, and then ligated to the pVT2 vector using techniques as described in (Zhang et al. 2004). This allows for the fusion of the single domain antibody to the N-terminal of verotoxin B subunit encoded in the vector. The vector also introduces a 6xHis-tag to facilitate purification. The clone was transformed, and expressed as described above. Cells were then harvested by centrifugation at 5,000 rpm (Beckman J2-21M/E centrifuge, J-10 rotor) for 20 min and the supernatant discarded. The pellet was resuspended in 100 mL of lysis buffer (500 mM Tris-HCl pH 8.0, 25 mM NaCl, 2 mM EDTA) and placed at -20°C overnight. The following day, PMSF and DTT were added to 1 mM and 2 mM final concentrations, respectively. The cells were lysed by adding lysozyme to 150 µg/mL final concentration and incubated at room temperature for 30-50 min. Two hundred µL of 15 unit/µL DNase I (Sigma, Oakville, ON, Canada) was added and incubated until the suspension became fluidic. The soluble fraction was separated by

centrifugation for 30 min at 4°C and 10,000 rpm (Beckman J2-21M/E centrifuge, J-17 rotor). After confirmation of expression of pentabodies by SDS-PAGE and Western blotting, the supernatant containing the antibody was dialyzed against IMAC buffer A and purified by IMAC as described above. The aggregation status was determined by size exclusion chromatography on a Superdex^{TM} 200 10/300 GL column as described above.

3.2.4. Antibody characterization

3.2.4.1. Determining affinity and pan-reactivity by Surface plasmon resonance (SPR)

The binding of all VHHs and VHs to immobilized strain QCD SLP High- and Low-MW subunits (QCD H/L complex), strain CD630 High- and Low-MW subunits (CD630 H/L complex), and strain QCD Low-MW subunit only (QCD Low) was determined by SPR using BIACORE 3000 biosensor system (GE Healthcare). The antigens were gel purified as described above prior to immobilization at a concentrations of 50 µg/mL in 10 mM acetate buffer on Sensorchip CM5 (GE Healthcare) using the amine coupling kit supplied by the manufacturer. All monomer sdAbs were passed through a Superdex^{TM} 75 column to eliminate any possible aggregates prior to BIACORE analysis. In all instances, analyses were carried out at 25°C in 10 mM HEPES buffer, pH 7.4 containing 150 mM NaCl, 3 mM EDTA and 0.005% surfactant P 20 at a flow rate of 20 µL/min. The surfaces were washed thoroughly with the running buffer for regeneration. Data were analyzed with BIAevaluation 4.1 software. The thermal refolding efficiency (TRE) of VH3 was determined as previously described (Arbabi-Ghahroudi et al., 2010). Briefly, 3 µM VH3 was heated to 80°C for 20 min and allowed to cool at 22°C for 30 min. The sample was then centrifuged and binding

was assayed to QCD SLP by SPR using several concentrations of the antibody. The steady state binding was plotted against concentration for the native and the heated-cooled antibody, and the slopes were used to determine the TRE.

3.2.4.2. Determining the epitope nature by Western blot

To determine which subunit the single-domain antibodies bound to, and the epitope conformation, SDS-PAGE of 5 μg of strain QCD SLPs was preformed to separate the subunits. They were then blotted onto PVDF membranes, blocked with 2% milk-PBS for 2 h, and treated with 5 mL of 10 μg/mL sdAb in 0.05% Tween 20-PBS for 1 h at room temperature. Three washes of 5 min each with 0.05% Tween 20-PBS were preformed followed by the addition of 1:10,000 dilution of mouse anti-His monoclonal IgG conjugated to alkaline phosphatase in 10 mL 0.05% Tween 20-PBS. The membranes were incubated at room temperature for 1 h, washed thrice for 5 min per wash with 10 mL 0.05% Tween 20-PBS, and developed with AP developing reagents (BIORAD, Mississauga, ON, Canada). Precision Plus^{TM} molecular weight standards (BIORAD) were used for each membrane. A 1:1,000 dilution of antiserum from the immunized llama in 10 mL 0.05% Tween 20-PBS was used as a positive control. A corresponding stained SDS-polyacrylamide gel of the SLPs was used for comparison.

3.2.4.3. Thermal unfolding analysis

The Thermal unfolding profile of each antibody was obtained using circular dichroism (CD) according to a previously described method (Hussack et al., 2011b) with minor modifications. Briefly, after dialysis into 10 mM sodium phosphate buffer pH 7.0, CD spectra from 180 - 260 nm of the antibody were obtained using a J-810 spectropolarimeter

(Jasco Inc. Easton, MD). The temperature was constantly increased from 30°C to 96°C and the molar ellipticity was taken at the wavelength corresponding to the maximal signal variation between spectra, at a scan speed of 50 nm/min, a 1 mm bandwidth and a temperature ramp of 1°C/min. Data was collected every 2°C with 1 accumulation. The molar ellipticity data was then blank-subtracted and a non-linear regression, using the Boltzman sigmoidal equation, was preformed. The T_m of each antibody was calculated as the inflection point of its non-linear regression curve. The non-linear regression curve was then normalized, and the T_{onset} value was extrapolated; the T_{onset} is defined as the temperature at which 5% of the protein is unfolded.

3.2.4.4. Pepsin resistance assay

To assess the resistance of each antibody to the most common protease encountered in the digestive tract, antiSLP antibodies were subjected to pepsin digestion as previously described (Hussack et al., 2011b). Briefly, a gradient of concentrations was used to determine the degree of resistance. All reactions were preformed in 20 µL final volume. Antibodies were diluted in PBS pH 7.4, and 1 µL of 1 M HCl was added to each reaction to bring the pH to ~1.5-2.0. Porcine stomach pepsin (Sigma) was diluted in 1 mM HCl, and 4.8 µg of antibody were digested with 2 µL of 100, 50, 25, 10, 2.5, and 1.25 µg/mL of pepsin. Controls received 2 µL 1 mM HCl instead. Reactions were incubated for 1 h at 37°C. All reactions were stopped by the addition of 1 µL 1 M NaOH followed by 10 µL of 3x non reducing SDS-PAGE sample buffer, and then boiled at 95°C for 5 min prior to loading 15 µL on an SDS-polyacrylamide gel. The gels were coomassie-stained, destained, photographed, and densitometric analysis using AlphaEaseFc™ software package (version 7.0.1; Alpha Innotech Corp., San Leandro, CA) was preformed. Antibodies which were resistant to pepsin

digestion retained a band corresponding to their respective molecular weight. The % Ab resistant was then calculated based on the signal intensity of that band relative to its undigested control.

3.2.4.5. *In vitro* motility assay

An *in vitro* motility assay was used to determine if the isolated sdAbs are able to bind whole *C. difficile* cells and prevent motility. Sterile culture tubes containing 5 mL 0.175% agar-BHI media supplemented with 0.5% w/v Bacto-yeast extract, 0.12% w/v NaCl, and 25 µg/mL or 50 µg/mL sdAb, were stabbed with a fresh culture of strain QCD as previously described (Twine et al., 2009) and incubated in anaerobic conditions at 37°C for 23 h. Photographs were taken at 17 h and 23 h post inoculation to monitor the effects of each antibody on motility of the strain relative to a control which did not receive antibody treatment. The experiment was done in duplicates and the degree of motility was qualitatively scored (on a scale of 0-3, where 0= no motility inhibition, and 3=complete motility inhibition), by three individuals, according to degree of motility inhibition relative to the control. The antibodies were stored for 10 months, and the assay was repeated at antibody concentration 50 µg/mL of sdAb, and scored as before; the values were averaged across the two experiments.

3.2.4.6. *C. difficile* cell ELISA

Formalin-killed whole cells from strain QCD were obtained from Susan Logan's lab, and 100 µL of cells (O.D.=0.2) were immobilized per well in microwell titer plates as follows: the cells were incubated at 55°C for 2 h, followed by further incubation overnight at 4°C. The following day, the plate was washed once to remove non-immobilized cells, and

wells were blocked with 2% milk-PBS for 30 min at 37°C. Hundred microliter of sdAb in 0.05% Tween 20-PBS (10 μg/mL, and 1 μg/mL, or approximately 625 nM and 62.5 nM) were added and incubated at 37°C for 1 h in a shaker incubator. The plate was washed three times with 0.05% Tween 20-PBS and a 100 μL of 1:5000 rabbit anti-6xHis conjugated to HRP in 0.05% Tween 20-PBS was added, and incubated at 37°C for 1 h in a shaker incubator. The plate was washed three times and developed with HRP substrate developer as before. Control wells in which no cells were immobilized received the same treatment as wells with immobilized cells. Blank control wells did not receive antibody treatment. The positive control well received a 1:500 dilution of llama anti-SLP serum, and was detected with anti-llama IgG conjugated to HRP.

3.3. Results

3.3.1. Size exclusion profiles of SLPs from strains QCD and CD630

SLPs from strains QCD and CD630 were purified by a Superdex^{TM} 200 gel filtration column post low pH glycine extraction (Figure 7). Fractions from the two major peaks and one minor peak were analyzed by 12% SDS-PAGE (Figure 7, inset image). The first peak eluted at an expected MW of 320 kDa, and SDS-PAGE analysis confirmed the presence of both subunits of SLPs in these fractions. The second small peak corresponds to the Low-MW subunit only. The Low-MW subunit could only be isolated from strain QCD. The last major peak was not detectable on SDS-PAGE despite the UV signal, which could represent breakdown products of the High-MW subunit, as it is unstable in the absence of the Low-MW subunit, and since High-MW subunit was not isolated in free-form from any of the fractions collected.

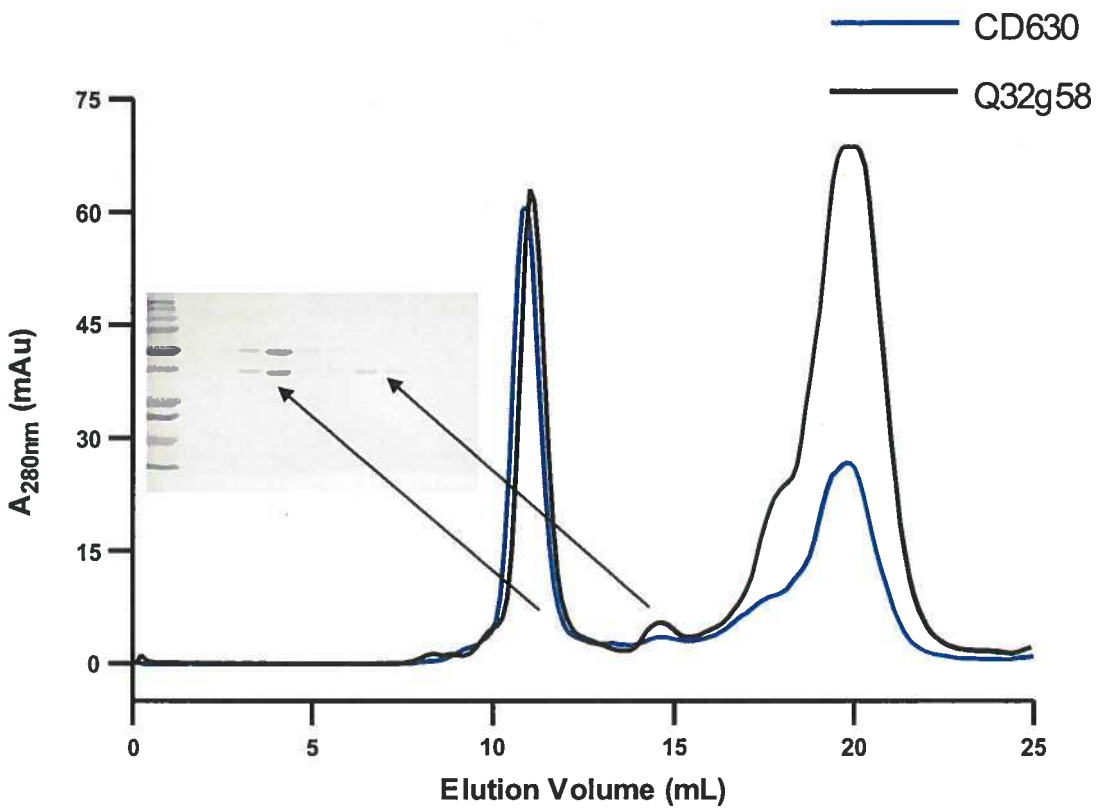
CD630
Q32g58
75
60
45
30
15
0
A_{280nm} (mAu)
0
5
10
15
20
25
Elution Volume (mL)

Figure 7: Size exclusion profiles of SLPs from *C. difficile* strains QCD and CD630. Approximately 500 µg (of each protein) were loaded on a Superdex^{TM} 200 chromatography column and eluted over 1 column volume (QCD – blue trace, CD630 – black trace). Proteins were eluted in 150 mM NaCl with 10 mM HEPES buffer pH 7.4 as the running buffer, at a flow rate of 0.4 mL/min. Fractions were analyzed on 12% SDS-PAGE; fractions from the first major peak were determined as the H/L SLP complex, while fractions from the small peak were identified as the Low-MW subunit alone.

3.3.2. Isolation of llama sdAbs to *C. difficile* SLPs

The naïve library was subjected to four rounds of selection using 100 µg of a crude low pH extracted SLP preparation from strain QCD. To identify QCD specific binders after three rounds of panning, a total of 40 plaques were picked at random (from a titer plate) for sequencing. Sequence analysis and predicted amino acid compositions revealed two distinct sequences of conventional (VH) origin as defined by residues Gly44, Leu45, and Trp47 (Figure 8). The two VH sdAbs isolated were termed antiSLP VH2 and antiSLP VH3, or VH2 and VH3 for short. VH3 was repeated in 38 out of the 39 sequenced clones while VH2 was a unique sequence. The CDR3 of VH2 is 10 amino acids long, while that of VH3 is 21 amino acids in length. Sequencing analysis of 40 clones from a fourth round of panning revealed that VH2 was eliminated from the phage pool. Both phages were isolated and propagated for further screening using 0.5 µg of QCD SLPs by monoclonal phage ELISA. Bound phages were detected with anti-M13 IgG conjugated to HRP. VH3-displaying monoclonal phage did not bind to QCD SLPs (Figure 9A); VH2-displaying phage did bind to the SLPs with an absorbance of 1.53. Despite the ELISA results, VH3 was not discarded as a potential SLP binder since it was the only sequence enriched in rounds three and four.

Clones isolated from this naïve library tend to have low affinities (µM) (Tanha et al., 2002), therefore, an immune library was constructed to isolate high affinity binders to SLPs, using both CD630 SLPs and QCD SLPs as immunogens. The immune library was subjected to four rounds of panning using 100 µg of gel purified QCD SLPs as antigen. To identify QCD specific binders after three rounds of panning as before, a total of 50 TG1 *E. coli* colonies containing the phagemid vector were picked from a titer plate at random for monoclonal phage ELISA (Figure 9B) and sequence analysis (Figure 8). Of the 40 returned

sequences and based on CDR sequence identity, we identified 10 unique amino acid sequences (Figure 8A) with varying frequency of occurrence (Table 1), which were confirmed to be VHHs, according to camelid VHH characteristics at positions 37, 44, 45, and 47 (Muyldermans et al., 1994; Vu et al., 1997). The VHHs are termed antiSLP VHH2, 5, 12, 22, 23, 26, 45, 46, 49, and 50 (Figure 8A, and Table 1). The 50 selected clones from round 3 were screened against 0.5 μg each of immobilized gel purified strain QCD and CD630 SLPs to identify cross-reactive antibodies to multiple strains (Figure 9B; one representative of each unique sequence is presented). In monoclonal phage ELISA, clones with an absorbance reading greater than 0.15 were considered positive for SLP binding. All 10 clones showed specific binding to strain QCD SLPs (Figure 9B, white bars). In contrast, only VHH2, and less strongly VHH26, showed binding to strain CD630 (Figure 9B, hatched bars). VH2 and VH3 were not assayed for binding to CD630 SLPs by phage ELISA. Controls not receiving phage treatment, or receiving non-specific phage were negative for binding to SLPs from both strains.

The library was subjected to a fourth round of panning and 40 colonies were picked at random for sequencing. Analysis of the predicted amino acid compositions of the 30 returned sequences revealed the presence of 7 distinct sequences, all of which were isolated in round three. VHH2 and VHH5 were the only clones whose sequences increased in frequency in round 4 based on sequence analysis (Table 1), while the frequency of the other clones decreased. VHHs 26, 45, and 50 were not selected in the fourth panning round.

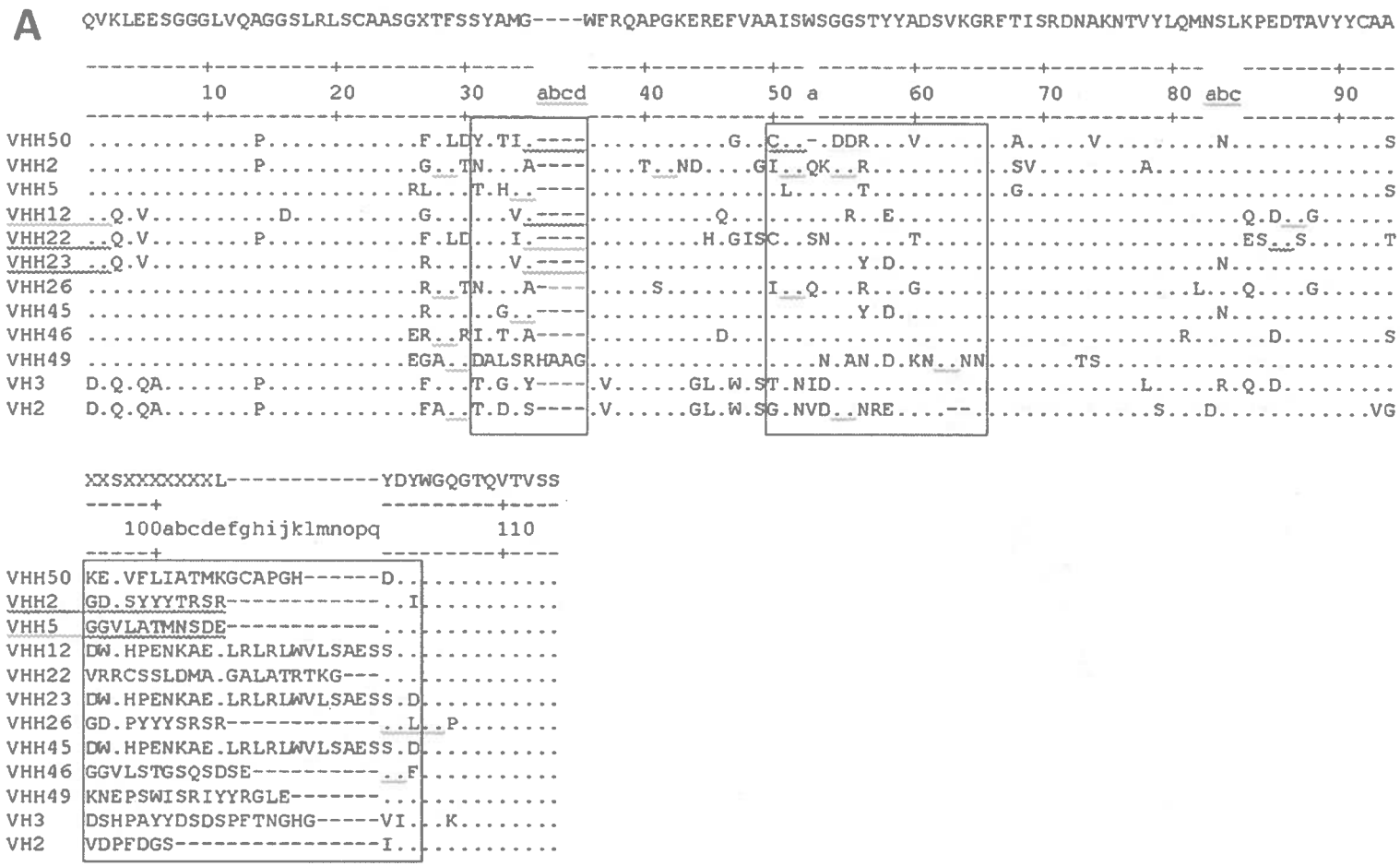
A
QVKLEESGGGLVQAGGSLRLSCAASGXTFSSYAMG----WFRQAPGKEREFVAAISWSGGSTYYADSVKGRFTISRDNAKNTVYLQMNSLKPEDTAVYYCAA
10
20
30
abcd
40
50 a
60
70
80 abc
90
VHH50 .....P.....F.LDY.TI.----.....G..C..-.DDR...V.....A.....V.....N.....S
VHH2 .....P.....G..TN...A----....T..ND....GI..QK..R.....SV.....A.....
VHH5 .....RL...T.H..----.....L.....T.....G.....S
VHH12 ..Q.V.....D.....G.....V.----.....Q.....R..E.....Q.D..G.....
VHH22 ..Q.V.....P.....F.LD...I.----.....H.GISC..SN.....T.....ES..S.....T
VHH23 ..Q.V.....R.....V.----.....Y.D.....N.....
VHH26 .....R..TN...A----.....S.....I..Q...R...G.....L...Q....G.....
VHH45 .....R.....G..----.....Y.D.....N.....
VHH46 .....ER..RI.T.A----.....D.....R.....D.....S
VHH49 .....EGA..DALSRHAAG.....N.AN.D.KN..NN.....TS.....
VH3 D.Q.QA.....P.....F...T.G.Y----.V.....GL.W.ST.NID.....L.....R.Q.D.....
VH2 D.Q.QA.....P.....FA..T.D.S----.V.....GL.W.SG.NVD..NRE....--.....S...D.....VG
XXSXXXXXXXL----------YDYWGQGTQVTVSS
100abcdefghijklmnopq
110
VHH50 KE.VFLIATMKGCAPGH------D.....
VHH2 GD.SYYYTRSR----------..I.....
VHH5 GGVLATMNSDE----------.....
VHH12 DW.HPENKAE.LRLRLWVLSAESS.....
VHH22 VRRCSSLDMA.GALATRTKG---.....
VHH23 DW.HPENKAE.LRLRLWVLSAESS.D.....
VHH26 GD.PYYYSRSR----------..L..P.....
VHH45 DW.HPENKAE.LRLRLWVLSAESS.D.....
VHH46 GGVLSTGSQSDSE----------..F.....
VHH49 KNEPSWISRIYYRGLE-------.....
VH3 DSHPAYYDSDSPFTNGHG-----VI..K.....
VH2 VDPFDGS----------I.....

B

Percent Identity

Divergence

	1	2	3	4	5	6	7	8	9	10	11	12		
1		69.8	73.4	64.7	71.2	68.3	70.5	69.8	71.2	66.2	64.7	61.9	**1**	VHH50
2	36.1		77.7	64.7	65.5	67.6	86.3	69.1	76.3	65.5	66.2	67.6	**2**	VHH2
3	29.8	30.8		69.8	67.6	72.7	79.1	74.8	84.9	71.2	68.3	69.8	**3**	VHH5
4	43.0	38.4	29.5		67.6	92.1	69.1	89.2	69.8	64.0	64.0	59.0	**4**	VHH12
5	35.2	41.1	37.1	41.3		69.1	66.2	66.9	66.9	61.2	65.5	62.6	**5**	VHH22
6	36.5	33.2	24.9	8.6	38.8		70.5	97.1	71.2	66.2	64.0	61.2	**6**	VHH23
7	34.8	17.3	28.4	30.8	39.8	28.4		71.9	79.9	68.3	66.9	66.2	**7**	VHH26
8	34.0	30.8	21.6	12.1	42.6	3.0	26.0		73.4	67.6	64.7	61.2	**8**	VHH45
9	35.4	30.8	17.3	31.3	40.3	29.0	24.9	25.5		70.5	65.5	65.5	**9**	VHH46
10	42.1	41.1	30.8	39.0	48.6	35.2	35.8	32.8	33.8		57.6	59.7	**10**	VHH49
11	50.1	42.5	38.4	46.2	47.6	46.2	41.1	44.8	45.8	59.5		71.9	**11**	VH3
12	46.0	43.9	39.5	43.9	41.0	39.5	47.0	39.5	45.5	47.0	26.4		**12**	VH2
	1	**2**	**3**	**4**	**5**	**6**	**7**	**8**	**9**	**10**	**11**	**12**		

C

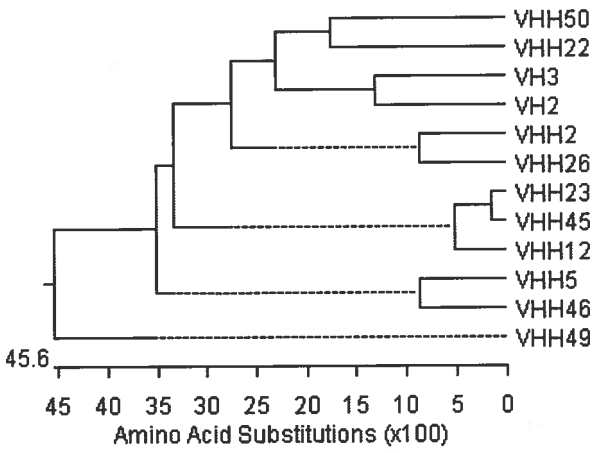

Figure 8: antiSLP sdAb sequences and relatedness. A) Sequence alignment of antiSLP sdAbs based on the Kabat numbering system (Kabat et al., 1992); boxes represent the CDR locations. B) Percent identity table of antiSLP sdAbs. C) Phylogenetic analysis of antiSLP sdAbs isolated from the naïve and immune llama phage display libraries, based on ClustalW alignment.

A

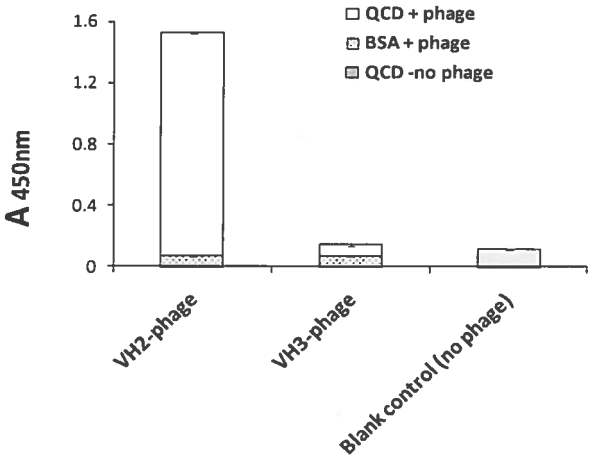
QCD + phage
BSA + phage
QCD -no phage
A 450nm
1.6
1.2
0.8
0.4
0
VH2-phage
VH3-phage
Blank control (no phage)

B

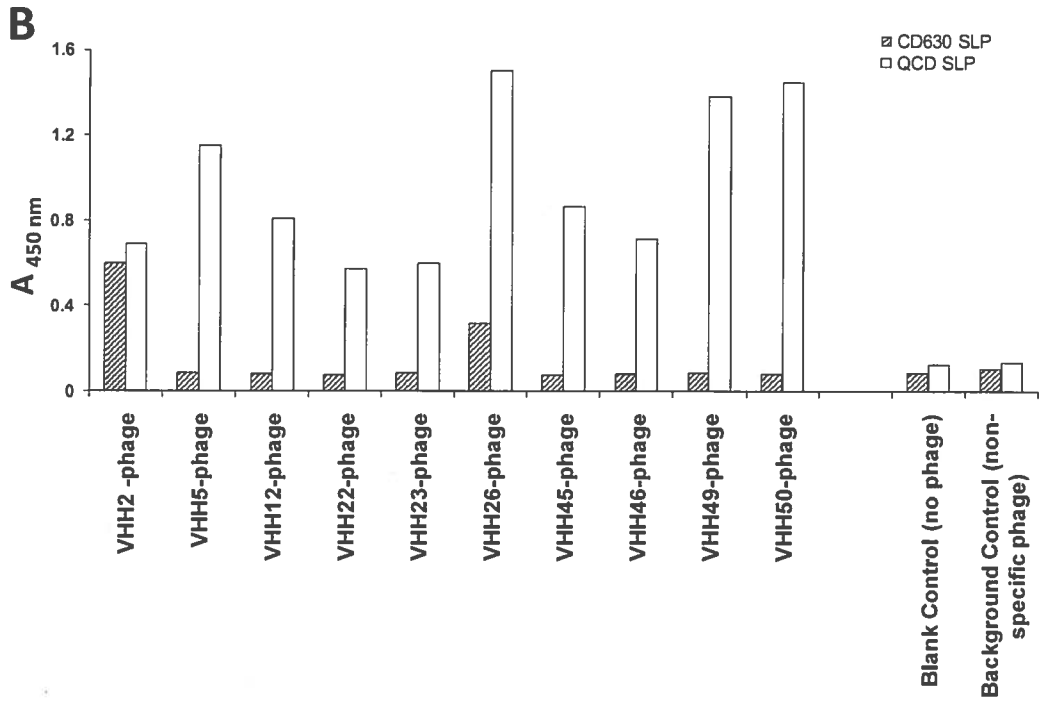
CD630 SLP
QCD SLP
A 450 nm
1.6
1.2
0.8
0.4
0
VHH2 -phage
VHH5-phage
VHH12-phage
VHH22-phage
VHH23-phage
VHH26-phage
VHH45-phage
VHH46-phage
VHH49-phage
VHH50-phage
Blank Control (no phage)
Background Control (non-specific phage)

Figure 9: Monoclonal phage ELISA of clones selected from the naïve and immune phage display library to SLPs. A) Phage ELISA of clones selected from the naïve llama phage display library. The phage supernatant was directly applied to immobilized strain QCD SLPs followed by detection with anti-M13-phage, HRP conjugated IgG. Negative control: BSA; Blank control: no phage. B) Phage ELISA of clones selected from the immune llama phage display library. Positive clones were grouped based on sequence identity of the CDRs to yield the 10 unique clones represented. All clones were screened for binding to SLPs from strains QCD and CD630 by directly applying phage-supernatants from overnight cultures to immobilized antigen, followed by detection with anti-M13-phage, HRP conjugated IgG. Blank control: no phage; Background control: M13 phage without sdAb fusion.

Table 1: AntiSLP single domain antibodies (VH/VHHs) isolated from the naïve and immune phage-display libraries. The pI of each sdAb was determined using the ExPASy online proteoparameter tool (Swiss Institute of Bioinformatics), excluding their c-Myc and 6xHis affinity tags. The sdAb were isolated from non-immune and immune phage display libraries using strain QCD SLPs as the antigen. Their frequency of selection during panning is indicated. QCD and CD630 are two different strains of *C. difficile;* QCD is recognized as a 'superbug'.

antiSLP	Molecular Weight (kDa)	Isoelectric Point	Relative Frequency (%)	
			Round 3	Round 4
VHH2	15.71	8.91	10	30
VHH5	15.61	6.77	27.5	43.3
VHH12	17.00	5.78	10	3.3
VHH22	16.38	6.75	5	3.3
VHH23	17.02	5.81	15	10
VHH26	15.72	8.93	5	0
VHH45	17.06	5.83	2.5	0
VHH46	15.83	5.33	2.5	3.3
VHH49	16.71	7.94	12.5	6.6
VHH50	16.25	5.79	7.5	0
VH3	14.69	4.37	97.4	100
VH2	16.32	6.05	2.6	0

Many of the clones shared high identity as revealed by the multiple sequence alignment of the unique SLP binders (Figure 8B and C). VHH22 and VHH50 contained additional cysteines which have the potential to form an interloop disulfide bond to constrict the relatively long CDR3, and enhance the stability of the antibodies. Interestingly, VHH50 was not selected during the fourth panning round. The presence of a cysteine at residue 50 is characteristic of VHH subfamilies 3 and 4 (Harmsen et al., 2000); these two VHHs were the only two to belong to the VHH subfamily 3 and grouped together in the phylogenetic sequence analysis. The remaining VHHs isolated in this study belonged to VHH subfamily 1.

The CDR3 length distribution among the 12 antibodies isolated varied. VHHs 2, 5, and 26 have the shortest CDR3 with 14 residues. VH3, a conventional VH, and VHH50 have a CDR3 with 21, and 20 residues respectively. VHH49 was distinct in that it has a 9 residue CDR1, and an asparagine-rich CDR2, likely to result in enhanced solubility. VHH12, VHH22, VHH23, and VHH45 all have a significantly long CDR3, with 23 residues for VHH22 and 26 residues for VHHs 12, 23, and 45. VHH23 and VHH45 were identical with the exception of 4 a.a., at positions 3 and 5 (FR1), and 33 and 34 (CDR1). VHH12 was the next most closely related antibody (92.1 and 89.2% to VHH23 and 45, respectively). VHH2 and VHH26 have an 86% sequence identity and almost all the substitutions (17/19) are either conserved or semi-conserved. Three of these substitutions are located in the CDR2, and 3 within the CDR3. In a similar manner, VHHs 5 and 46 grouped together in phylogenetic analysis. The molecular weights (MW) and isoelectric points (pI) of the sdAbs are summarized in Table 1; these SLP specific antibodies have acidic pIs resulting in a negative net charge at pH 7.4 (the pH at which they were selected at), and which is consistent with the observation that camelid VHHs tend to have acidic pIs (Arbabi-Ghahroudi et al., 2008), with the exception of VHHs 49, 2 and 26 which have basic pIs of 7.94, 8.91 and 8.93,

respectively. The pIs of the Low-MW and High-MW subunits of SLPs are 4.92 and 4.69, respectively.

3.3.3. Large scale expression and purification of antiSLP sdAbs and assessment of the aggregation state

The VH and VHH sequences were cloned into the pSJF2H vector for monomeric expression in *E. coli*, and were purified by IMAC. We observed high and variable expression yields of the clones (3-75 mg/L of bacterial culture). VH2 (not to be confused with VHH2) and VHH45 were poorly expressed despite multiple attempts; expression did not yield a sufficient quantity for full downstream characterization, and for that reason VH2 was discarded from the study, while VHH45 was only analyzed in terms of binding to SLPs. Normalized size exclusion profiles were obtained to study the aggregation state of each sdAb (Figure 10). The elution volumes observed for the major monomeric peaks correspond to the expected elution volumes of proteins with similar MWs (~15 kDa) (Ewert et al., 2002; Jespers et al., 2010). It was observed that VHH22 shows a slight degree of aggregation. Precipitate was also observed for VHH26 and VHH46 despite the presence of EDTA (a metal chelating agent that reduces protease activity and aggregation following IMAC purification), although it is important to note that both were stored at concentrations of > 3.0 mg/mL which has the potential to contribute to aggregate formation. Indeed when VHH26 was re-expressed and stored at 1.35 mg/mL, no precipitate was observed to date. This was not the case for VHH46 which repercipitated following dilution post size exclusion on a Superdex^{TM} 75 column. The elution volumes varied from 11.8 to 13.1 mL.

As VH3 was the first antibody isolated, it was cloned into pVT2 for homopentamerization (pVH3), in efforts to increase the avidity, since previous reports of a

pentamerized antibody showed a significant increase in it's apparent affinity (Zhang et al., 2004) when the antigen presentation provides for avidity, as is the case for SLPs on the cell surface of *C. difficile*. The expected MW of a single subunit of pVH3 is 27.07 kDa which results in a MW of 135.4 kDa upon pentamerization. The expression of pVH3 was comparable to its monomer. VH3 (Figure 10A) and pVH3 (Figure 10B) were 100% aggregate-free despite being of conventional origin, and eluted at 12.3 (Superdex^{TM} 75) and 13.9 mL (Superdex^{TM} 200), respectively. Interestingly, VH3 also has a slightly acidic pI (Table 1) which is consistent with the observation that non-aggregating VHs tend to have acidic pIs (Arbabi-Ghahroudi et al., 2008). Camelid VH/VHHs typically possess glutamic acid at position 6 (Vu et al., 1997), while our conventional VH3 contains an alanine at this position; therefore, a mutant VH3 (VH3-6E) was constructed to study the effects of an A6E residue substitution as this residue position was previously recognized to contribute to stability (Tanha et al., 2006). The mutation lowered the pI to 5.49. By size exclusion chromatography, VH3-6E is 100% aggregate-free, and elutes at 12.6 mL.

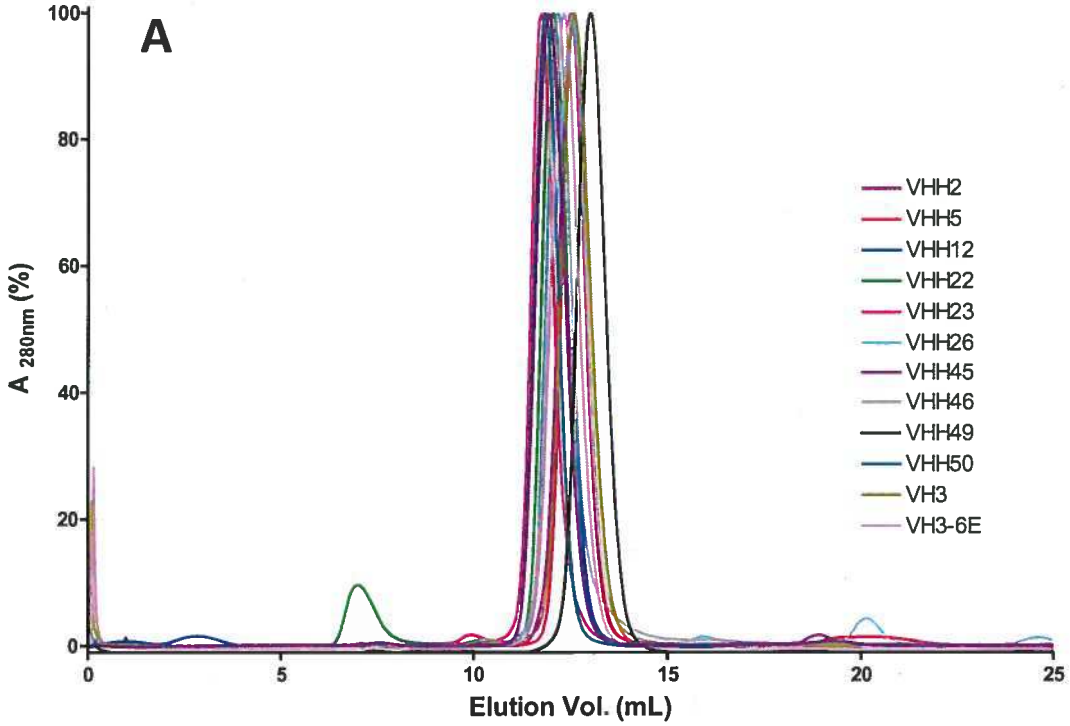
A
100
80
60
40
20
0
A 280nm (%)
0
5
10
15
20
25
Elution Vol. (mL)
VHH2
VHH5
VHH12
VHH22
VHH23
VHH26
VHH45
VHH46
VHH49
VHH50
VH3
VH3-6E

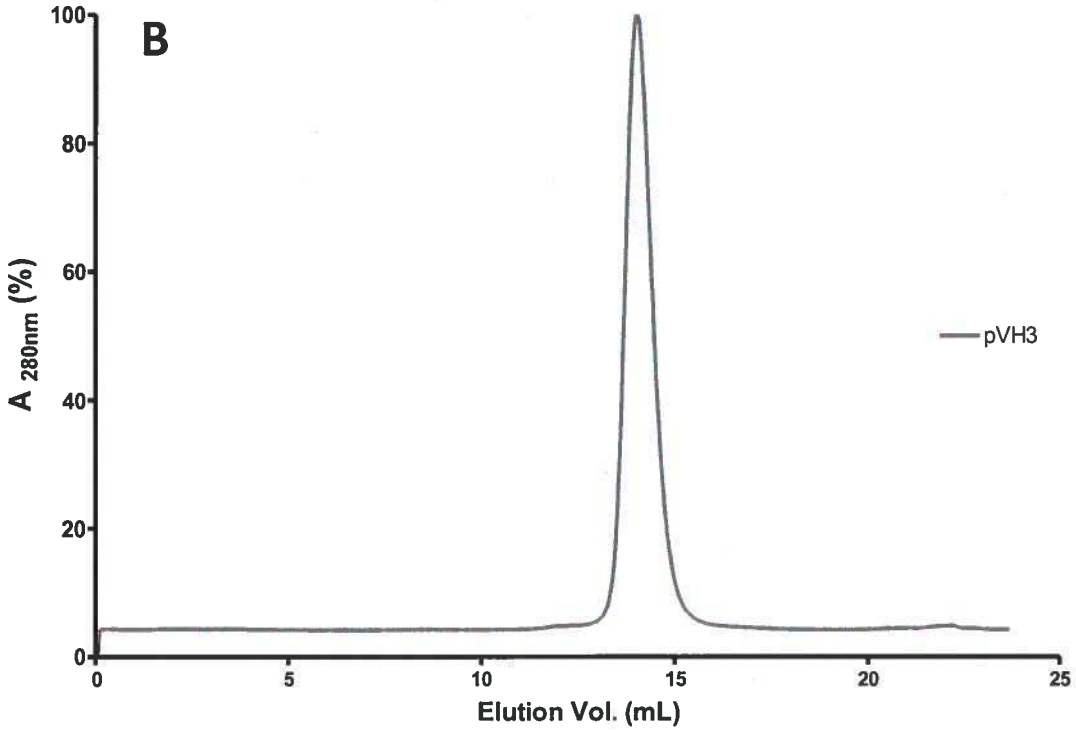
B
100
80
60
40
20
0
A 280nm (%)
0
5
10
15
20
25
Elution Vol. (mL)
pVH3

Figure 10: Size exclusion chromatography profiles of anti-SLP single domain antibodies. AntiSLP sdAbs were applied to a Superdex^{TM} 75 (A), or Superdex^{TM} 200 size exclusion column (B) for pVH3, to determine their aggregation state. VHH22 shows some degree of aggregation based on the small peak eluted at approximately 7.5 mL.

3.3.4. Binding anaylsis by surface plasmon resonance

The monomers were injected over sensorchip-bound QCD H/L complex SLPs, CD630 H/L complex SLPs, and QCD Low-MW SLP only, at various concentrations to characterize the binding to *C. difficile* SLPs by SPR.

3.3.4.1. Determining the affinity and specificity of the naïve VH3 to SLPs by SPR

VH3 clearly binds SLPs from both strains tested, and with higher affinity to CD630 (K_D= 600 nM) than to QCD SLPs (K_D= 900 nM) (Figure 11 A and B, and Table 2). No interactions were observed when VH3 was tested for binding to QCD Low-MW subunit (Figure 11C) strongly suggesting that the epitope is located on the High-MW subunit; CD630 Low-MW subunit could not be isolated in a quantity that lends itself to experimentation. In a parallel experiment, after heating and cooling of VH3 (3 μM), binding to QCD SLPs was assayed by SPR to determine the thermal refolding efficiency of the antibody. SPR analysis of refolded VH3 revealed that VH3 retained 96% of its binding capacity post denaturation and refolding (Figure 12) demonstrating that it exhibits reversible thermal unfolding. Upon the introduction of a mutation in the FR (A6E) of VH3 (termed VH3-6E), binding to SLPs was completely abolished (Figure 11, D-F), and the effects on the refolding efficiency imparted by this mutation could not be characterized by SPR, as was done for VH3. SPR analysis of pentamerized VH3 (pVH3) binding to QCD H/L and CD630 H/L SLPs revealed a 8-fold decrease in the dissociation rate constant of VH3 when in pentamer form (Figure 13 and Table 2; 1.6×10^{-2} *vs.* 2.0×10^{-3} 1/s, respectively), indicating that multiple antibody-antigen interactions occurred.

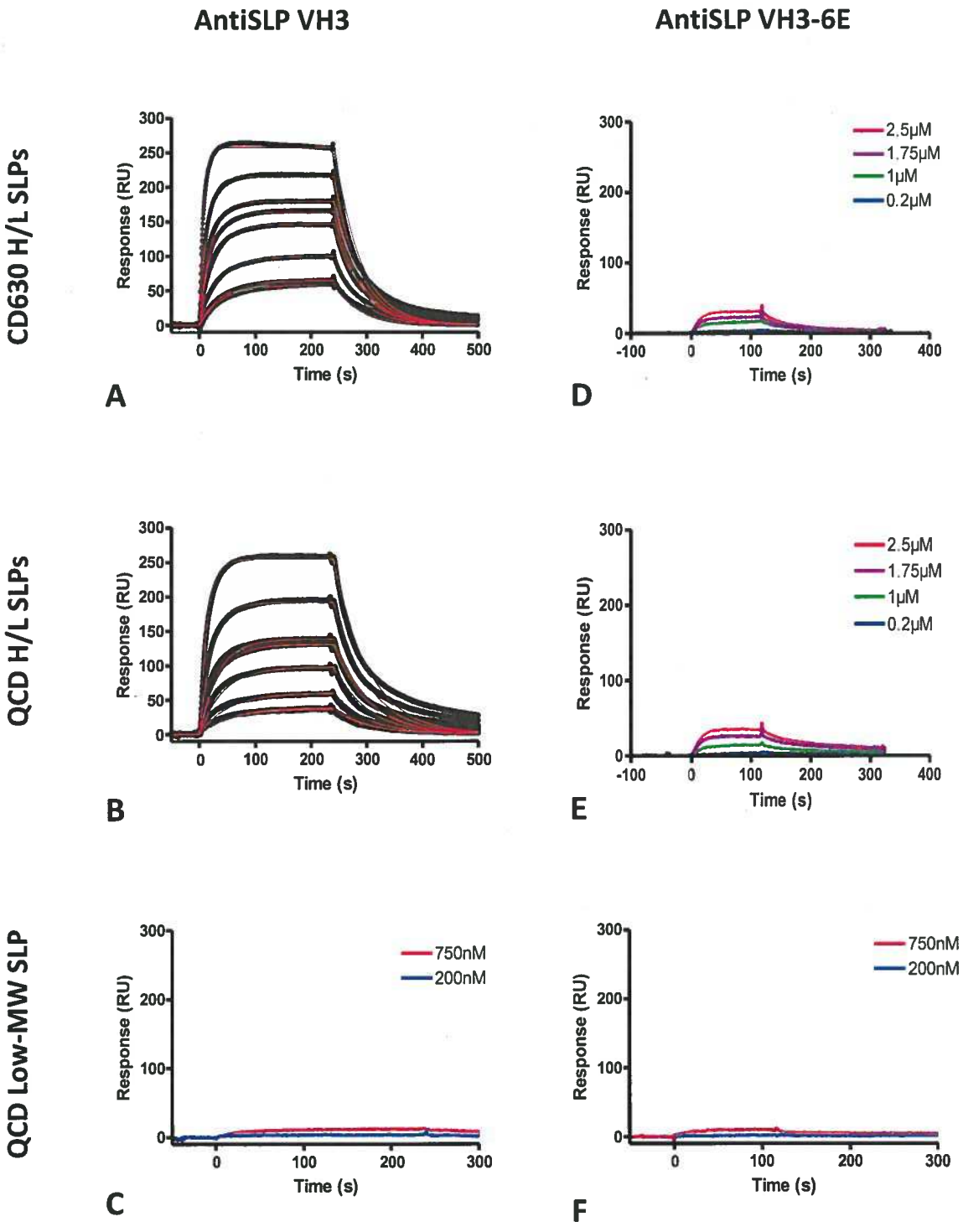
AntiSLP VH3
AntiSLP VH3-6E
CD630 H/L SLPs
QCD H/L SLPs
QCD Low-MW SLP
Response (RU)
Time (s)
2.5μM
1.75μM
1μM
0.2μM
750nM
200nM
A
B
C
D
E
F

Figure 11: Binding kinetics of antiSLP VH3 and VH3-6E to SLPs by SPR. Purified antigens (CD630 H/L complex SLPs, QCD H/L complex SLPs, or QCD Low-MW subunit only) were immobilized on sensorchip CM5 by amine-coupling, and antiSLPs were injected over the surface at various concentrations. The resonance caused by antibody-antigen interaction is detected and the association and dissociation rate constants were determined and used to calculate the binding affinity (K_D). Sensorgram overlays of the Ab-antigen interaction at Ab concentrations ranging from 200 nM – 3 μM are presented for antiSLP VH3 (panels A-C), and ranging from 200 nM - 2.5 μM for antiSLP VH3-6E (panels D-F). RU: resonance unit.

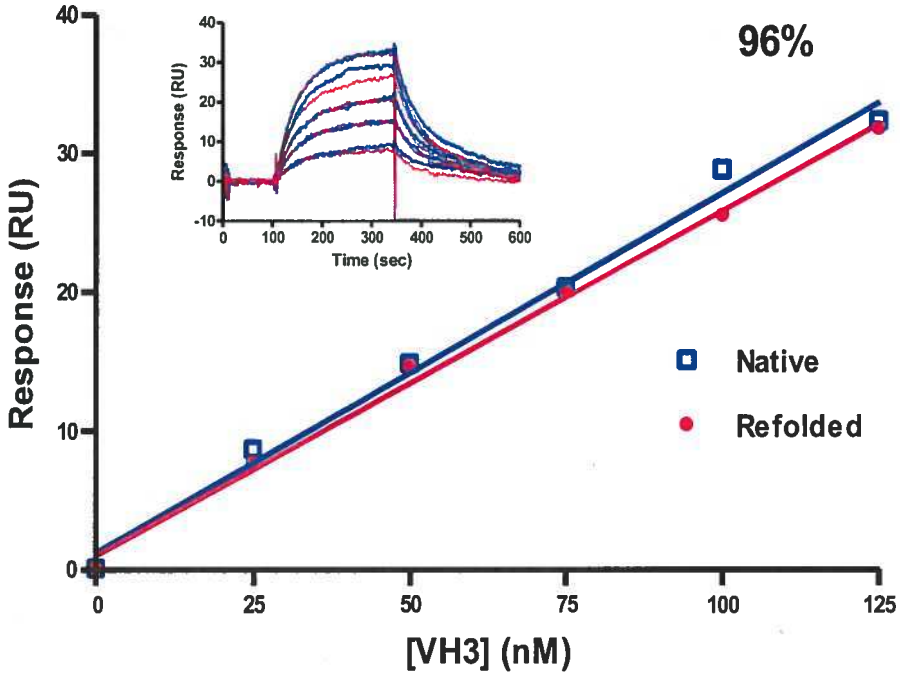
96%
Response (RU)
[VH3] (nM)
Native
Refolded
Response (RU)
Time (sec)

Figure 12: Thermal refolding efficiency of antiSLP VH3. AntiSLP3 (3 μM) was heated to 85°C for 20 min and allowed to cool at 22°C for 30 min and centrifuged even in the absence of aggregates. Binding of the native VH3 and "refolded" VH3 to QCD SLPs was assayed by SPR. Inset graph is an overlay of the sensorgrams obtained from the SPR experiment for the native *vs.* refolded antibody. RU: resonance unit.

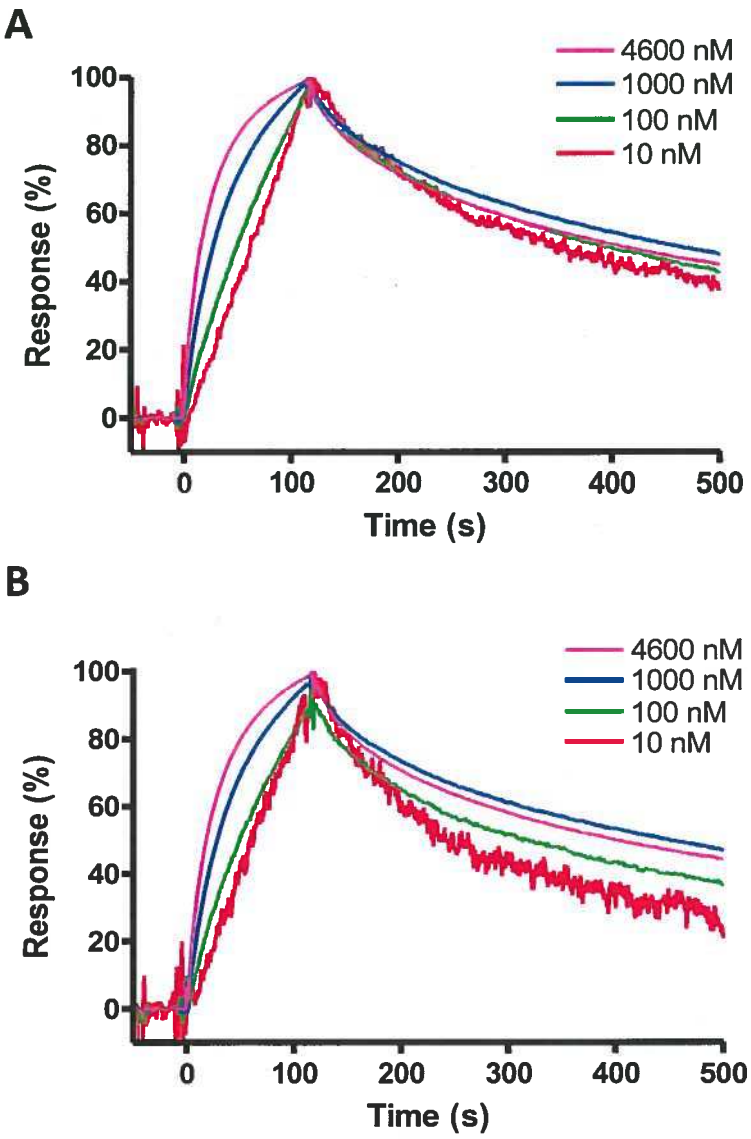
A
4600 nM
1000 nM
100 nM
10 nM
Response (%)
100
80
60
40
20
0
0
100
200
300
400
500
Time (s)
B
4600 nM
1000 nM
100 nM
10 nM
Response (%)
100
80
60
40
20
0
0
100
200
300
400
500
Time (s)

Figure 13: Binding of antiSLP VH3 pentamer (pVH3) to CD630 and QCD SLPs by SPR. Sensorgrams were obtained for binding of pVH3 CD630 (A) and QCD (B) at 10, 100, 1000, and 4200 nM antibody concentrations. The sensorgrams were normalized for comparison of the binding kinetics at the various concentrations.

Table 2: Binding kinetics of antiSLP VH3 and pVH3 to strains QCD and CD630 SLPs. QCD H/L SLPs and CD630 H/L SLPs were immobilized on a CM5 sensorchip and binding kinetics were obtained from a 1:1 binding model of antibody:antigen interactions at varrying antibody concentrations. The affinity constant (K_D), association (k_{on}) and dissociation (k_{off}) rate constants were determined by SPR analysis using BIACORE 3000. The resonance units (RU) returned during antibody-antigen interactions are tabulated as the R_{max}.

	Binding Kinetics to strain QCD H/L complex SLPs				Binding Kinetics to strain CD630 H/L complex SLPs			
antiSLP	**K_D (nM)**	**k_{on} (1/Ms)**	**k_{off} (1/s)**	**R_{max} (RU)[a]**	**K_D (nM)**	**k_{on} (1/Ms)**	**k_{off} (1/s)**	**R_{max} (RU)[b]**
VH3	900	2.0×10^{4}	1.6×10^{-2}	329	600	3.7×10^{4}	2.2×10^{-2}	273
pVH3	n/a	n/a	2.0×10^{-3}	n/a	n/a	n/a	2.0×10^{-3}	n/a--

a- Theoretical R_{max} is 437 RU
b- Theoretical R_{max} is 460.

3.3.4.2. Determining the affinity and specificity of the immune VHHs to SLPs by SPR

The monomers were injected over a CM5 sensorchip-bound QCD H/L complex SLPs at various concentrations to characterize the binding to *C. difficile* strain QCD by SPR. All 10 antiSLP VHHs were shown to be active by SPR analyses (Figures 14-16, and Table 3). VHH45 was included in this experiment to determine the effects of the four residue substitutions within the FR1 and CDR1 relative to VHH23 (97% identity). None of the VHHs bound to the reference surface on which a similar amount of a control antigen was immobilized (data not shown). Using kinetic analysis, VHHs 5, 12, 23, and 46 (Figure 14) were shown to have the highest affinities (K_Ds of 3-6 nM) to strain QCD SLPs, and the slowest k_{off} ($3.4 - 4.6 \times 10^{-4}$ s^{-1}). VHHs 12 and 23 required the use of low pH glycine for their complete dissociation from the antigen, which resulted in some loss of surface activity. VHHs 2, 22, 45, 49, and 50 were analyzed using steady state analysis. The affinities of VHHs 45, 49, and 50 to strain QCD SLPs are in the medium nM range (54, 50, and 75 nM respectively) (Figure 15). VHHs 2, 22, and 26 had the lowest affinities to strain QCD SLPs of the 10 VHHs (K_Ds of 230, 177, and 584 nM, respectively) (Figure 16, A-F); such affinities are probably too low for therapeutic applications. Note that kinetic analysis was used to obtain the K_D for VHH26, which also exhibits the fastest k_{on} and k_{off} from our panel of antibodies. Moreover, these three antibodies showed complex binding to strain QCD SLPs in that at low antibody concentrations (below 100 nM) high affinity binding was observed, while at high antibody concentration (above 100 nM), lower affinity binding was observed (Figure 16, F-H). Affinities of low nM to pM are preferred for therapeutic applications. Our antibodies can be ranked as either having high affinity (VHHs 5, 12, 23, and 46; K_D less than 10 nM), medium affinity (VHHs 45, 49, and 50; K_D less than 100 nM but greater than 10

nM), or low affinity (VHHs 2, 22, and 26; K_D greater than 100 nM). These results demonstrate the specificity of these sdAbs to strain QCD SLPs.

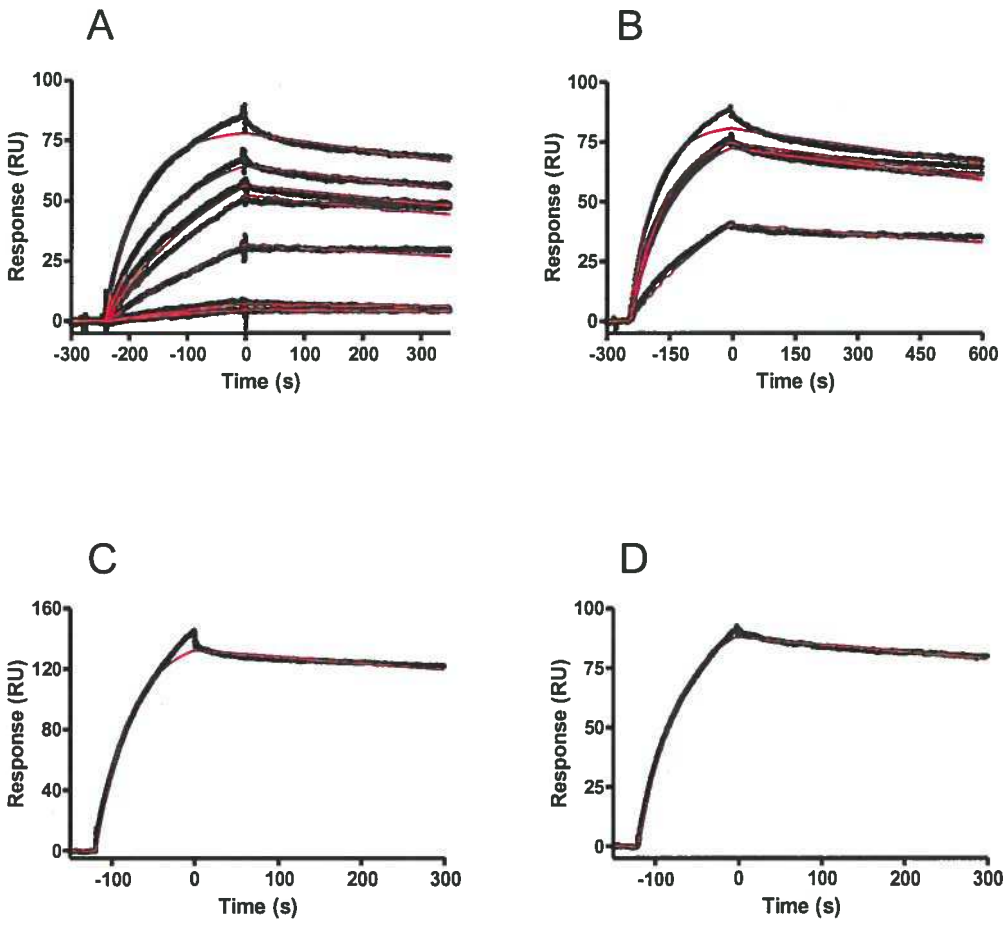
A
B
C
D
Response (RU)
Time (s)
100
75
50
25
0
-300
-200
-100
0
100
200
300
-150
150
450
600
160
120
80
40

Figure 14: SPR analysis of antiSLP VHHs 5, 46, 12 and 23 binding to strain QCD H/L complex SLPs. Several antibody concentrations of A) VHH5 (1-200 nM) or B) VHH46 (25-150 nM) were injected over a CM5 sensorchip with immobilized strain QCD SLPs. Only one concentration (200 nM) was used for VHHs 12 and 23 as they poorly dissociated from SLPs, resulting in decreased surface capacity. Sensorgrams were fitted to the 1:1 binding model (red lines). All 4 VHHs had affinities (K_Ds) in the low nM range (3-6 nM). The theoretical R_{max} for the sensorchip is 513 RU.

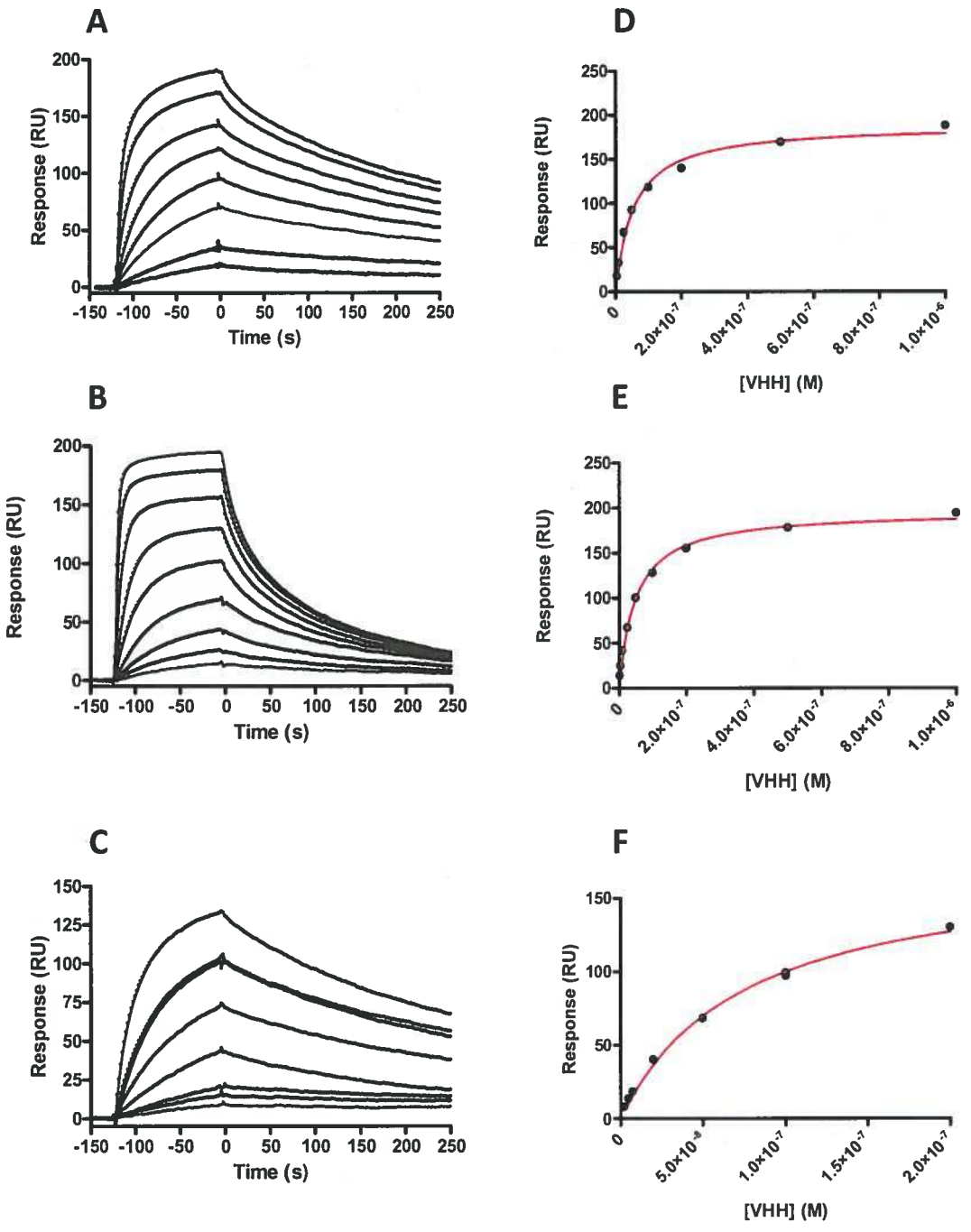
A
Response (RU)
Time (s)
B
Response (RU)
Time (s)
C
Response (RU)
Time (s)
D
Response (RU)
[VHH] (M)
E
Response (RU)
[VHH] (M)
F
Response (RU)
[VHH] (M)

Figure 15: SPR analysis of antiSLP VHHs 45, 49, and 50 binding to strain QCD H/L complex SLPs. Several antibody concentrations of A) VHH45 (5-2000 nM), or B) VHH49 (2.5-1000 nM), or C) VHH50 (2.5-500 nM) were injected over a CM5 sensorchip with immobilized strain QCD SLPs. Steady state analysis (D-F) results in K_Ds of 54 nM, 50 nM, and 75 nM for each antibody, respectively. The theoretical R_{max} for the sensorchip is 513 RU. RU: resonance unit.

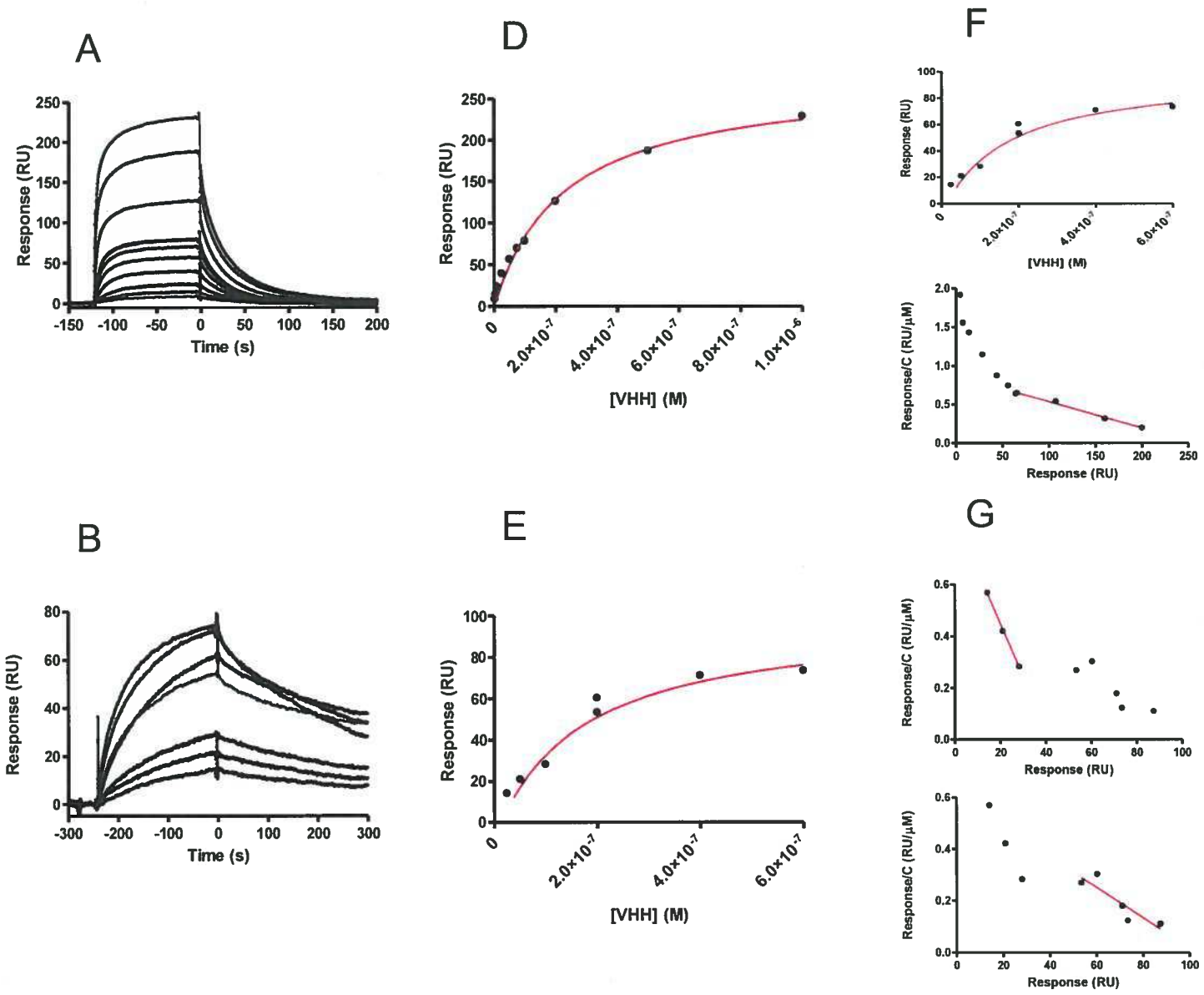
A
Response (RU)
Time (s)
B
Response (RU)
Time (s)
D
Response (RU)
[VHH] (M)
E
Response (RU)
[VHH] (M)
F
Response (RU)
[VHH] (M)
Response/C (RU/µM)
Response (RU)
G
Response/C (RU/µM)
Response (RU)
Response/C (RU/µM)
Response (RU)

C

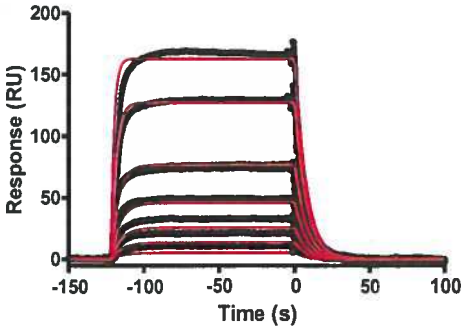
Response (RU)
200
150
100
50
0
-150
-100
-50
0
50
100
Time (s)

H

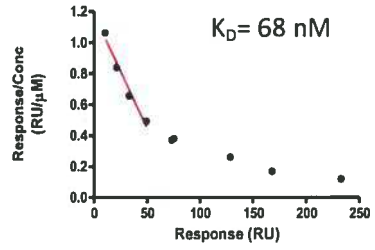
K_D= 68 nM
Response/Conc (RU/μM)
1.2
1.0
0.8
0.6
0.4
0.2
0.0
0
50
100
150
200
250
Response (RU)

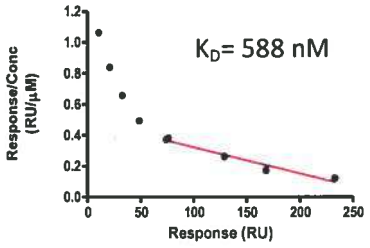
K_D= 588 nM
Response/Conc (RU/μM)
1.2
1.0
0.8
0.6
0.4
0.2
0.0
0
50
100
150
200
250
Response (RU)

Figure 16: SPR analysis of antiSLP VHHs 2, 22, and 26 binding to strain QCD H/L complex SLPs. Several antibody concentrations of A)VHH2 (2.5-1000 nM), or B) VHH22 (25-800 nM) or C) VHH26 (10-2000 nM) were injected over a CM5 sensorchip with immobilized strain QCD SLPs. Steady state analysis of VHH2 and VHH22 (D-E) results in K_Ds of 230 nM, and 180 nM, respectively. VHH26 was analyzed using the 1:1 binding model (K_D=390 nM).The scatchard plots (F-H) reveal that at low antibody concentrations (less than 100 nM; upper panels) high affinity binding is observed, and at high antibody concentrations (more than 100 nM; lower panels) low affinity binding was observed. The theoretical R_{max} for the sensorchip is 513 RU.

Table 3: Binding kinetics of antiSLP sdAbs to strain QCD H/L complex SLPs obtained from multiple antibody concentrations. QCD H/L SLPs were immobilized on a CM5 sensorchip for the characterization of antibody-antigen interactions. antiSLPs were injected at different concentrations, and the affinities (K_D), association (k_{on}), and dissociation (k_{off}) rate constants were determined by SPR analysis using BIACORE 3000. Kinetic analysis was used when interactions fit the 1:1 binding model. Alternatively, steady state analysis was used for antibodies which exhibit complex binding characteristics, in which case no k_{on} or k_{off} could be calculated. The resonance units (RU) returned during antibody-antigen interactions are tabulated as the R_{max}.

	Binding kinetics to QCD H/L complex SLPs			
	K_D (nM)	**k_{on} (1/Ms)**	**k_{off} (1/s)**	**R_{max} (RU)[a,b]**
VHH2	230	n/a	n/a	277
VHH5	5.6	8.2×10^{4}	4.6×10^{-4}	100
VHH12	3	1.2×10^{5}	3.4×10^{-4}	142
VHH22	180	n/a	n/a	100
VHH23	4	9.4×10^{4}	3.7×10^{-4}	98
VHH26	390	3.5×10^{5}	0.1	288
VHH45	54	n/a	n/a	189
VHH46	3	1.1×10^{5}	3.4×10^{-4}	n/a[c]
VHH49	47.8	n/a	n/a	197
VHH50	74.5	n/a	n/a	175

a- The theoretical R_{max} is 513RU
b- The R_{max} is dependent on the [VHH]
c- The local R_{max} was used after each injection

All 10 antiSLP VHHs were also tested for their ability to bind CD630 H/L complex SLPs in order to identify pan-reactive antibodies. Interactions with CD630 H/L complex SLPs were observed for VHH2, and VHH26 (Figure 17 and Table 4), consistent with phage ELISA observations (Figure 9B). The affinities of these VHHs to strain CD630 SLPs were lower than the affinities to strain QCD SLPs (Table 3 and Table 4); the affinities of VHH2 and VHH26 to CD630 are 1 and 2 μM, indicating a 4-fold and a 5-fold decrease in affinities compared to the higher affinity for QCD SLPs, respectively. Although binding to CD630 SLPs was observed for VHH23, it was only tested at 200 nM antibody concentration, and the respective R_{max} is significantly lower for CD630 when compared to QCD SLPs (23, and 98 RU), therefore no reliable conclusions can be made as to the cross-reactivity without further detailed studies. The association (k_{on}) and dissociation (k_{off}) rate constants, as well as the affinity constant (K_D) are summarized in Table 4. VHH26 had the fastest k_{on} and k_{off} for both SLP antigens.

A

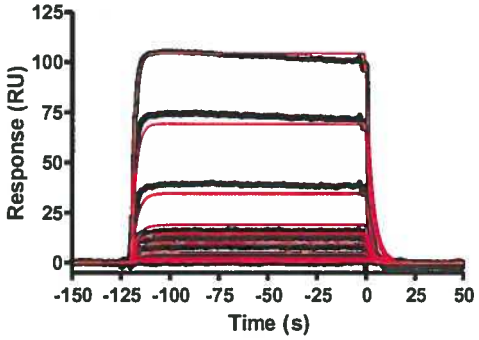
125
100
75
50
25
0
Response (RU)
-150 -125 -100 -75 -50 -25 0 25 50
Time (s)

B

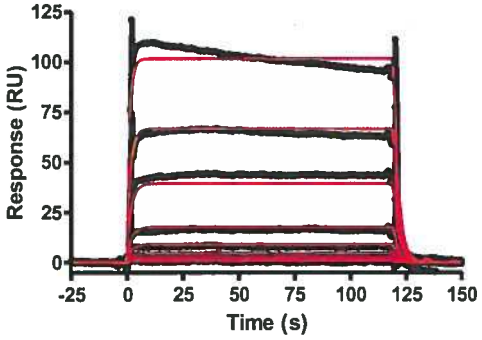
125
100
75
50
25
0
Response (RU)
-25 0 25 50 75 100 125 150
Time (s)

C

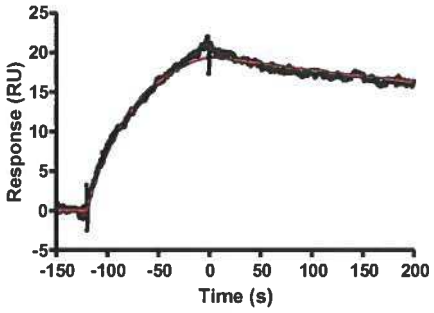
25
20
15
10
5
0
-5
Response (RU)
-150 -100 -50 0 50 100 150 200
Time (s)

Figure 17: Sensorgrams of antiSLP sdAbs binding to strain CD630 H/L complex SLPs. Strain CD630 H/L complex SLPs were immobilized on a CM5 sensorchip and antibodies were injected over the surface at different concentrations. The theoretical R_{max} for this sensorchip is 497 RU. A) Sensorgram overlays of VHH2 binding to strain CD630 SLPs at antibody concentrations of 2.5-1000 nM with a 1:1 kinetic analysis (black line). K_D=1 μM. B) Sensorgram overlays of VHH26 binding to CD630 at antibody concentrations of 10-1000 nM with a 1:1 kinetic analysis (black line). K_D=2 μM. C) Sensorgram of VHH23 binding to CD630 SLPs at 200 nM antibody concentration with a 1:1 kinetic analysis (black line). Only one concentration was injected due to the poor dissociation of the antibody. K_D=9 nM. RU: resonance units.

Table 4: Binding kinetics of antiSLP sdAbs to strain CD630 SLPs. CD630 H/L SLPs were immobilized on a CM5 sensorchip for the characterization of antibody-antigen interactions using the 1:1 binding model. antiSLPs were injected at different concentrations (with the exception of VHH23 which was injected at 200 nM only) and the association (k_{on}) and dissociation (k_{off}) rate constants were determined by SPR analysis using BIACORE 3000. The resonance units (RU) returned during antibody-antigen interactions are tabulated as the R_{max}.

	Binding Kinetics to CD630 H/L SLPs			
antiSLPs	**K_D (nM)**	**k_{on} (1/Ms)**	**k_{off} (1/s)**	**R_{max} (RU)[a]**
VHH2	1000	2.8×10^{5}	3.0×10^{-1}	216
VHH23[b]	9	8.6×10^{4}	8.8×10^{-4}	23
VHH26	2000	1.5×10^{5}	4.0×10^{-1}	223

a- The theoretical R_{max} is 497RU

b- Data collected using one antibody concentration (200 nM)

3.3.4.2.1. Determining the SLP epitope nature

In order to determine whether these Abs bind the high- or Low-MW subunit of the SLPs, antiSLP VHHs were also tested for binding against the QCD Low-MW subunit only by SPR. At 200 nM results revealed that all of our antiSLP VHHs bound the low MW subunit alone. VHHs 5, 12, 23, and 46 had lowest dissociation rate constants. Although VHH26 bound the QCD Low-MW subunit, the K_D (500 nM) may not be reliable as the returned R_{max} falls below the error range for such experiments; multiple antibody concentrations should be used to verify this value. At 200 nM antibody concentrations, the calculated antibody dissociation rate constants from strain QCD Low-MW subunit correlate well with the antibody dissociation rate constants from strain QCD H/L complex SLPs (Figure 18). The calculated K_Ds also correlate well for the two antigens at 200 nM antibody concentrations (Table 5), collectively indicating that the epitope lies on the Low-MW subunit of the protein. Interestingly, although the binding kinetics, as well as affinities, correlate well for the two antigens as indicated by a slope of 1.11, there are significant differences in the observed R_{max}s for each protein (discussed below).

Table 5: Binding kinetics of antiSLP sdAbs to strain QCD H/L complex and Low-MW SLP by SPR. QCD H/L SLPs and Low-MW SLP were immobilized on a CM5 sensorchip and binding kinetics were obtained from a 1:1 binding model of antibody:antigen interactions at 200 nM antibody concentrations. The affinity constant (K_D), association (k_{on}) and dissociation (k_{off}) rate constants were determined by SPR analysis using BIACORE 3000. The resonance units (RU) returned during antibody-antigen interactions are tabulated as the R_{max}.

	Binding kinetics to strain QCD H/L complex SLPs at 200 nM				Binding kinetics to strain QCD Low-MW SLP at 200 nM			
antiSLP	**K_D (nM)**	**k_{on} (1/Ms)**	**k_{off} (1/s)**	**R_{max} (RU)[a]**	**K_D (nM)**	**k_{on} (1/Ms)**	**k_{off} (1/s)**	**R_{max} (RU)[b]**
VHH2	71	4.3×10^5	3.1×10^{-2}	221	90	1.5×10^5	1.3×10^{-2}	26
VHH5	5	1.2×10^5	6.2×10^{-4}	336	3	1.4×10^5	4.1×10^{-4}	151
VHH12	3	1.1×10^5	3.4×10^{-4}	286	1	1.4×10^5	1.2×10^{-4}	131
VHH22	18	8.4×10^4	1.5×10^{-3}	97	10	1.3×10^5	1.1×10^{-3}	114
VHH23	4	9.4×10^4	3.7×10^{-4}	137	3	1.1×10^5	3.2×10^{-4}	72
VHH26	92	1.1×10^6	1.0×10^{-1}	205	500	--[d]	--[d]	5[c]
VHH45	19	1.8×10^5	3.4×10^{-3}	78	10	2.3×10^5	2.3×10^{-3}	171
VHH46	3	9.5×10^4	2.8×10^{-4}	93	2	1.5×10^5	3.2×10^{-4}	181
VHH49	51	4.3×10^5	2.2×10^{-2}	74	20	5.9×10^5	1.2×10^{-2}	231
VHH50	20	1.6×10^5	3.0×10^{-3}	66	10	1.9×10^5	2.7×10^{-3}	154

a- The theoretical R_{max} for the sensorchip is 513RU
b- The theoretical R_{max} for the sensorchip is 492RU
c- R_{max} falls below the acceptable lower response limit
d- response too low to calculate rate constants

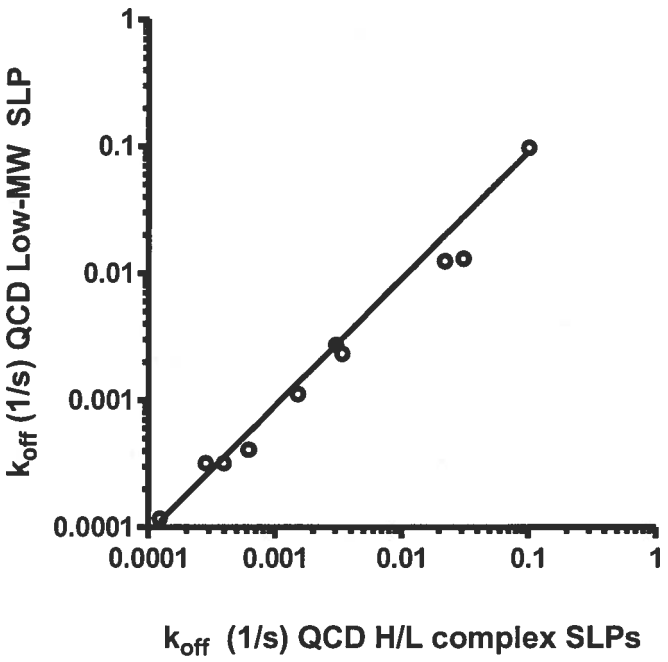
1
0.1
0.01
0.001
0.0001
koff (1/s) QCD Low-MW SLP
0.0001
0.001
0.01
0.1
1
koff (1/s) QCD H/L complex SLPs

Figure 18: Correlation of antiSLP VHHs binding to strain QCD H/L complex SLPs and QCD Low-MW subunit only. A linear regression of the dissociation rate constants of each antiSLP (at 200 nM) obtained from the 1:1 binding model to strain QCD H/L complex SLPs and QCD Low-MW SLP results in a slope of 1.11. R^2=0.966, p=0.0001.

To determine if the epitope is linear or conformational, a Western blot was performed where the antibodies were applied to SLPs that were separated in a 12% SDS-PAGE and transferred to a PVDF membrane, followed by detection with anti-5xHis IgG conjugated to alkaline phosphatase (AP) (Figure 19). SDS-PAGE was used to demonstrate the presence of both SLP subunits in the QCD SLP samples, and the blots are presented in order of decreasing affinity. A signal was observed for antibodies which recognize a linear epitope. VHHs 12, 23, 46, 5, 49, and less strongly VHHs 22 and 26 (consistent with their lower affinity), clearly bind the Low-MW subunit of the SLPs, providing support for the SPR results, and indicating that the epitope recognized by these antibodies is in a linear conformation.

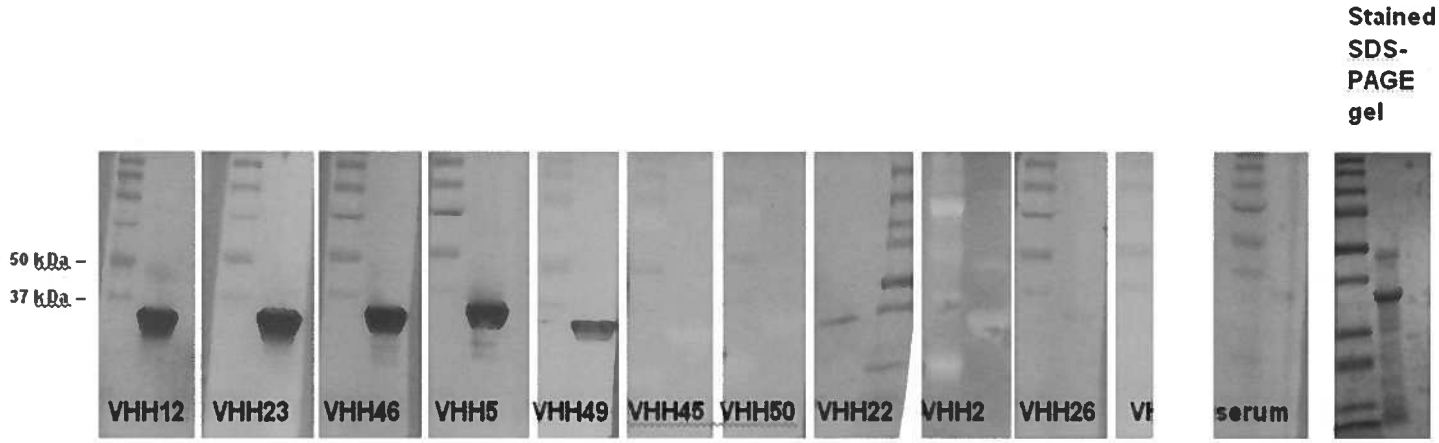
Stained SDS-PAGE gel
50 kDa –
37 kDa –
VHH12
VHH23
VHH46
VHH5
VHH49
VHH45
VHH50
VHH22
VHH2
VHH26
serum

Figure 19: Western blot analysis of antiSLP sdAbs to strain QCD SLPs. 5 μg of QCD SLPs were separated in a 12% SDS-polyacrylamide gel and proteins were transferred onto a PVDF membrane. antiSLP sdAbs were applied at 10 μg/mL (~625 nM) to determine the subunit specificity, and detected with anti-5xHis IgG conjugate to AP. The membrane was developed using AP substrate developer. A 1:1000 llama anti-serum was used as a positive control. An SDS-PAGE gel demonstrates the presence of both subunits. The blots are arranged in order of decreasing K_Ds.

3.3.5. Binding of antiSLPs to whole *C. difficile* cells

The antibodies were also tested for their ability to bind whole *C. difficile* cells *in vitro* by means of whole cell ELISA (figure 20). Formalin-killed *C. difficile* cells were immobilized in microtiter plates, and antibodies were added at 10 μg/mL (~625 nM) and 1 μg/mL (~62.5 nM) concentrations. All our antiSLP sdAbs bound whole *C. difficile* cells with the exception of VHH2. VHH50 only weakly bound cells by whole cell ELISA. When the antibody concentration was decreased 10-fold, the signal intensity observed from binding to whole cells decreased for VH3. The signal for VHH2 was lost at 1 μg/mL. For the remaining antibodies, the signal intensity remained relatively the same, indicating that in this assay, surface saturation was reached at or below antibody concentrations of 1 μg/mL.

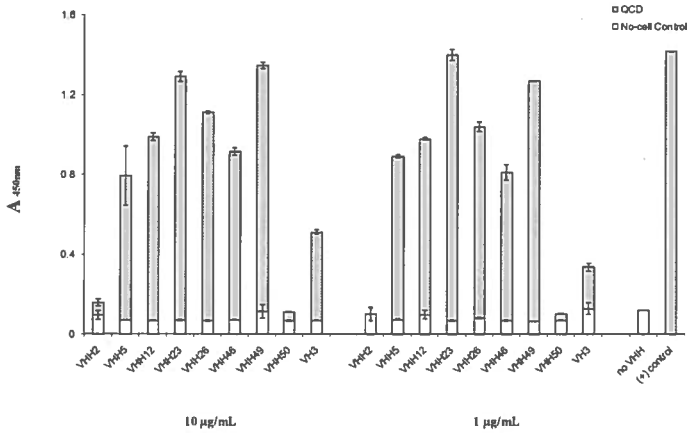
QCD
No-cell Control
1.6
1.2
0.8
0.4
0
A 450nm
VHH2
VHH5
VHH12
VHH23
VHH26
VHH46
VHH49
VHH50
VH3
10 µg/mL
1 µg/mL
no VHH
(+) control

Figure 20: AntiSLP sdAbs bind *C. difficile* whole cells. Formaline killed strain QCD whole cells were immobilized on 96well plates, wells were blocked with 2% milk-PBS, and antiSLP sdAbs were applied at 10 μg/mL (~625 nM), and 1 μg/mL (~62.5 nM) per well, and detected with anti-5xHis conjugated to HRP. The experiment is a representative of two independent experiments, with duplicates within each experiment (n=2); error bars represent the standard error within the experiment. Blank wells were blocked with 2% milk-PBS and received the same treatment as wells with immobilized strain QCD cells (no-cell control). Two wells with immobilized strain QCD cells and not receiving antibody treatment serve as a no-VHH control. (+) control is a 1:500 dilution of llama antiserum to SLPs, followed by detection with anti-llama antibody conjugated to HRP.

3.3.6. The ability of antiSLP antibodies to inhibit *C. difficile* motility

Although the antibodies were not selected using a motility antigen, we sought to determine if antiSLPs could interfere with the motility of strain QCD using a motility inhibition assay. Culture tubes containing 0.175% BHI-agar supplemented with either 25 µg/mL or 50 µg/mL antiSLP antibody were inoculated with *C. difficile* and cultured for 23 h. Growth was monitored at 17 h and 23 h post inoculation (Figure 21,A and B; upper panel). Results demonstrate that at 23 h post inoculation, and 25 µg/mL antibody concentrations, VHH5, and VHH46 completely inhibit motility of *C. difficile*. VHH45 and VHH50 show slight inhibition of motility at 25 µg/mL. The remaining sdAbs do not inhibit motility at concentrations of 25 µg/mL.

To test whether motility inhibition is concentration dependent we doubled the antibody concentration to 50 µg/mL (Figure 21A and B; lower panel). Results indicate that at antibody concentrations of 50 µg/mL, VHH5 and VHH46 clearly inhibit *C. difficile* motility. VHH45 also inhibits *C. difficile* motility, whereas VHH23 only slightly inhibits motility at this concentration, despite having 97% identity; however, motility inhibition was only assayed once for VHH45 (with duplicates within the experiment) due to limited antibody availability, and data should be interpreted with caution. Interestingly, the affinity of VHH45 to QCD SLPs is 14-fold lower than the affinity of VHH23 to the same antigen. Increasing the concentration of VHH50 resulted in complete inhibition of *C. difficile* motility, wherein only slight inhibition was observed at 25 µg/mL. Results of two independent experiments are summarized in Table 6. The growth could not be scored at 17 h due to insufficient cell growth of the control. Antibodies with motility inhibition values above 2 were considered effective at inhibiting motility. Although VHH45, was not included in our whole cell ELISA,

it's ability to inhibit motility indicates that it binds SLPs when they are present on the cell surface.

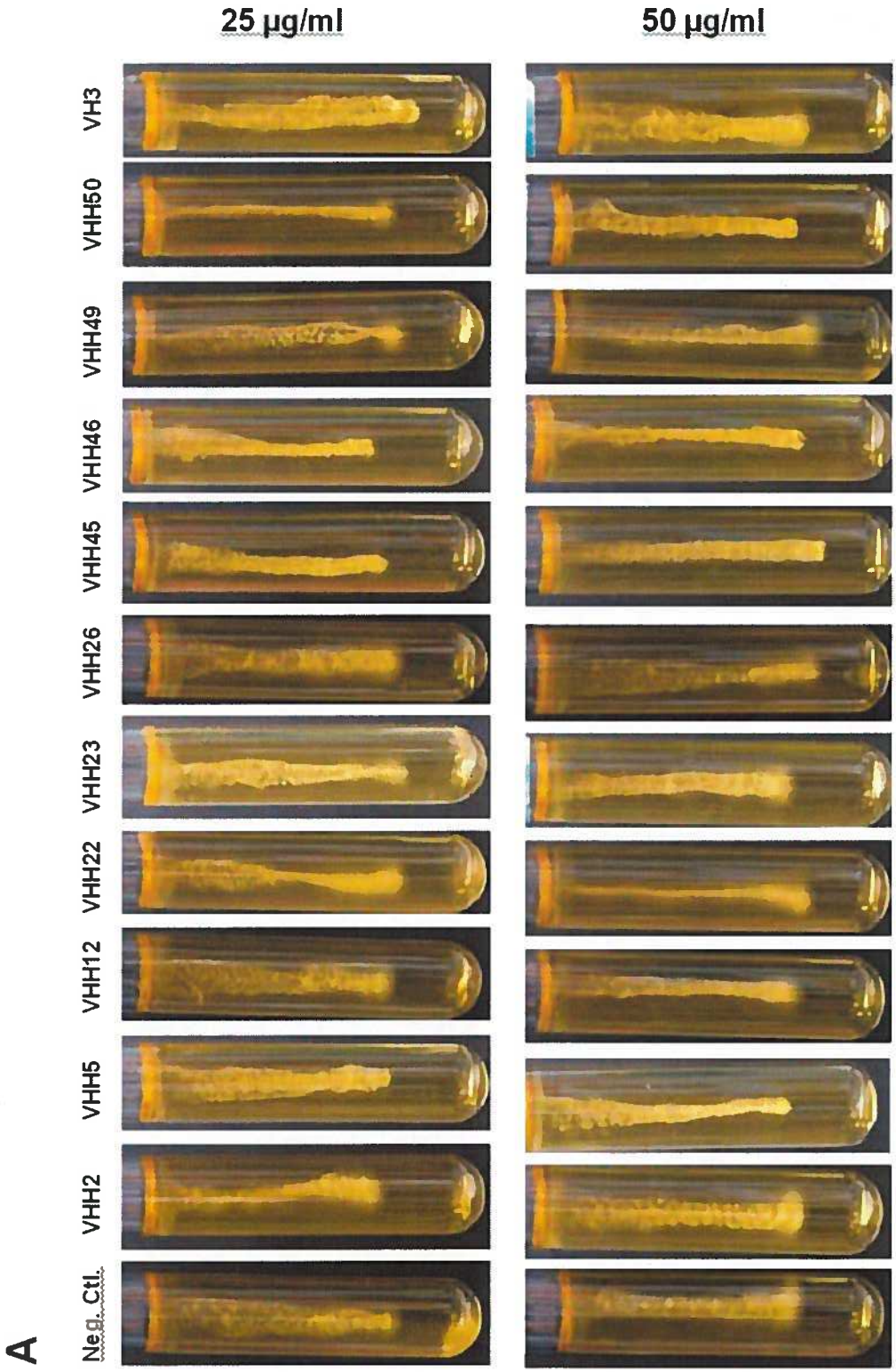
A
25 µg/ml
50 µg/ml
Neg. Ctl.
VHH2
VHH5
VHH12
VHH22
VHH23
VHH26
VHH45
VHH46
VHH49
VHH50
VH3


B
25µg/ml
50µg/ml
VH3
VHH50
VHH49
VHH46
VHH45
VHH26
VHH23
VHH22
VHH12
VHH5
VHH2
Neg. Ctl.

Figure 21: *C. difficile* motility in the presence of anti-SLP single domain antibodies. *C. difficile* strain QCD was inoculated in 0.175% agar-BHI with or without the presence of anti-SLP sdAbs, and incubated overnight under anaerobic conditions. Images were taken at A) 17, and B) 23 h post-inoculation. Two concentrations of antibody (25 µg/mL and 50 µg/mL) were used to assay *C. difficile* motility. VHHs 5, 45, 46, and 50 inhibit *C. difficile* motility. Images represent one set of tubes, from one independent experiment.

Table 6: *C. difficile* motility in the presence of anti-SLP single domain antibodies. *C. difficile* QCD was inoculated in 0.175% agar-BHI with or without the presence of antiSLP antibody at two different concentrations (25 µg/mL and 50 µg/mL), and incubated for 23 h, at 37°C and anaerobic conditions. The tubes were scored based on the degree of bacterial diffusion from the original stab point, relative to the control. Antibodies with a score >2 were considered successful at inhibiting *C. difficile* motility.

	25 µg/mL[a]	50 µg/mL[b]		
	Trial 1	Trial 1[c]	Trial 2[c,e]	Average[d]
Control[g]	0	0	0	0
VHH2	0	0	0.3	0.15
VHH5	3	3	2.3	2.65
VHH12	0	1.5	2.3	1.9
VHH22	0	0.5	0.3	0.4
VHH23	0	1.5	1.3	1.4
VHH26	0	0.5	0.3	0.4
VHH45[f]	2.5	3	n/a	3
VHH46	3	3	2.3	2.65
VHH49	0	0.5	1.3	0.9
VHH50	1	3	3	3
VH3	0	1	0.3	0.65

a- One independent experiment, with two replicates per antibody; scored by 1 individual.
b- Two independent experiments, with two replicates per antibody within each experiment.
c- The experiment was scored by three individuals and the average was taken.
d- The average of c (n=2).
e- Same antibody preparation as was used in trial 1 but after 10 month storage in PBS pH 7.4, 4°C .
f- Only assayed once due to insufficient antibody yield.
g- Control tube without sdAb.

3.3.7. Melting temperature (T_m) analysis of antiSLP sdAbs

The melting temperature is often indicative of the stability of the antibody molecule under non-ideal conditions. The T_m was determined for all antiSLP sdAbs using the circular dichroism spectra which were obtained as temperature was linearly increased at 1°C/min from 30-96°C (Figure 22 and Table 7). Antibody unfolding appears as a single phase as previously described in (Jespers et al., 2004). The melting temperature of VHH23 was the highest at 75.36°C, followed closely by VHH22 (74.62°C), and VHH12 (73.68°C). The lowest T_m determined was that of VHH2 (62.31°C) also followed closely by VH3 (65.53°C). There appears to be a slight increase in T_m of VH3-6E (66.2°C) relative to VH3. The T_{onset} of each antibody was also determined as the temperature at which 5% of the antibody in solution is unfolded (Table 7). This value also gives an indication of the antibody stability, as a molecule which begins to unfold at a lower temperature (low T_{onset}) is less stable than a molecule which begins to unfold at a relatively higher temperature (high T_{onset}), despite having the same T_m, especially if it unfolds at 37°C. There was also a slight increase of the T_{onset} of VH3-6E compared to VH3 (+0.7°C). VHH12, 22, and 23 all had high T_{onset}. The maximal signal difference from the zero occurred at 205 nm for VHHs 12, 23, and 26. The maximal signal difference from the zero for the remaining antibodies occurred at 210 nm.

Table 7: Thermal unfolding characteristics of antiSLP VHs and VHHs. Following a linear temperature gradient from 30°C to 96°C, a non-linear regression analysis on the circular dichroism (CD) data was used to determine the T_m of each antibody. The T_{onset} was obtained from the normalized linear-regression curve, as the temperature at which 5% of the antibody is unfolded. The assay was performed in 100 mM NaPi buffer pH 7.0. The standard error, and R^2 values, from the non-linear regression, are tabulated for each antibody.

	Thermal unfolding characteristics			
antiSLP	T_m (°C)	SE (+/-°C)[a]	R^2	T_{onset} (°C)
VHH2	62.31	0.339	0.989	58.20
VHH5	70.32	0.125	0.998	58.60
VHH12	73.68	0.183	0.995	67.80
VHH22	74.62	0.133	0.998	68.25
VHH23	75.36	0.253	0.990	69.75
VHH26	71.87	0.457	0.990	63.20
VHH46	66.33	0.273	0.993	53.90
VHH49	64.78	0.214	0.994	58.65
VHH50	70.26	0.248	0.992	59.70
VH3	65.52	0.079	0.999	58.79
VH3-6E	66.21	0.17	0.996	59.50

a- The standard error was calculated based on the 95% confidence interval of the non-linear regression curve of each antibody

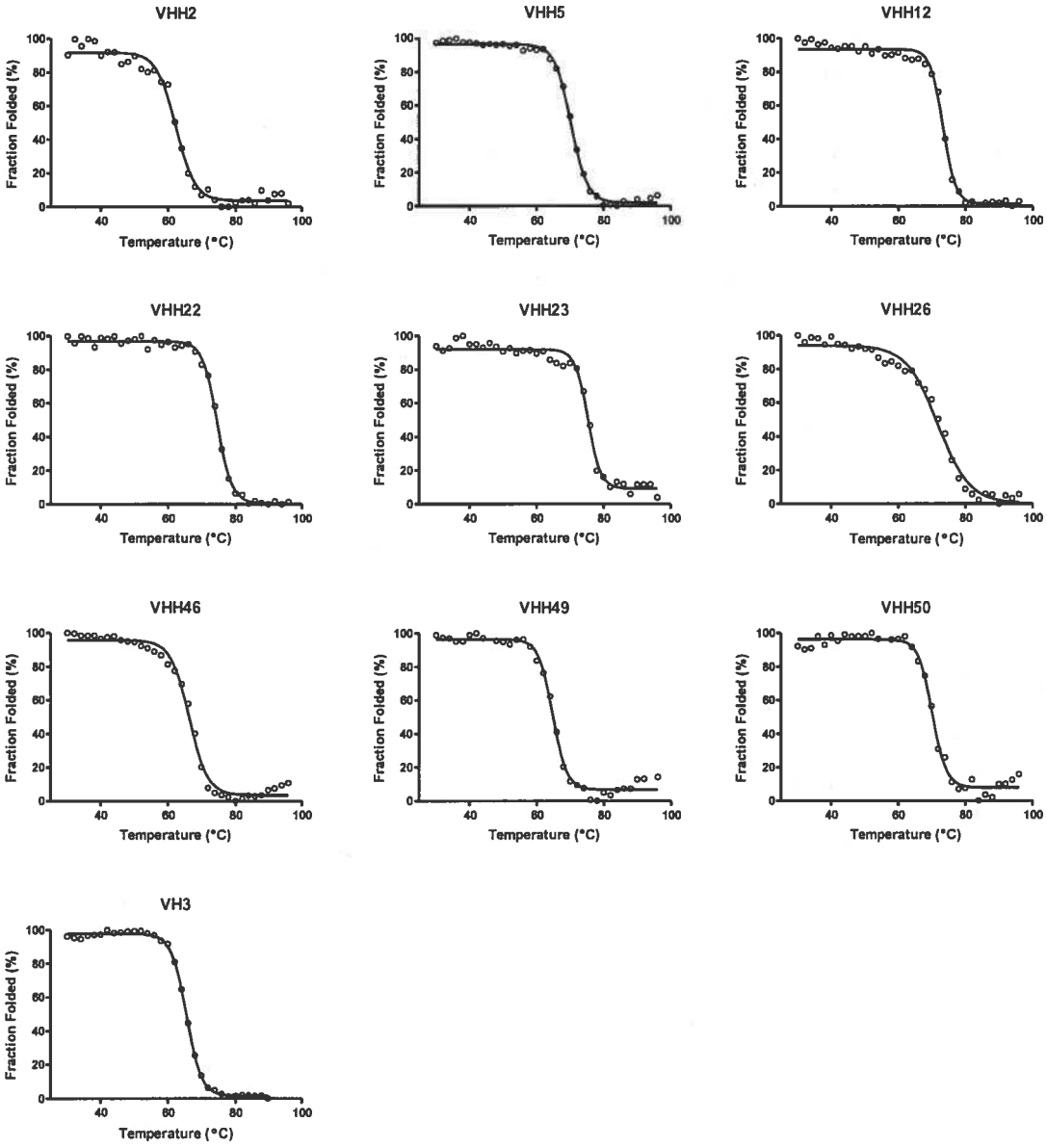
VHH2
VHH5
VHH12
VHH22
VHH23
VHH26
VHH46
VHH49
VHH50
VH3
Fraction Folded (%)
Temperature (°C)
0
20
40
60
80
100
40
60
80
100

Figure 22: Thermal unfolding curves of anti-SLP VH and VHHs. The melting curves were generated by collecting the CD spectra from 180-260 nm for each antibody, and following the wavelength corresponding to the maximal signal variation with respect to zero, as the temperature was increased from 30°C to 96°C. A non-linear regression was performed on the normalized CD values, in order to determine the melting point, T_m, for each antiSLP antibody. The assay was performed in 100 mM NaPi buffer pH 7.0

3.3.8. Pepsin resistance of antiSLP sdAbs

All VH/VHHs were subjected to pepsin digestion at decreasing concentration of enzyme, beginning with the concentration normally found in the digestive tract (100 µg/mL) (Figure 23 and Figure 24). VHH2 and VHH22 exhibited the highest degree of resistance with an average of 12% and 19.6% antibody remaining undigested respectively, after digestion for 1 h with 100 µg/mL of enzyme (Table 8). At the second highest enzyme concentration (50 µg/mL), 21.9% of VHH23 and 2.8% of VHH12 remain undigested after one h incubation with pepsin. Most of our antibodies were fully digested with 25 µg/mL of pepsin (Figure 24). Moreover, there appears to be a correlation between the T_m, and the T_{onset} obtained and the degree of pepsin resistance (Figure 25) however, VHHs 2 and 46 were excluded from the population (discussed below). It is important to note that the thermal unfolding of proteins is highly dependent on salt concentrations, and pH; all of our unfolding experiments were performed in 10 mM NaPi buffer, pH 7.0, while the pH of the pepsin digestion was approximately 1.5-2. Under digestion conditions, the antibodies exhibit loss of the C-terminal His-tag, consistent with previous findings (Hussack et al., 2011b), and therefore, lower bands corresponding to a MW that is ~2 kDa less than the band corresponding to the full antibody were considered as resistant to enzymatic digestion. VHHs 5 and 46, and VHHs 12 and 23, which share 84.9% and 92.1% sequence identity and similar binding properties (as indicated by SPR and our motility assay), also exhibit similar T_m and pepsin resistance characteristics. VH3-6E was excluded from this assay since we were primarily interested in characterizing sdAbs with binding activity. No obvious correlation was found between the number of pepsin digestion sites present in each antibody, and its relative resistance to pepsin digestion.

VHH2

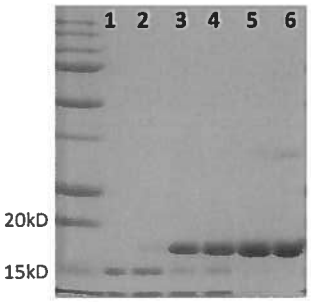

VHH5

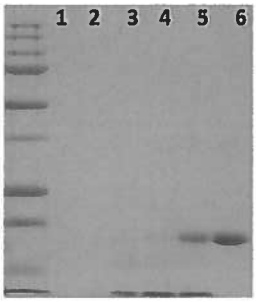

VHH12

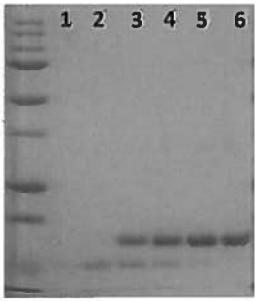

VHH22

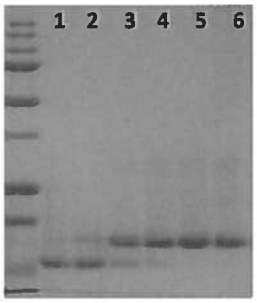

VHH23

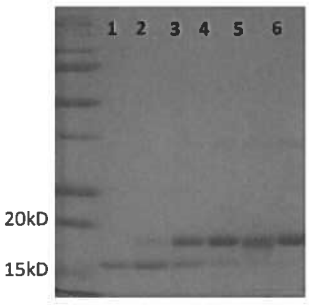

VHH26

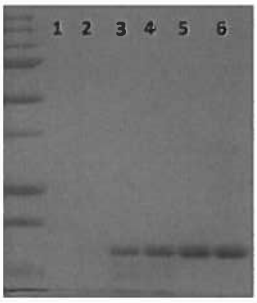

VHH46

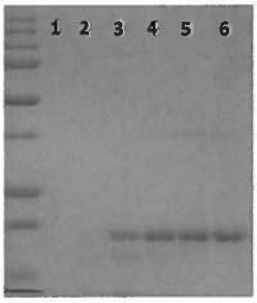

VHH49

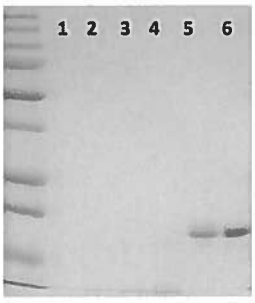

VHH50

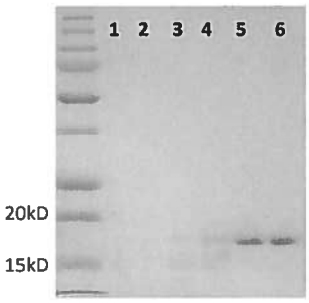

VH3

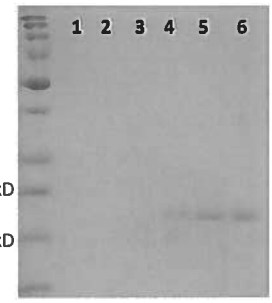

Figure 23: SDS-PAGE profiles of anti-SLP single domain antibodies following pepsin digestion. Antibodies were digested with pepsin at final enzyme concentrations of 100, 50, 25, 10, 5, 1.25 µg/mL (lanes 1-5, respectively) for 1 h at 37°C, and analyzed in a 12% SDS-PAGE gel. Lane 6 in all panels - undigested control. Figures are representative of three independent experiments. Molecular weight markers are indicated on the left hand side. The calculated percentage of undigested Ab are recorded in Table 6.

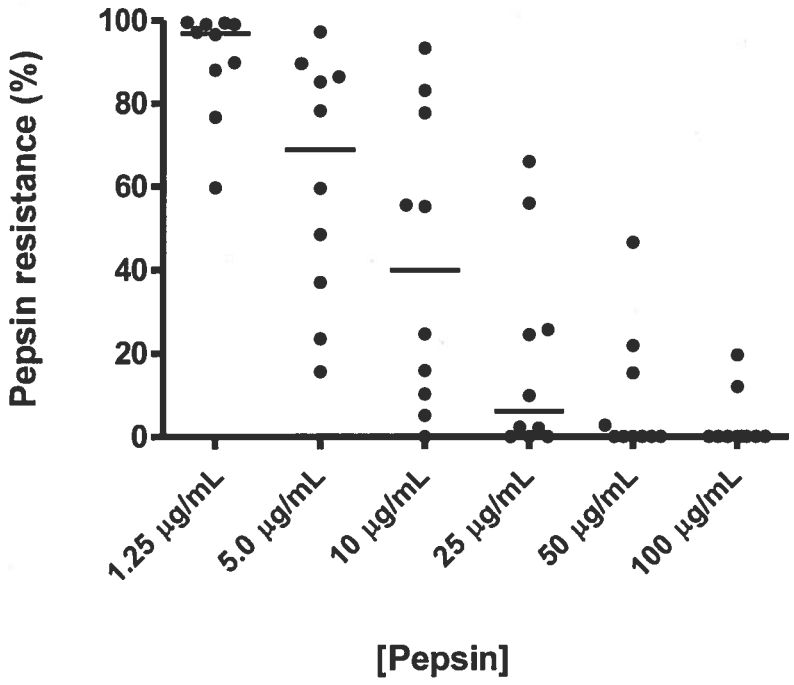
Pepsin resistance (%)
100
80
60
40
20
0
1.25 µg/mL
5.0 µg/mL
10 µg/mL
25 µg/mL
50 µg/mL
100 µg/mL
[Pepsin]

Figure 24: Pepsin resistance profiles of antiSLP sdAbs. The percent resistance of each antibody was determined by densitometric analysis following a 1 h digestion with various pepsin concentrations. The median value is indicated.

Table 8: Resistance profiles of anti-SLP sdAbs to pepsin digestion. sdAbs were digested with pepsin at final enzyme concentrations of 1.25, 5, 10, 25, 50, or 100 µg/mL for 1 h at 37°C to determine the degree of resistance to pepsin digestion, and analyzed on SDS-PAGE by densitometric analysis relative to an undigested control. The % Ab undigested value (+/- standard error, n=3) represents the amount of antibody remaining intact post-digestion as indicated by its band intensity on an SDS-PAGE gel, relative to its undigested control. The antibodies are ranked from most to least resistant. The number of pepsin digestion sites within the whole antibody *vs.* within the CDRs are indicated, and were obtained using the Expasy PeptideCutter tool courtesy of the Swiss Institute of Bioinformatics (http://ca.expasy.org/cgi-bin/peptidecutter/peptidecutter.pl).

	# of pepsin cleavage sites (pH 1.3-2.0)		Pepsin resistance (%)					
Anti-SLP	**Whole**	**CDRs**	**1.25 µg/mL**	**5 µg/mL**	**10 µg/mL**	**25 µg/mL**	**50 µg/mL**	**100 µg/mL[a]**
VHH22	47	19	99.0 +/- 1.5	85.2 +/- 7.3	83.1 +/- 3.3	56.0 +/- 7.0	46.5 +/- 10.0	19.6 +/- 0.8
VHH2	41	13	99.0 +/- 1.3	78.2 +/- 3.4	55.3 +/- 13.1	24.5 +/- 8.5	15.3 +/- 5.0	12.0 +/- 3.1
VHH23	47	19	97.2 +/- 1.7	97.3 +/- 2.5	93.4 +/- 5.9	66.0 +/- 2.3	21.9 +/- 9.8	0.00
VHH12	48	19	99.4 +/- 1.9	89.6 +/- 8.0	77.8 +/- 3.9	25.7 +/- 3.6	2.8 +/- 2.0	0.00
VHH46	36	14	96.6 +/- 1.6	86.4 +/- 7.7	55.6 +/- 4.5	9.9 +/- 4.6	0.00	0.00
VHH5	45	17	76.7 +/- 15.1	23.5 +/- 9.7	10.3 +/- 1.5	2.1 +/- 2.1	0.00	0.00
VHH26	40	11	96.6 +/- 0.1	72.8 +/- 8.8	50.8 +/- 2.5	1.9 +/- 1.3	0.00	0.00
VHH50	42	14	89.9 +/- 3.1	48.5 +/- 4.4	15.9 +/- 7.9	0.00	0.00	0.00
VH3	46	15	88.0 +/- 6.9	37.0 +/- 12.7	5.1 +/- 2.7	0.00	0.00	0.00
VHH49	44	17	59.7 +/- 14.2	15.6 +/- 0.6	0.00	0.00	0.00	0.00

a- n=2

A

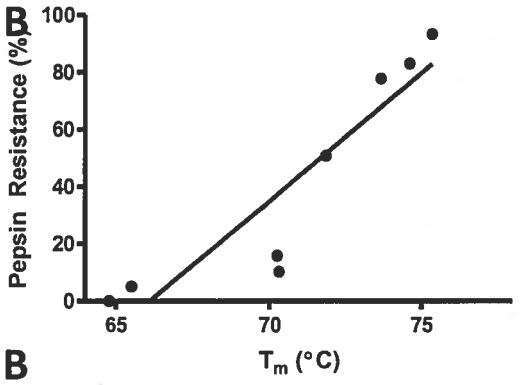
B
Pepsin Resistance (%)
100
80
60
40
20
0
65
70
75
T_m (°C)

B

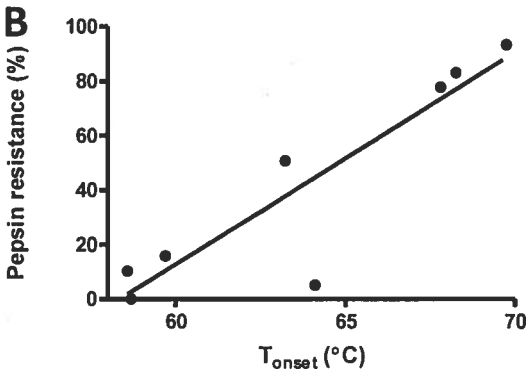
B
Pepsin resistance (%)
100
80
60
40
20
0
60
65
70
T_{onset} (°C)

Figure 25: Correlation between pepsin resistance and thermal unfolding. A linear-regression analysis was performed; values for VHH2 and VHH46 were excluded from the group analysis. A) Correlation of pepsin resistance with T_m; R^2=0.837, p=0.0014. B) Correlation of pepsin resistance with T_{onset}; R^2=0.817, p=0.0021.

4. Discussion

C. difficile is the leading cause of hospital acquired infections in developed countries. 1-3% of all healthy adults are asymptomatic carriers, but this rate increases to 20% upon antibiotic treatment (McFarland et al., 1989). Currently, the only available treatment for *C. difficile* infection is the administration of antibiotics; However, there is a 20% chance of relapse even after prolonged antibiotic treatment, and a further 30-50% will experience a third relapsing episode (Kyne et al., 2001; Barbut et al., 2000). With the rise of antibiotic resistance, it is necessary to develop alternative therapeutic strategies to treat infections.

C. difficile SLPs mediate adherence to host cells (Takumi et al., 1991; Karjalainen et al., 2001; Drudy et al., 2001; Calabi et al., 2002) and passive immunization with anti-SLP serum has been shown to significantly enhance survival in a stringent hamster model (O'Brien et al., 2005). Moreover, mucosal immunization of hamsters with cell wall extracts in combination with flagellar protein FliD significantly reduces bacterial load during infection and prolongs survival (Pechine et al., 2007). In a similar study, hamsters that were protected against *C. difficile* challenge following active immunization with toxoids A, B, and whole cell antigens, produced antisera with high agglutinating activity (Torres et al., 1995). Together these studies suggest that antibody-mediated bacterial neutralization may be an effective therapeutic strategy for *C. difficile* infections, and provide the rational for our current study which aimed to isolate and characterize high affinity sdAb binders to *C. difficile* SLPs for the potential use as potential therapeutic agents.

4.1. Isolation and functional characterization of anti-SLP sdAbs

In the context of alternative oral therapy for *C. difficile* infections, llama sdAbs offer several advantages: (i) they are cost efficient to produce, (ii) they are stable molecules with a

long shelf-life, (iii) they are highly specific, (iv) they are highly amenable to antibody engineering for improving affinity, stability, and function, (v) they are closely related to the human VH subfamily III (Vu et al., 1997; Nguyen et al., 2000), and are likely only minimally immunogenic (Cortez-Retamozo et al., 2004), and (vi) no selective pressure is applied where the emergence of resistance is a concern. Moreover, since sdAbs do not lyse bacteria, bacterial endotoxins are not released.

A naïve and an immune VHH llama phage display library were panned for SLP-specific sdAbs. A total of 12 unique sequences were isolated – 2 and 10 clones from the naïve and immune library, respectively. However, only 11 were successfully expressed and shown to be aggregate-free. Based on sequence analysis, all the anti-SLP antibodies isolated from the immune library contained the characteristic camelid heavy chain tetrad residues at positions 37, 44, 45, and 47 (Muyldermans et al., 1994), while VH3 isolated from the naïve library was of conventional origin (Val 37, Gly44, Leu45, and Trp47). Many of the clones shared high sequence identity (60-97% among the VHHs; Figure 8). Sequence analysis revealed the presence of a long CDR1 (9 residues) in VHH49, while all other antibodies identified possess 5 residues. Although antigen recognition is generally accepted to be shared by all three CDRs, it relies heavily on the CDR3 of antibodies. However, it is likely that the CDR1 of VHH49 plays an important role in antigen recognition, and the occurrence of a long CDR1 is not unprecedented (Harmsen et al., 2000). In fact, there has been previous evidence for the involvement of the CDR1 pairing with the CDR3 of VHHs in antigen interactions but not CDR2 (Decanniere et al., 1999). Interestingly, both VHH50 and VHH22 possess additional cysteines in CDR2 and CDR3 which likely forms a disulfide bond and aids in the stabilization of the antibodies, as indicated by their relatively high T_m (70.26 and

74.62 °C, respectively). These VHHs belong to the VHH subfamily 3 which is characterized by the presence of a cysteine at position 50 and a longer CDR3 (an average llama CDR3 length is 14-16 a.a.) (Harmsen et al., 2000;. Indeed both VHHs possess a 20- and 23 residue CDR3 respectively, and many of the anti-SLP VHHs isolated in this study share the same characteristic. A long CDR3 is thought to increase the stability and solubility of the VHH by folding over the VL-interface (Desmyter et al., 1996; Spinelli et al., 1996; Decanniere et al., 1999). Moreover, a long CDR3 can protrude into crevices that are rather inaccessible by conventional antibodies. In an example, a lysozyme-specific VHH (cAb-Lys3) possesses a stretch of residues within its long CDR3 which protrudes and inserts into the cleft of the enzyme (Desmyter et al., 1996). This highlights the potential of VHHs as potent enzyme inhibitors as was also demonstrated by Lauwereys et al. (1998). Additionally, a llama VHH which neutralizes HIV-1 IIIB was shown to possess a CDR3 with structural flexibility which counters the plasticity of the antigen (Hinz et al., 2010). Together these studies support the notion that it may be desirable for us to select from a pool of antibodies with larger antigen-binding components (i.e. CDRs) as to increase the likelihood of neutralization by either covering a larger antigenic surface, or by accessing crevices that are key for host-cell interactions, given the narrow and elongated shape of SLPs (Fagan et al., 2009), as well as their arrayed arrangement on the surface of *C. difficile.*

Two additional interesting observations were the sequence similarities of VHHs 2 and 26, VHHs 5 and 46, and VHHs 23 and 45. Upon sequence analysis of VHHs 2 and 26 we observed 19 residue substitutions, 6 of which are distributed in CDRs 2 and 3. VHH23 and VHH45 shared the highest sequence identity (97 % identity) as they differed by 4 residues, two of which are at the N-terminal and 2 of which were in CDR1. VHHs 5 and 46

share 84.9% identity, and differ mainly in CDR1 and CDR3. The binding kinetics of our VHHs were determined by SPR and all of our antibodies bound to strain QCD SLPs. Interestingly, binding kinetics revealed that VHH26 had a 3-fold faster dissociation rate constant and a ~2-fold lower K_D relative to VHH2 for strain QCD SLPs, which is likely the reason for its elimination in the fourth panning round. VHH45 was also not selected in the fourth panning round, and a 14-fold higher affinity of VHH23 to QCD SLPs relative to VHH45 was observed. This difference is probably attributed by the G33A and M34V substitutions during *in vivo* maturation from VHH45 to VHH23. Although there is no significant difference in their association rate constants (1.23 and 1.77 x 10^{-5} $M^{-1} \cdot s^{-1}$ for VHH23 and VHH45, respectively) for strain QCD SLP, VHH45 did exhibit a 17-fold faster dissociation rate constant, which translates to the decreased affinity. Interestingly, when De Genst *et al.* (2004) constructed a germline revertant of a cAb-Lys3 to study the plasticity and interaction strength of the antigen binding residues during affinity maturation, they found that while the association rate constants remained relatively constant, their germline precursor variants differed significantly in their dissociation rate from the mature cAb-Lys3, and that the replacement mutations from the germline to the mature VHH occur at the paratope periphery of the antibody-antigen interface. Somatic hypermutation for diversification is common at this location during the *in vivo* selection process (Tomlinson et al., 1996). Furthermore, the residue replacements at the N-terminal (K3Q, and E5V) could have conferred a structural change that translates to the antigen-binding paratopes which resulted in more favorable binding energetic, and therefore increased affinity of VHH23 to SLPs, relative to VHH45.

Camelids typically have a glutamic acid at position 6. A mutant VH3 (VH3-6E) was constructed by a single residue substituting (A6E) in order to study the effects on the antibody (Tanha et al., 2006). The introduction of this mutation in the framework region completely disrupted antigen binding. It is difficult to speculate why this occurred but perhaps the mutation conferred a slight overall structural change that altered the conformation of the antigen binding loops such that antigen-interactions were no longer energetically favorable. This is further supported by computer modeling of the structure of VH3 and VH3-6E (Appendix II), where a local charge disruption is observed around residue 6E in VH3-6E, when compared to the area around residue 6A in VH3. However, the results are only qualitatively useful as the electrostatics were generated *in vacuo*, using PyMOL (The PyMOL Molecular Graphics System, version 1.2r3pre, Schrodinger, LLC). The structural effects imparted by this mutation warrant further investigation. We also sought to increase the affinity of VH3 by increasing the avidity through pentamerization. The pentamerization of VH3 resulted in an approximately 10-fold decrease in the dissociation rate constant, indicating that multiple antibody-antigen interactions occurred. However, full valency was not achieved as was previously described for this platform (Zhang et al., 2004), due to the orientation of the antibodies and the rigidity of the platform, in combination with the number of epitopes and the geometry of the epitopes which results in steric hindrance of multivalent interactions.

All of our VHHs were specific to strain QCD SLPs (PCR ribotype 027), and were further shown to be specific to the Low-MW subunit of the protein by SPR. However, VH3 did not bind the Low-MW subunit of SLPs suggesting that the epitope likely lies on the High-MW subunit. VHH26 showed slight binding to the QCD Low-MW subunit by SPR and

by Western blot, however, the R_{max} for the SPR experiment was significantly lower in comparison to the R_{max} for the H/L experiment (Table 5) and the binding kinetics need to be re-examined. The SPR data obtained in this study highlights the complexity of SLPs as antigens. Although the K_Ds of our VHHs to H/L complex SLPs and to the Low-MW subunit alone (Table 5) were relatively the same, there were significant differences in the R_{max}s observed between the two sets of data, despite using the same antibody concentration. The increase in R_{max} (as is the case for VHH45, 46, 49, and 50) is likely the result of better accessibility to QCD Low-MW subunit due to the absence of steric hindrance from the High-MW subunit. Instances where the R_{max} decreases can be explained by the fact that the Low-MW SLP can be present as a homodimer in the absence of the High-MW subunit (Fagan et al., 2009). This homo-dimerization could result in masking of an epitope that is normally surface exposed when the Low-MW subunit is in complex with the High-MW subunit, thereby resulting in a decrease of the theoretical surface capacity. The complexity of the antigen is further illustrated by the observation that in certain instances, high affinity binding is observed at low antibody concentrations and low affinity binding is observed at high antibody concentrations. This variability can be explained in a simplified model (Figure 26), based on the knowledge that H/L complex SLPs form dimers in solution (Fagan et al., 2009), and as indicated by the gel filtration results (Figure 7), where an elution volume of ~320 kDa corresponds to a long-shaped molecule as that of the H/L complex SLPs (the MW of QCD H/L complex SLPs = 73 kDa). In this simple model of VHH-SLP interactions, SLPs are present as dimers and are therefore randomly immobilized on the sensorchip as such (Figure 26 A). In instances where the epitope if fully accessible in the dimer, the R_{max} for that given SPR experiment will be high (i.e. close to 80% of the theoretical R_{max}), however, in instances where the epitope is only partially exposed in the dimer, the R_{max} values will be relatively

lower (Figure 26 B Case 1 and 2) as not all epitopes will be occupied by the antibody. In instances where the affinity is concentration dependent, as is the case for VHHs 2, 22, and 26, the epitope may be partially accessible such that at low [VHH], the epitopes which are most easily accessible are occupied first, and as the concentration increases, the epitopes which are partially accessible can be occupied though by less than favorable kinetics (i.e. only part of that epitope is accessible thereby resulting in decreased affinity for the antigen; Figure 26 B, Case 3). Our model presents a plausible explanation for the observed SPR results, however, it's speculative and would benefit from further epitope mapping experiments.

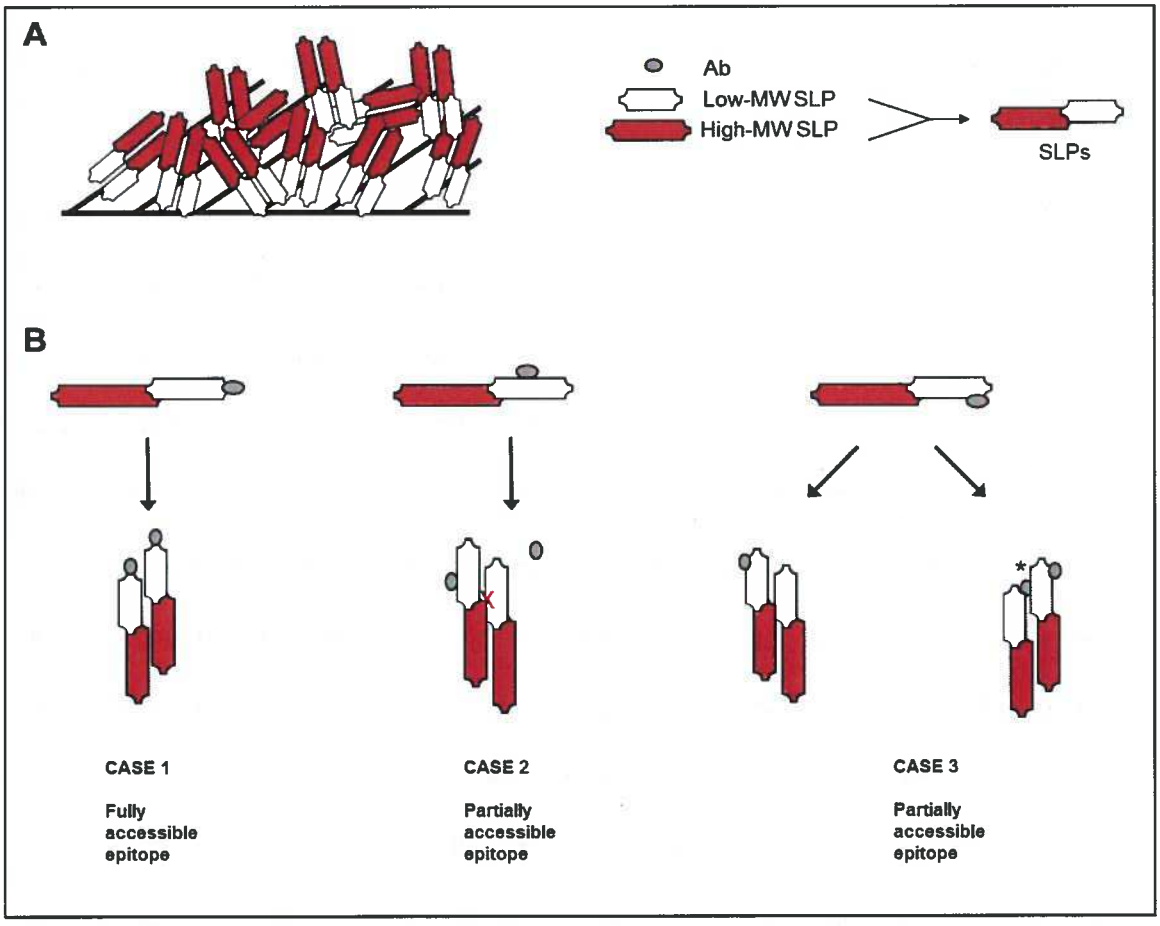

Figure 26: A model for VHH:SLP interactions during SPR. A) Purified SLPs form dimers in solution, and as a result they are immobilized on a CM5 sensorchip as such. B) Antibodies can either bind a fully accessible epitope (Case 1), or a partially accessible (Cases 2 and 3). The 1:1 binding model of antibody-antigen interactions can be applied in cases where the epitope is fully accessible (Case 1). In cases where the epitope is partially accessible, the outcome of the SPR experiment will depend on the degree of accessibility. In Case 2, the epitope is partially accessible and low R_{max} values will be observed as not all potential epitopes can be occupied, as indicated by the red "X" symbols. In Case 3, the accessibility of the epitope is greater than that of Case 2, however, at low antibody concentrations, the fully accessible epitopes will be occupied first, and as the antibody concentration increases, the partially accessible epitopes will begin to be occupied, however, due to steric hindrance low affinity to the antigen will be observed.

All of our antibodies were shown to bind SLPs on *C. difficile* cells with the exception of VHH2. The isolation of an antibody that does not bind whole cells is possible as the antibody was selected using the purified antigen in which certain epitopes were available during the immunization and selection but is not surface exposed when SLPs are present on the bacterial cell surface, which explains the disagreement between the high affinity of VHH2 and its low signal intensity in the *C. difficile* ELISA. Interestingly, VHH5, 45, 46 and 50 significantly inhibited motility of strain QCD in a motility assay. Inhibiting motility is another determinant for the identification of candidate therapeutic antibodies from our pool, even though the antibodies were not selected with a motility antigen. The ability of an antibody to simultaneously inhibit motility is a desirable quality since motility is a pathogenic determinant (Ramos et al., 2004). Moreover, a mAb which modifies the LPS of *Salmonella enterica* was shown to inhibit motility (Forbes et al., 2008). In a similar manner, P22, a phage tailspike protein was also able to inhibit the motility of *S. enterica* (Waseh et al., 2010). In both these studies, the antigen covered the surface of the bacteria, and given that the infection process often requires motility and/or surface antigens, mechanically

interfering with these interactions has the potential to reduce the bacterial infectivity (Waseh et al., 2010). Although not all strains of *C. difficile* possess flagella for motility (Delmee et al., 1990), hypervirulent strains, which are of great importance, did acquire enhanced motility (Stabler et al., 2009), and the presence of flagella on the surface of *C. difficile* enhances its adherence to host cells (Tasteyre et al., 2001). It is important to note that in the study by Tasteyre *et al.*, purified *C. difficile* flagella only weakly associated with host tissue cells, suggesting that flagella are not heavily relied upon for adherence. To date, there is no known report of SLP interactions with motility factors in *C. difficile*, and SLPs remain the primary adherence factors of *C. difficile*. Independent sequence alignment of QCD SLPs with a select number of the relevant flagellar proteins FliC, FliD, FliE, FliR/FlhB, FlgE, FlgG, FlhA, as well as a hook protein, a putative hook-length control protein, and two HAP proteins did not identify any potentially shared epitopes (data not shown). The mechanism by which a select number of our antibodies inhibit motility remains unknown, as gram-positive bacteria do not possess LPS. However, the theme of blocking a surface antigen which is high in abundance, wherein motility is reduced is present in this study and warrants further investigation.

In this study, we aimed to isolate broadly neutralizing antibodies to *C. difficile*, in order to prevent adherence and enhance bacterial clearance. Ideally, our antibodies should target a conserved epitope of SLPs within the different serogroups of *C. difficile*. This is likely to be established by isolating antibodies to the High-MW subunit of SLPs since this subunit is highly conserved among members of the same group, and anti-sera to this subunit has the ability to cross-react with members of different groups (Takeoka et al., 1991; Calabi et al., 2001). In our study, VHHs 2, 23, and 26 were shown to cross react with strain CD630

(PCR ribotype 012) SLPs by SPR. While this maybe a desirable quality, VHHs 2 and 26 did have the lowest affinity of the VHHs, a characteristic that is not ideal for a therapeutic antibody. Moreover, these antibodies recognize the Low-MW subunit of QCD SLPs (therefore, also likely the Low-MW subunit of strain CD630 SLPs), and the likelihood of cross-reactivity across a wide variety of isolates is low using this antigen, as it is not well conserved (Calabi and Fairweather, 2002; Spigaglia et al., 2011). While the ability to recognize the well-conserved High-MW subunit is desirable for providing cross-reactive neutralization activity, antibodies to the Low-MW subunit of PCR ribotype 027 are highly likely to cross-react with the Low-MW subunit of PCR ribotype 001, and are only slightly likely to cross-react with ribotype 012, as was previously demonstrated (Spigaglia et al., 2011). A peptide with 100% identity between all the groups tested was not recognized by ribotype 027, 001, or 012 anti-sera suggesting that it is not immunogenic, and provides evidence that the high variation observed among the Low-MW SLPs functions in host immune response evasion. Sequence alignment of the Low-MW portion of SlpA reveals very few conserved sites likely to be both surface-exposed, and immunogenic; therefore, the expectation of cross-reactivity of QCD selected sdAbs in this study with CD630 SLPs is extremely low. However, since the Low-MW SLP is conserved among strains *within* each group (Spigaglia et al., 2011) and is partly involved in adherence to host cells (Takumi et al., 1991), the antibodies isolated in this study can provide a proof-of-principle model for the future development of cross-reacting SLP-specific therapeutic antibodies, especially for ribotype 027 strains which are now the most prevalent hospital acquired strains. In contrast to the antibodies isolated from the immune library, VH3 did not bind the Low-MW subunit of SLPs, and was shown to be cross-reactive between the two different strains of *C. difficile*, strongly suggesting that it targets the conserved High-MW subunit of SLPs.

A more effective strategy to isolating therapeutic cross-reactive High-MW-specific sdAbs would be to immunize the llama with SLPs from several strains and then pan against a variety of SLPs. Alternatively, one could initially separate the two subunits by ion exchange chromatography, and use the single subunit during panning in place of whole SLPs. However, isolating the High-MW subunit is not straightforward and bacterial expression results in misfolded proteins that must be denatured and refolded post purification (Fagan et al., 2009). Moreover, the lone High-MW subunit is extremely unstable in solution and truncation products are highly likely during short-term storage. In hindsight, an alternative approach to select High-MW-specific antibodies would have been to employ a process termed subtractive panning, as previously described for the selection of antibodies to antigens that are difficult to isolate (Ridgway et al., 1999; Muruganandam et al., 2002). The process would entail panning the library with the Low-MW SLP to remove phage displaying antibodies specific to that subunit, followed by panning the remaining pool with whole SLPs. However, the likelihood of success may not be as high as anticipated for our current immune library; the llama was immunized with multiple antigens and subsequent panning of the library indicated that the immune response was strongly geared towards the Low-MW subunit consistent with previous observations that the Low-MW subunit is immunodominant (Pantosti et al., 1989). Therefore, the chances of successfully isolating high-affinity binders to the High-MW SLP from the current library may be relatively low.

4.2. Physicochemical characterization of antiSLP sdAbs

To be used in oral therapy, the therapeutic agent must be partially resistant to proteolysis by the digestive tract proteases (i.e. pepsin, trypsin, and chymotrypsin), and physically stable in order to resist the harsh environment of the digestive tract. The second

part of this study was to biophysically and chemically characterize these antibodies. It was previously demonstrated that aggregation resistant VHHs selected under acid-pressure had higher apparent melting temperatures (Famm et al., 2008). Our anti-SLPs were screened for high melting temperatures as a means to predict the stability of each antibody, and the T_{onset} and the T_m were determined at neutral pH using CD. The anti-SLPs were also screened for their resistance to pepsin digestion, as this is the harshest proteolytic enzyme to be encountered in the GI tract. VHH22 and VHH2 were the most resistant to pepsin digestion, and survived digestion with the 100 μg/mL, which is comparable to physiological pepsin concentrations. However, while the T_m of VHH22 was relatively high (74.62°C), the T_m of VHH2 was the lowest of the antibodies isolated (62.31°C). VHH23 was a close third in its relative resistance to pepsin digestion (21.9% resistant at 50 μg/mL), and also possessed a high T_m (75.4°C). Interestingly, despite having a relatively lower T_m, the refolding efficiency of VH3 was determined by SPR to be 96%, and although the refolding efficiencies of the VHHs were not investigated, they are likely to remain highly functional following refolding as this is a characteristic of llama VHHs. Ironically, there's no obvious correlation between the number of theoretical pepsin digestion sites *vs.* the relative sensitivity to pepsin digestion, however, we did observe a correlation between pepsin resistance and the T_m and T_{onset} of these antibodies, although VHH2 and VHH46 were excluded from this analysis. The T_m is strongly influenced by the environmental conditions in which the antibody is present, and different T_m values could be observed under lower pH conditions. Perhaps a stronger correlation could have been observed if the melting curves were obtained under acidic pH rather than neutral pH, as pepsin requires a pH of ~1.5 for efficient function. Nevertheless, proteolytic digestion of antibodies within the GI tract could be minimized by engineering, or by applying the appropriate formulation and dosage. One potential approach is the

administration of *Lactobacillus casei* expressing our therapeutic antibody on its cell surface. This was successfully demonstrated in an *in vivo* animal model for the protection against rotavirus-induced diarrhea (Pant et al., 2006). Alternatively, high concentrations of protein additives such as BSA can be formulated with the therapeutic agent, which provides an excess of pepsin and chymotrypsin digestion sites thereby becoming the digestive target (Waseh et al., 2010; Schmidt et al., 1989; Morgavi et al., 2000; Harmsen et al., 2005b). Additionally, since pepsin is highly dependent on hydrogen ion concentrations for efficient function, formulations that either encapsulate, or control the pH such as carbonate buffer, will inactivate pepsin, and neutralize the protein denaturation ability of gastric fluids (Schmidt et al., 1989; Wiedemann et al., 1990; Northrop, 1920; Worledge et al., 2000; Shimizu et al., 1993).

Interestingly, VHHs 12 and 23 shared similar biophysical properties throughout this study which is probably due to their high degree of sequence identity; based on 92% identity these properties include low nM affinities, specificity to the same SLP subunit, partial ability to inhibit motility, and comparable T_ms, and pepsin resistance profiles. In a similar manner, VHHs 5 and 46 grouped together by phylogenetic analysis, and they shared low nM affinities and subunit specificity, the ability to inhibit motility, and similar pepsin resistance profiles. Interestingly, VHHs 2 and 26 share a 86% identity however, they differed in their binding properties, their T_ms, and degree of pepsin resistance as a result in sequence differences which are concentrated in the FR.

4.3. Future directions

The next chapter of this study will aim to characterize the trypsin and chymotrypsin resistance profiles of these antibodies, as well as try to identify the epitopes recognized by

each antibody. In the future, in addition to the geared selection for High-MW specific antibodies, we also plan to apply selective pressure during the panning process, such as panning in the presence of pepsin (Harmsen et al., 2006) to select for pepsin resistant antibodies, or by panning following heat denaturation of the library (Jespers et al., 2004) to select for thermodynamically stable antibodies with high degree of pepsin resistance (since T_m is correlated with pepsin resistance), or by panning under low pH (Famm et al., 2008) in order to isolate aggregation resistant antibodies that are thermodynamically stable in the digestive tract. Additionally, the *in vivo* efficacy of the antibodies must be tested in an animal model in order to identify the best candidates for oral therapeutics. The efficacy of our anti-SLP antibodies when administered in combinations, or with toxin-specific VHHs, or with antibiotics should also be evaluated. Moreover, if our antibodies prove effective in controlling *in vivo C. difficile* infections, by epitope mapping we can precisely identify key regions within SLPs that are responsible for host-pathogen interactions, which will aid in developing fine-tuned therapeutic alternatives, rather than rely on large blind screens as is the case in our study. Aside from direct crystallization of our antibody in complex with SLPs, panning a commercially available peptide library with our antibodies can be the first step in identifying the epitope in the case of linear epitope-recognizing VHHs. Alternatively, using our antibodies as bait, a gene-fragment library which displays different segments of *C. difficile* SLPs on the surface of phage can be used to potentially isolate the specific epitope for that antibody (Fack et al., 1997).

Cross-reactive anti-SLP antibodies also have the potential to function as biological sensors in clinical settings. For example, sdAbs conjugated to superparamagnetic nanoparticles (silica encapsulated iron-oxide capsules) are effective at specifically detecting

Staphylococcus aureus with high sensitivity (Ryan et al., 2009), as are nanoaggregate-embedded bead probes (aggregates of gold particles embedded in silica) (Huang et al., 2009). Since the antibodies described in these studies target protein A, which is present in tens of thousands molecules per cell, and approximately 4 and 125 sdAb molecules are conjugated per nanoparticle and bead respectively in a multidirectional orientation, bacterial capture and agglutination is possible. This approach may translate for *C. difficile*, since SLPs constitute the majority of proteins on the cell surface. These platforms maybe more geometrically suitable to apply than the currently employed pentameric platform in the context of SLPs, as the number and orientation of the sdAbs can be manipulated, which will theoretically provide the appropriate spatial relationship and orientation for achieving full valency.

5. CONCLUSION

We successfully isolated and extensively characterized 11 llama sdAbs specific to QCD SLPs for their potential use as oral therapeutic agents. sdAbs are superior in the context of alternative therapies for *C. difficile* infections, as they avoid giving rise to antibiotic-resistance and decrease incidence of relapse, and are more cost effective in terms of production. Our antiSLP sdAbs are soluble and are specific to the Low-MW subunit of QCD SLPs, with the exception of VH3. VH3 is a conventional llama antibody specific to the High-MW subunit of strains QCD and CD630 SLPs, and has the potential to be cross-reactive among additional strains of the different PCR ribotypes, however, it requires *in vitro* affinity maturation in order to achieve therapeutic potential. Moreover, several lead candidates possess desirable biophysical characteristics such as high affinity, high intrinsic stability or the ability to inhibit motility. While it is preferred to isolate antibodies to the High-MW subunit, it maybe advantageous to target both subunits of the antigen in order to enhance the neutralizing potential, and consequently increase the therapeutic effect. This maybe possible if we can identify a neutralizing antibody to the Low-MW subunit which recognizes a highly conserved, surface exposed epitope among the different subgroups of *C. difficile*. The antibodies isolated in this study provide the basis for developing a novel therapeutic for treating ribotype 027 *C. difficile*, and additionally provide a proof-of-principle model, with which to develop highly specific and broadly neutralizing antibodies for the oral therapy of *C. difficile* infections.

Reference List

Arbabi Ghahroudi,M., Desmyter,A., Wyns,L., Hamers,R., and Muyldermans,S. (1997). Selection and identification of single domain antibody fragments from camel heavy-chain antibodies. FEBS letters *414*, 521-526.

Arbabi-Ghahroudi, M., MacKenzie, C. R., and Tanha, J. Site-directed mutagenesis for improving biophysical properties of V. (2010). Methods Mol Biol 634, 309-330.

Arbabi-Ghahroudi,M., MacKenzie,R., and Tanha,J. (2009). Selection of non-aggregating VH binders from synthetic VH phage-display libraries. Methods Mol Biol *525*, 187-216.

Arbabi-Ghahroudi,M., Tanha,J., and MacKenzie,R. (2005). Prokaryotic expression of antibodies. Cancer and Metastasis Rev. *24*, 501-519.

Arbabi-Ghahroudi,M., To,R., Gaudette,N., Hirama,T., Ding,W., MacKenzie,R., and Tanha,J. (2008). Aggregation-resistant VHs selected by in vitro evolution tend to have disulfide-bonded loops and acidic isoelectric points. Protein Eng Des Sel. *2,* 59-66.

Aronsson,B., Granström,M., Möllby,R., and Nord,C.E. (1985). Serum antibody response to *Clostridium difficile* toxins in patients with *Clostridium difficile* diarrhoea. Infection *13*, 97-101.

Babcock,G.J., Broering,T.J., Hernandez,H.J., Mandell,R.B., Donahue,K., Boatright,N., Stack,A.M., Lowy,I., Graziano,R., and Molrine,D. (2006). Human monoclonal antibodies directed against toxins A and B prevent *Clostridium difficile*-induced mortality in hamsters. Infect Immun. *74*, 6339.

Barbass III,C.F., Burton,D.R., Scott,J.K., and Silverman,G.J. (2004). Phage display: a laboratory manual. Cold Spring Harbor Laboratory Press.

Barbut,F., Richard,A., Hamadi,K., Chomette,V., Burghoffer,B., and Petit,J.C. (2000). Epidemiology of recurrences or reinfections of *Clostridium difficile*-associated diarrhea. J Clin Microbiol. *38*, 2386.

Behar,G., Siberil,S., Groulet,A., Chames,P., Pugniere,M., Boix,C., Sautes-Fridman,C., Teillaud,J.L., and Baty,D. (2007). Isolation and characterization of anti-Fc {gamma} RIII (CD16) llama single-domain antibodies that activate natural killer cells. Protein Eng Des Sel. *1*, 1-10.

Borriello,S.P. (1998). Pathogenesis of *Clostridium difficile* infection. J Antimicrob Chemother. *41*, 13.

Burton,D.R., Barbas,C.F., Persson,M.A., Koenig,S., Chanock,R.M., and Lerner,R.A. (1991). A large array of human monoclonal antibodies to type 1 human immunodeficiency virus

from combinatorial libraries of asymptomatic seropositive individuals. Proc Natl Acad Sci U S A. *88*, 10134.

Calabi,E., Calabi,F., Phillips,A.D., and Fairweather,N.F. (2002). Binding of *Clostridium difficile* surface layer proteins to gastrointestinal tissues. Infect Immun. *70*, 5770.

Calabi,E. and Fairweather,N. (2002). Patterns of sequence conservation in the S-layer proteins and related sequences in *Clostridium difficile*. J Bacteriol. *184*, 3886.

Calabi,E., Ward,S., Wren,B., Paxton,T., Panico,M., Morris,H., Dell,A., Dougan,G., and Fairweather,N. (2001). Molecular characterization of the surface layer proteins from *Clostridium difficile*. Mol Microbiol. *40*, 1187-1199.

Carayannopoulos,L., Max,E.E., and Capra,J.D. (1994). Recombinant human IgA expressed in insect cells. Proc Natl Acad Sci U S A..*91*, 8348.

Carter,P. (2001). Improving the efficacy of antibody-based cancer therapies. Nat Rev Cancer. *1*, 118-129.

Cartman,S.T., Heap,J.T., Kuehne,S.A., Cockayne,A., and Minton,N.P. (2010). The emergence of hypervirulence in *Clostridium difficile*. Int J Med Microbiol. *300(6)*:387-395.

Cerquetti,M., Molinari,A., Sebastianelli,A., Diociaiuti,M., Petruzzelli,R., Capo,C., and Mastrantonio,P. (2000). Characterization of surface layer proteins from different *Clostridium difficile* clinical isolates. Microb pathog. *28*, 363-372.

Chan,P.H., Pardon,E., Menzer,L., De Genst,E., Kumita,J.R., Christodoulou,J., Saerens,D., Brans,A., Bouillenne,F., and Archer,D.B. (2008). Engineering a Camelid Antibody Fragment That Binds to the Active Site of Human Lysozyme and Inhibits Its Conversion into Amyloid Fibrils. Biochemistry. *47*, 11041-11054.

Clackson,T., Hoogenboom,H.R., Griffiths,A.D., and Winter,G. (1991). Making antibody fragments using phage display libraries. Nature. *352*, 624-628.

Conrath,K.E., Wernery,U., Muyldermans,S., and Nguyen,V.K. (2003). Emergence and evolution of functional heavy-chain antibodies in Camelidae. Dev Comp Immunol. *27*, 87-103.

Coppieters,K., Dreier,T., Silence,K., Haard,H.D., Lauwereys,M., Casteels,P., Beirnaert,E., Jonckheere,H., Wiele,C.V.D., and Staelens,L. (2006). Formatted anti-tumor necrosis factor VHH proteins derived from camelids show superior potency and targeting to inflamed joints in a murine model of collagen induced arthritis. Arthritis & Rheum. *54*, 1856-1866.

Cortez Retamozo,V. and Lauwereys,M. (2002). Efficient tumor targeting by single domain antibody fragments of camels. Int J Cancer. *98*, 456-462.

Cortez-Retamozo,V., Backmann,N., Senter,P.D., Wernery,U., De Baetselier,P., Muyldermans,S., and Revets,H. (2004). Efficient cancer therapy with a nanobody-based conjugate. Cancer Res. *64*, 2853.

Davies,J. and Riechmann,L. (1996). Single antibody domains as small recognition units: design and in vitro antigen selection of camelized, human VH domains with improved protein stability. Protein Eng Des Sel. *9*, 531.

De Genst,E., Handelberg,F., Van Meirhaeghe,A., Vynck,S., Loris,R., Wyns,L., and Muyldermans,S. (2004). Chemical basis for the affinity maturation of a camel single domain antibody. J Biol Chem. *279*, 53593.

De Genst,E., Silence,K., Decanniere,K., Conrath,K., Loris,R., Kinne,J., Muyldermans,S., and Wyns,L. (2006). Molecular basis for the preferential cleft recognition by dromedary heavy-chain antibodies. Proc Natl Acad Sci U S A. *103*, 4586.

Decanniere,K., Desmyter,A., Lauwereys,M., Ghahroudi,M.A., Muyldermans,S., and Wyns,L. (1999). A single-domain antibody fragment in complex with RNase A: non-canonical loop structures and nanomolar affinity using two CDR loops. Structure *7*, 361-370.

Delmee,M., Avesani,V., Delferriere,N., and Burtonboy,G. (1990). Characterization of flagella of *Clostridium difficile* and their role in serogrouping reactions. J Clin Microbiol. *28*, 2210.

Demarest, S. J., Hariharan, M., Elia, M., Salbato, J., Jin, P., Bird, C., Short, J. M., Kimmel, B. E., Dudley, M., and Woodnutt, G. (2010). Neutralization of *Clostridium difficile* toxin A using antibody combinations. mAbs. *2(2)*, 190-198.

Desmyter,A., Spinelli,S., Payan,F., Lauwereys,M., Wyns,L., Muyldermans,S., and Cambillau,C. (2002). Three camelid VHH domains in complex with porcine pancreatic -amylase. Journal of Biol Chem. *277*, 23645.

Desmyter,A., Transue,T.R., Ghahroudi,M.A., Thi,M.H.D., Poortmans,F., Hamers,R., Muyldermans,S., and Wyns,L. (1996). Crystal structure of a camel single-domain VH antibody fragment in complex with lysozyme. Nat Struct Biol. *3*, 803-811.

Drudy,D., Calabi,E., Kyne,L., Sougioultzis,S., Kelly,E., Fairweather,N., and Kelly,C.P. (2004). Human antibody response to surface layer proteins in *Clostridium difficile* infection. FEMS Immunol Med Microbiol. *41*, 237-242.

Drudy,D., O'donoghue,D.P., Baird,A., Fenelon,L., and O'farrelly,C. (2001). Flow cytometric analysis of *Clostridium difficile* adherence to human intestinal epithelial cells. J Med Microbiol *50*, 526.

Dörsam,H., Rohrbach,P., Knrschner,T., Kipriyanov,S., Renner,S., Braunagel,M., Welschof,M., and Little,M. (1997). Antibodies to steroids from a small human naive IgM library. FEBS letters *414*, 7-13.

Estell,D. (2006). Adapting industry practices for the rapid, large-scale manufacture of pharmaceutical proteins. Bridge *36(3)*.

Fack, F., Hugle-Dorr, B., Song, D., Queitsch, I., Petersen, G., and Bautz, E. K. F. (1997). Epitope mapping by phage display: random versus gene-fragment libraries. J Immunolog Meth. *206[1-2]*, 43-52.

Fagan,R.P., Albesa-Jove,D., Qazi,O., Svergun,D.I., Brown,K.A., and Fairweather,N.F. (2009). Structural insights into the molecular organization of the S-layer from *Clostridium difficile*. Mol Microbiol. *71*, 1308-1322.

Famm,K., Hansen,L., Christ,D., and Winter,G. (2008). Thermodynamically stable aggregation-resistant antibody domains through directed evolution. J Mol Biol. *376*, 926-931.

Fellouse,F.A., Esaki,K., Birtalan,S., Raptis,D., Cancasci,V.J., Koide,A., Jhurani,P., Vasser,M., Wiesmann,C., and Kossiakoff,A.A. (2007). High-throughput generation of synthetic antibodies from highly functional minimalist phage-displayed libraries. J Mol Biol. *373*, 924-940.

Filpula,D. (2007). Antibody engineering and modification technologies. Biomol Eng. *24*, 201-215.

Forbes,S.J., Eschmann,M., and Mantis,N.J. (2008). Inhibition of Salmonella enterica serovar Typhimurium motility and entry into epithelial cells by a protective antilipopolysaccharide monoclonal immunoglobulin A antibody. Infect Immun. *76*, 4137.

Francisco,J.A., Campbell,R., Iverson,B.L., and Georgiou,G. (1993a). Production and fluorescence-activated cell sorting of Escherichia coli expressing a functional antibody fragment on the external surface. Proc Natl Acad Sci U S A. *90*, 10444.

Fuchs,P., Breitling,F., Dnbel,S., Seehaus,T., and Little,M. (1991). Targeting recombinant antibodies to the surface of Escherichia coli: fusion to a peptidoglycan associated lipoprotein. Nat Biotech. *9*, 1369-1372.

Georgiou,G., Poetschke,H.L., Stathopoulos,C., and Francisco,J.A. (1993). Practical applications of engineering Gram-negative bacterial cell surfaces. Trends Biotechnol. *11*, 6-10.

Georgiou,G., Stathopoulos,C., Daugherty,P.S., Nayak,A.R., Iverson,B.L., and Curtiss III,R. (1997). Display of heterologous proteins on the surface of microorganisms: from the screening of combinatorial libraries to live recombinant vaccines. Nature Biotech. *15*, 29-34.

Giannasca,P.J. and Warny,M. (2004). Active and passive immunization against *Clostridium difficile* diarrhea and colitis. Vaccine *22*, 848-856.

Goldman,E.R., Anderson,G.P., Liu,J.L., Delehanty,J.B., Sherwood,L.J., Osborn,L.E., Cummins,L.B., and Hayhurst,A. (2006). Facile generation of heat-stable antiviral and

antitoxin single domain antibodies from a semisynthetic llama library. Anal. Chem. *78*, 8245-8255.

Goncalves,C., Decre,D., Barbut,F., Burghoffer,B., and Petit,J.C. (2004). Prevalence and characterization of a binary toxin (actin-specific ADP-ribosyltransferase) from *Clostridium difficile*. J Clinl Microbiol. *42*, 1933.

Griffiths,A.D., Malmqvist,M., Marks,J.D., Bye,J.M., Embleton,M.J., McCafferty,J., Baier,M., Holliger,K.P., Gorick,B.D., and Hughes-Jones,N.C. (1993). Human anti-self antibodies with high specificity from phage display libraries. EMBO J. *12*, 725.

Gräslund,S., Nordlund,P., Weigelt,J., Bray,J., Gileadi,O., Knapp,S., Oppermann,U., Arrowsmith,C., Hui,R., and Ming,J. (2008). Protein production and purification. Nat Methods. *5*, 135-146.

Gunneriusson,E., Samuelson,P., Uhlen,M., Nygren,P.A., and Stahl,S. (1996). Surface display of a functional single-chain Fv antibody on staphylococci. J Bacteriol. *178*, 1341.

Jean-Benoit Legault. Deadly C. difficile outbreak sparks lawsuit against Quebec hospital. 1-9-2008. The Okanagan Valley Group of Newspapers. Online Source

Hagihara,Y., Mine,S., and Uegaki,K. (2007). Stabilization of an immunoglobulin fold domain by an engineered disulfide bond at the buried hydrophobic region. J Biolog Chem. *282*, 36489.

Hamers-Casterman,C., Atarhouch,T., Muyldermans,S., Robinson,G., Hamers,C., Songa,E.B., Bendahman,N., and Hamers,R. (1993). Naturally occurring antibodies devoid of light chains. Nature. 363 *446*, 448.

Harmsen,M.M. and De Haard,H.J. (2007). Properties, production, and applications of camelid single-domain antibody fragments. Appl Microbiol Biotechnol. *77*, 13-22.

Harmsen,M.M., Ruuls,R.C., Nijman,I.J., Niewold,T.A., Frenken,L.G.J., and de Geus,B. (2000). Llama heavy-chain V regions consist of at least four distinct subfamilies revealing novel sequence features. Mol Imm. *37*, 579-590.

Harmsen,M.M., Van Solt,C.B., Fijten,H.P.D., and Van Setten,M.C. (2005a). Prolonged in vivo residence times of llama single-domain antibody fragments in pigs by binding to porcine immunoglobulins. Vaccine *23*, 4926-4934.

Harmsen,M.M., Van Solt,C.B., Hoogendoorn,A., van Zijderveld,F.G., Niewold,T.A., and Van der Meulen,J. (2005b). Escherichia coli F4 fimbriae specific llama single-domain antibody fragments effectively inhibit bacterial adhesion in vitro but poorly protect against diarrhoea. Vet Microbiol. *111*, 89-98.

Harmsen,M.M., Van Solt,C.B., van Zijderveld-van Bemmel,A., Niewold,T.A., and van Zijderveld,F.G. (2006). Selection and optimization of proteolytically stable llama single-

domain antibody fragments for oral immunotherapy. Appl Microbiol Biotechnol. *72*, 544-551.

He,M. and Taussig,M.J. (1997). Antibody-ribosome-mRNA (ARM) complexes as efficient selection particles for in vitro display and evolution of antibody combining sites. Nucleic Acids Res. *25*, 5132.

Hendershot,L., Bole,D., Köhler,G., and Kearney,J.F. (1987). Assembly and secretion of heavy chains that do not associate posttranslationally with immunoglobulin heavy chain-binding protein. J Cell Biol. *104*, 761.

Hermeling,S., Crommelin,D.J.A., Schellekens,H., and Jiskoot,W. (2004). Structure-immunogenicity relationships of therapeutic proteins. Pharm Res. *21*, 897-903.

Hilschmann,N. and Craig,L.C. (1965). Amino acid sequence studies with Bence-Jones proteins. Proc Natl Acad Sci U S A.*53*, 1403.

Hinz,A., Hulsik,D.L., Forsman,A., Koh,W.W.L., Belrhali,H., Gorlani,A., de Haard,H., Weiss,R.A., Verrips,T., and Weissenhorn,W. (2010). Crystal Structure of the Neutralizing Llama VHH D7 and Its Mode of HIV-1 gp120 Interaction. PloS one. *5*, e10482.

Hmila,I., Abdallah,R., Ben,A.B., Saerens,D., Benlasfar,Z., Conrath,K., Ayeb,M.E., Muyldermans,S., and Bouhaouala-Zahar,B. (2008). VHH, bivalent domains and chimeric Heavy chain-only antibodies with high neutralizing efficacy for scorpion toxin AahI'. Mol Imm. *45*, 3847-3856.

Holliger,P. and Hudson,P.J. (2005). Engineered antibody fragments and the rise of single domains. Nat Biotech. *23*, 1126-1136.

Holt,L.J., Herring,C., Jespers,L.S., Woolven,B.P., and Tomlinson,I.M. (2003). Domain antibodies: proteins for therapy. Trends in biotechnol. *21*, 484-490.

Hoogenboom,H.R. (1997). Designing and optimizing library selection strategies for generating high-affinity antibodies. Trends in biotechnol. *15*, 62-70.

Hoogenboom,H.R. (2005). Selecting and screening recombinant antibody libraries. Nat Biotechnol. *23*, 1105-1116.

Hoogenboom,H.R., de,B.n., Hufton,S.E., Hoet,R.M., Arends,J.W., and Roovers,R.C. (1998). Antibody phage display technology and its applications. Immunotechnology *4*, 1-20.

Hoogenboom,H.R., Griffiths,A.D., Johnson,K.S., Chiswell,D.J., Hudson,P., and Winter,G. (1991). Multi-subunit proteins on the surface of filamentous phage: methodologies for displaying antibody (Fab) heavy and light chains. Nucleic Acids Res. *19*, 4133.

Huang,P.J., Tay,L.L., Tanha,J., Ryan,S., and Chau,L.K. (2009). Single Domain Antibody Conjugated Nanoaggregate Embedded Beads for Targeted Detection of Pathogenic Bacteria. Chemistry. *15*, 9330-9334.

Hudson,P.J. (1998). Recombinant antibody fragments. Curr Opin Biotechnol. *9*, 395-402.

Huse,W.D., Sastry,L., Iverson,S.A., Kang,A.S., Alting-Mees,M., Burton,D.R., Benkovic,S.J., and Lerner,R.A. (1989). Generation of a large combinatorial library of the immunoglobulin repertoire in phage lambda. Science. *246*, 1275.

Hussack,G., Arbabi-Ghahroudi,M., van Faassen,H., Songer,J.G., Ng,K.K.S., MacKenzie,R., and Tanha,J. (2011a). Neutralization of *Clostridium difficile* toxin A with single-domain antibodies targeting the cell-receptor binding domain. J Biolog Chem. *286(11)*:8961-76.

Hussack,G., MacKenzie,C.R., and Tanha,J. (2011b). Characterization of Single Domain Antibodies with an Engineered Disulfide Bond. Submitted.

Hussack,G. and Tanha,J. (2010). Toxin-Specific Antibodies for the Treatment of *Clostridium difficile*: Current Status and Future Perspectives. Toxins *2*, 998-1018.

Jank,T. and Aktories,K. (2008). Structure and mode of action of clostridial glucosylating toxins: the ABCD model. Trends in microbiol. *16*, 222-229.

Jank,T., Giesemann,T., and Aktories,K. (2007). Rho-glucosylating *Clostridium difficile* toxins A and B: new insights into structure and function. Glycobiology *17*, 15R.

Jespers,L., Schon,O., Famm,K., and Winter,G. (2004). Aggregation-resistant domain antibodies selected on phage by heat denaturation. Nat Biotechnol. *22*, 1161-1165.

Joosten,V., Lokman,C., Van Den Hondel,C.A., and Punt,P.J. (2003). The production of antibody fragments and antibody fusion proteins by yeasts and filamentous fungi. Microb Cell Fact. *2*, 1.

Kabat,E.A., Te Wu,T., Perry,H.M., Gottesman,K.S., and Foeller,C. (1992). Sequences of proteins of immunological interest. Diane Pub Co.

Karjalainen,T., Waligora-Dupriet,A.J., Cerquetti,M., Spigaglia,P., Maggioni,A., Mauri,P., and Mastrantonio,P. (2001). Molecular and genomic analysis of genes encoding surface-anchored proteins from *Clostridium difficile*. Infect Imm *69*, 3442.

Kawata,T., Takeoka,A., Takumi,K., and Masuda,K. (1984). Demonstration and preliminary characterization of a regular array in the cell wall of *Clostridium difficile*. FEMS Microbiol Let. *24*, 323-328.

Kirby,J.M., Ahern,H., Roberts,A.K., Kumar,V., Freeman,Z., Acharya,K.R., and Shone,C.C. (2009). Cwp84, a surface-associated Cysteine Protease, plays a role in the maturation of the surface layer of *Clostridium difficile*. J Biolog Chem. *284*, 34666.

Knappik,A., Ge,L., Honegger,A., Pack,P., Fischer,M., Wellnhofer,G., Hoess,A., Wölle,J., Plückthun,A., and Virnekäs,B. (2000). Fully synthetic human combinatorial antibody libraries (HuCAL) based on modular consensus frameworks and CDRs randomized with trinucleotides1. J Mol Biol. *296*, 57-86.

Knappik,A. and Plückthun,A. (1995). Engineered turns of a recombinant antibody improve its in vivo folding. Protein Eng Des Sel. *8*, 81.

Kyne,L., Warny,M., Qamar,A., and Kelly,C.P. (2001). Association between antibody response to toxin A and protection against recurrent *Clostridium difficile* diarrhoea. The Lancet. *357*, 189-193.

Köhler,G. and Milstein,C. (1975). Continuous cultures of fused cells secreting antibody of predefined specificity.Reprint, 2005, J Immunol. *174(5)*:2453-5.

Lauwereys,M., Ghahroudi,M.A., Desmyter,A., Kinne,J., Hölzer,W., De Genst,E., Wyns,L., and Muyldermans,S. (1998). Potent enzyme inhibitors derived from dromedary heavy-chain antibodies. EMBO J. *17*, 3512-3520.

Lee,A.S.Y. and Song,K.P. (2005). LuxS/autoinducer-2 quorum sensing molecule regulates transcriptional virulence gene expression in *Clostridium difficile*. Biochem Biophys Res Commun. *335*, 659-666.

Leung,D.Y., Kelly,C.P., Boguniewicz,M., Pothoulakis,C., LaMont,J.T., and Flores,A. (1991). Treatment with intravenously administered gamma globulin of chronic relapsing colitis induced by *Clostridium difficile* toxin. J Pediatr. *118*, 633.

Li,M. (2000). Applications of display technology in protein analysis. Nat Biotechnol. *18*, 1251-1256.

Little,M., Breitling,F., Dnbel,S., Fuchs,P., Braunagel,M., Seehaus,T., and Klewinghaus,I. (1993). Universal antibody libraries on phage and bacteria. Year Immunol. *7*, 50.

Lyerly,D.M., Krivan,H.C., and Wilkins,T.D. (1988). *Clostridium difficile*: its disease and toxins. Clin Microbiol Rev. *1*, 1-18.

Lyerly,D.M., Saum,K.E., MacDonald,D.K., and Wilkins,T.D. (1985). Effects of *Clostridium difficile* toxins given intragastrically to animals. Infect Immun. *47*, 349.

MacCannell,D.R., Louie,T.J., Gregson,D.B., Laverdiere,M., Labbe,A.C., Laing,F., and Henwick,S. (2006). Molecular analysis of *Clostridium difficile* PCR ribotype 027 isolates from Eastern and Western Canada. J Clin Microbiol. *44*, 2147.

Marks,J.D., Hoogenboom,H.R., Bonnert,T.P., McCafferty,J., Griffiths,A.D., and Winter,G. (1991). By-passing immunization:: Human antibodies from V-gene libraries displayed on phage. JMol Biol. *222*, 581-597.

Maynard,J. and Georgiou,G. (2000). Antibody engineering. Annu Rev Biomed Eng. *2*, 339.

McCafferty,J., Griffiths,A.D., Winter,G., and Chiswell,D.J. (1990). Phage antibodies:

filamentous phage displaying antibody variable domains. Nature. *348(6301)*:552-554.

McFarland,L.V., Mulligan,M.E., Kwok,R.Y.Y., and Stamm,W.E. (1989). Nosocomial acquisition of *Clostridium difficile* infection. N Eng J Med. *320*, 204-210.

Mehdiratta,R. and Saberwal,G. (2007). Bio-business in brief: Many a monoclonal. Current Science *93*, 789-796.

Miao,Q., Liu,X., Shang,B., Ouyang,Z., and Zhen,Y. (2007). An enediyne-energized single-domain antibody-containing fusion protein shows potent antitumor activity. Anticancer drugs. *18*, 127.

Morgavi,D.P., Newbold,C.J., Beever,D.E., and Wallace,R.J. (2000). Stability and stabilization of potential feed additive enzymes in rumen fluid*. Enzyme Microb Technol. *26*, 171-177.

Muruganandam,A., Tanha,J., Narang,S., and Stanimirovic,D. (2002). Selection of phage-displayed llama single-domain antibodies that transmigrate across human blood-brain barrier endothelium. FASEB J. *16*, 240.

Muyldermans,S. (2001). Single domain camel antibodies: current status. Rev Mol Biotechnol. *74*, 277-302.

Muyldermans,S., Atarhouch,T., Saldanha,J., Barbosa,J., and Hamers,R. (1994). Sequence and structure of VH domain from naturally occurring camel heavy chain immunoglobulins lacking light chains. Protein Eng Des Sel. *7*, 1129.

Muyldermans,S. and Lauwereys,M. (1999). Unique single-domain antigen binding fragments derived from naturally occurring camel heavy-chain antibodies. J Mol Recognit. *12*, 131-140.

Nguyen,V.K., Hamers,R., Wyns,L., and Muyldermans,S. (2000). Camel heavy-chain antibodies: diverse germline VHH and specific mechanisms enlarge the antigen-binding repertoire. EMBO J. *19*, 921-930.

Northrop,J.H. (1920). The significance of the hydrogen ion concentration for the digestion of proteins by pepsin. J Gen Physiol. *3*, 211.

Nowakowski,A., Wang,C., Powers,D.B., Amersdorfer,P., Smith,T.J., Montgomery,V.A., Sheridan,R., Blake,R., Smith,L.A., and Marks,J.D. (2002). Potent neutralization of botulinum neurotoxin by recombinant oligoclonal antibody. Proc Natl Acad Sci U S A. *99*, 11346.

O'Brien,J.A., Lahue,B.J., Caro,J.J., and Davidson,D.M. (2007). The emerging infectious challenge of *Clostridium difficile*-associated disease in Massachusetts hospitals: clinical and economic consequences. Infect Control Hosp Epidemiol. *28*, 1219.

O'Brien,J.B., McCabe,M.S., Athiq-Morales,V., McDonald,G.S.A., Eidhin,D.B.N., and Kelleher,D.P. (2005). Passive immunisation of hamsters against *Clostridium difficile* infection using antibodies to surface layer proteins. FEMS Microbiol Let. *246*, 199-205.

Orum,H., Andersen,P.S., Oster,A., Johansen,L.K., Riise,E., Bj°rnvad,M., Svendsen,I., and Engberg,J. (1993). Efficient method for constructing comprehensive murine Fab antibody libraries displayed on phage. Nucleic Acids Res. *21*, 4491.

Padlan,E.A. (1994). Anatomy of the antibody molecule. Mol Immunol. *31*, 169-217.

Pant,N., Hultberg,A., YAOFENG,Z., Svensson,L., Pan-Hammarström,Q., Johansen,K., Pouwels,P.H., Ruggeri,F.M., Hermans,P., and Frenken,L. (2006). Lactobacilli expressing variable domain of llama heavy-chain antibody fragments (lactobodies) confer protection against rotavirus-induced diarrhea. J Infect Dis. *194*, 1580-1588.

Pantosti,A., Cerquetti,M., Viti,F., Ortisi,G., and Mastrantonio,P. (1989). Immunoblot analysis of serum immunoglobulin G response to surface proteins of *Clostridium difficile* in patients with antibiotic-associated diarrhea. J Clin Microbiol. *27*, 2594.

Paschke,M. (2006). Phage display systems and their applications. Appl Microbiol Biotechnol. *70*, 2-11.

Patel,D., Vitovski,S., Senior,H.J., Edge,M.D., Hockney,R.C., Dempsey,M.J., and Sayers,J.R. (2001). Continuous affinity-based selection: rapid screening and simultaneous amplification of bacterial surface-display libraries. Biochem J. *357*, 779.

Pechine,S., Janoir,C., Boureau,H., Gleizes,A., Tsapis,N., Hoys,S., Fattal,E., and Collignon,A. (2007). Diminished intestinal colonization by *Clostridium difficile* and immune response in mice after mucosal immunization with surface proteins of *Clostridium difficile*. Vaccine. *25*, 3946-3954.

Peeters,K., De Wilde,C., De Jaeger,G., Angenon,G., and Depicker,A. (2001). Production of antibodies and antibody fragments in plants. Vaccine *19*, 2756-2761.

Pelaez,T., Alcala,L., Alonso,R., Rodriguez-Creixems,M., Garcia-Lechuz,J.M., and Bouza,E. (2002). Reassessment of *Clostridium difficile* susceptibility to metronidazole and vancomycin. Antimicrob Agents Chemother. *46*, 1647.

Persson,M.A., Caothien,R.H., and Burton,D.R. (1991). Generation of diverse high-affinity human monoclonal antibodies by repertoire cloning. Proc Natl Acad Sci U S A. *88*, 2432.

Plückthun,A. (1991). Antibody engineering: advances from the use of Escherichia coli expression systems. Biotechnology *9*, 545.

Porath,J. and Olin,B. (1983). Immobilized metal affinity adsorption and immobilized metal affinity chromatography of biomaterials. Serum protein affinities for gel-immobilized iron and nickel ions. Biochemistry *22*, 1621-1630.

Pothoulakis,C. (2000). Effects of *Clostridium difficile* toxins on epithelial cell barrier. Ann N Y Acad Sci. *915*, 347-356.

Ramos,H.C., Rumbo,M., and Sirard,J.C. (2004). Bacterial flagellins: mediators of pathogenicity and host immune responses in mucosa. Trends in microbiol. *12*, 509-517.

Rea,M.C., Sit,C.S., Clayton,E., O'Connor,P.M., Whittal,R.M., Zheng,J., Vederas,J.C., Ross,R.P., and Hill,C. (2010). Thuricin CD, a posttranslationally modified bacteriocin with a narrow spectrum of activity against *Clostridium difficile*. Proc Natl Acad Sci U S A. *107*, 9352.

Ridder,R., Schmitz,R., Legay,F., and Gram,H. (1995). Generation of rabbit monoclonal antibody fragments from a combinatorial phage display library and their production in the yeast Pichia pastoris. Nat Biotechnol. *13*, 255-260.

Ridgway,J.B.B., Ng,E., Kern,J.A., Lee,J., Brush,J., Goddard,A., and Carter,P. (1999). Identification of a human anti-CD55 single-chain Fv by subtractive panning of a phage library using tumor and nontumor cell lines. Cancer Res. *59*, 2718.

Riechmann,L., Foote,J., and Winter,G. (1988). Expression of an antibody Fv fragment in myeloma cells. J Mol Biol. *203*, 825-828.

Roberts,R.W. and Ja,W.W. (1999). In vitro selection of nucleic acids and proteins: what are we learning? Curr Opin Struct Biol. *9*, 521-529.

Roovers,R.C., Laeremans,T., Huang,L., De Taeye,S., Verkleij,A.J., Revets,H., De Haard,H.J., and van Bergen en Henegouwen,P. (2007). Efficient inhibition of EGFR signalling and of tumour growth by antagonistic anti-EGFR Nanobodies. Cancer Immunol Immunother. *56*, 303-317.

Ryan,S., Kell,A.J., van Faassen,H., Tay,L.L., Simard,B., MacKenzie,R., Gilbert,M., and Tanha,J. (2009). Single-Domain Antibody-Nanoparticles: Promising Architectures for Increased Staphylococcus aureus Detection Specificity and Sensitivity. Bioconjugate Chem. *20*, 1966-1974.

Saerens,D., Conrath,K., Govaert,J., and Muyldermans,S. (2008a). Disulfide bond introduction for general stabilization of immunoglobulin heavy-chain variable domains. J Mol Biol. *377*, 478-488.

Saerens,D., Ghassabeh,G.H., and Muyldermans,S. (2008b). Single-domain antibodies as building blocks for novel therapeutics. Curr Opin Pharmacol. *8*, 600-608.

Salcedo,J., Keates,S., Pothoulakis,C., Warny,M., Castagliuolo,I., LaMont,J.T., and Kelly,C.P. (1997). Intravenous immunoglobulin therapy for severe *Clostridium difficile* colitis. Gut. *41*, 366.

Sara,M. and Sleytr,U.B. (2000). S-layer proteins. J Bacteriol. *182*, 859.

Schaffitzel,C., Hanes,J., Jermutus,L., and Plückthun,A. (1999). Ribosome display: an in vitro method for selection and evolution of antibodies from libraries. J Immunolog Meth. *231*, 119-135.

Schmidt,P., Wiedemann,V., Knhlmann,R., Wanke,R., and Linckh,E. (1989). Chicken egg antibodies for prophylaxis and therapy of infectious intestinal diseases. II: *in vitro* studies on gastric and enteric digestion of egg yolk antibodies specific against pathogenic Escherichia coli strains. Zentralbl Veterinarmed B. *36(8):*619-628.

Schwan,C., Stecher,B., Tzivelekidis,T., Van Ham,M., Rohde,M., Hardt,W.D., Wehland,J., and Aktories,K. (2009). *Clostridium difficile* toxin CDT induces formation of microtubule-based protrusions and increases adherence of bacteria. PLoS Pathog. *5*, e1000626.

Shimizu,M., Miwa,Y., Hashimoto,K., and Goto,A. (1993). Encapsulation of chicken egg yolk immunoglobulin G (IgY) by liposomes. Biosci Biotechnol Biochem. *57*, 1445.

Sleytr,U.B. and Beveridge,T.J. (1999). Bacterial S-layers. Trends microbiol. *7*, 253-260.

Smith,G.P. (1985). Filamentous fusion phage: novel expression vectors that display cloned antigens on the virion surface. Science *228*, 1315.

Spigaglia,P., Galeotti,C.L., Barbanti,F., Scarselli,M., Van Broeck,J., and Mastrantonio,P. (2011). *Clostridium difficile* PCR-ribotypes 027 and 001 share common immunogenic properties of the low-molecular-weight (LMW) surface layer (S-layer) protein. J Med Microbiol. [Epub ahead of print].

Spinelli,S., Frenken,L., Bourgeois,D., De Ron,L., Bos,W., Verrips,T., Anguille,C., Cambillau,C., and Tegoni,M. (1996). The crystal structure of a llama heavy chain variable domain. Nat Struct Biol. *3*, 752-757.

Spinelli,S., Frenken,L.G.J., Hermans,P., Verrips,T., Brown,K., Tegoni,M., and Cambillau,C. (2000). Camelid Heavy-Chain Variable Domains Provide Efficient Combining Sites to Haptens. Biochemistry *39*, 1217-1222.

Stabler,R., He,M., Dawson,L., Martin,M., Valiente,E., Corton,C., Lawley,T., Sebaihia,M., Quail,M., and Rose,G. (2009). Comparative genome and phenotypic analysis of *Clostridium difficile* 027 strains provides insight into the evolution of a hypervirulent bacterium. Genome Biol. *10*, R102.

Stewart,C.S., MacKenzie,C.R., and Christopher Hall,J. (2007). Isolation, characterization and pentamerization of [alpha]-cobrotoxin specific single-domain antibodies from a na ve phage display library: Preliminary findings for antivenom development. Toxicon *49*, 699-709.

Szynol,A., De Haard,J.J.W., Veerman,E.C., De Soet,J.J., and van Nieuw Amerongen,A.V. (2006). Design of a Peptibody Consisting of the Antimicrobial Peptide dhvar5 and a llama Variable Heavy chain Antibody Fragment. Chem Biol Drug Des. *67*, 425-431.

Takeoka,A., Takumi,K., KOGA,T., and Kawata,T. (1991). Purification and characterization of S layer proteins from *Clostridium difficile* GAI 0714. Microbiology. *137*, 261.

Takumi,K., KOGA,T., OKA,T., and Endo,Y. (1991). Self-assembly, adhesion, and chemical properties of tetragonarly arrayed S-layer proteins of Clostridium. J Gen Appl Microbiol. *37*, 455-465.

Tanha,J., Dubuc,G., Hirama,T., Narang,S.A., and MacKenzie,C.R. (2002). Selection by phage display of llama conventional VH fragments with heavy chain antibody VHH properties. J Immunolog Meth. *263*, 97-109.

Tanha,J., Nguyen,T.D., Ng,A., Ryan,S., Ni,F., and MacKenzie,R. (2006). Improving solubility and refolding efficiency of human VHs by a novel mutational approach. Protein Eng Des Sel. *19*, 503.

Tanha,J., Xu,P., Chen,Z., Ni,F., Kaplan,H., Narang,S.A., and MacKenzie,C.R. (2001). Optimal design features of camelized human single-domain antibody libraries. J Biol Chem. *276*, 24774.

Tasteyre,A., Barc,M.C., Collignon,A., Boureau,H., and Karjalainen,T. (2001). Role of FliC and FliD flagellar proteins of *Clostridium difficile* in adherence and gut colonization. Infect Immun. *69*, 7937.

Taylor,C.P., Tummala;S., Molrine,D., Davidson,L., Farrell,R.J., Lembo,A., Hibberd,P.L., Lowy,I., and Kelly,C.P. (2008). Open-label, dose escalation phase I study in healthy volunteers to evaluate the safety and pharmacokinetics of a human monoclonal antibody to *Clostridium difficile* toxin A. Vaccine *26*, 3404-3409.

Te Wu,T., Johnson,G., and Kabat,E.A. (1993). Length distribution of CDRH3 in antibodies. Proteins: Struct Funct Bioinform. *16*, 1-7.

The Immunology Link. FDA approved antibodies. 2011. 4-16-2011. Ref Type: Online Source

Tomlinson,I.M., Walter,G., Jones,P.T., Dear,P.H., Sonnhammer,E.L.L., and Winter,G. (1996). The imprint of somatic hypermutation on the repertoire of human germline V genes. J Mol Biol. *256*, 813-817.

Tonegawa,S. (1983). Somatic generation of antibody diversity. Nature. *302(5909)*:575-581.

Torres,J.F., Lyerly,D.M., Hill,J.E., and Monath,T.P. (1995). Evaluation of formalin-inactivated *Clostridium difficile* vaccines administered by parenteral and mucosal routes of immunization in hamsters. Infect Immun. *63*, 4619.

Twine,S.M., Reid,C.W., Aubry,A., McMullin,D.R., Fulton,K.M., Austin,J., and Logan,S.M. (2009). Motility and flagellar glycosylation in *Clostridium difficile*. J Bacteriol. *191*, 7050.

van der Linden,R., de Geus,B., Stok,W., Bos,W., van Wassenaar,D., Verrips,T., and Frenken,L. (2000). Induction of immune responses and molecular cloning of the heavy chain antibody repertoire of Lama glama. J Immunolog Meth. *240*, 185-195.

Van der Linden,R.H.J., Frenken,L.G.J., de Geus,B., Harmsen,M.M., Ruuls,R.C., Stok,W., De Ron,L., Wilson,S., Davis,P., and Verrips,C.T. (1999). Comparison of physical chemical properties of llama VHH antibody fragments and mouse monoclonal antibodies. Biochimica et Biophysica Acta (BBA)-Protein Struc Mol Enzymol. *1431*, 37-46.

Van der Vaart,J.M., Pant,N., Wolvers,D., Bezemer,S., Hermans,P.W., Bellamy,K., Sarker,S.A., van der Logt,C.P.E., Svensson,L., and Verrips,C.T. (2006). Reduction in morbidity of rotavirus induced diarrhoea in mice by yeast produced monovalent llama-derived antibody fragments. Vaccine *24*, 4130-4137.

Vaughan,T.J., Williams,A.J., Pritchard,K., Osbourn,J.K., Pope,A.R., Earnshaw,J.C., McCafferty,J., Hodits,R.A., Wilton,J., and Johnson,K.S. (1996). Human antibodies with sub-nanomolar affinities isolated from a large non-immunized phage display library. Nat Biotechnol. *14*, 309-314.

Voth,D.E. and Ballard,J.D. (2005). *Clostridium difficile* toxins: mechanism of action and role in disease. Clin Microbiol Rev. *18*, 247.

Vu,K.B., Ghahroudi,M.A., Wyns,L., and Muyldermans,S. (1997). Comparison of llama VH sequences from conventional and heavy chain antibodies. Mol Immunol. *34*, 1121-1131.

Waligora,A.J., Hennequin,C., Mullany,P., Bourlioux,P., Collignon,A., and Karjalainen,T. (2001). Characterization of a cell surface protein of *Clostridium difficile* with adhesive properties. Infect Immun. *69*, 2144.

Ward,E.S., Gussow,D., Griffiths,A.D., Jones,P.T., and Winter,G. (1989). Binding activities

of a repertoire of single immunoglobulin variable domains secreted from Escherichia coli.

Nature. *341(6242)*:544-546.

Warny,M., Vaerman,J.P., Avesani,V., and Delmee,M. (1994). Human antibody response to *Clostridium difficile* toxin A in relation to clinical course of infection. Infect Immun. *62*, 384.

Waseh,S., Hanifi-Moghaddam,P., Coleman,R., Masotti,M., Ryan,S., Foss,M., MacKenzie,R., Henry,M., Szymanski,C.M., and Tanha,J. (2010). Orally Administered P22 Phage Tailspike Protein Reduces Salmonella Colonization in Chickens: Prospects of a Novel Therapy against Bacterial Infections. PloS one *5*, 541-549.

Wesolowski,J., Alzogaray,V., Reyelt,J., Unger,M., Juarez,K., Urrutia,M., Cauerhff,A., Danquah,W., Rissiek,B., and Scheuplein,F. (2009). Single domain antibodies: promising

experimental and therapeutic tools in infection and immunity. Med Microbiol Immunol. *198*, 157-174.

Wiedemann,V., Kuhlmann,R., Schmidt,P., and Erhardt,W. (1990). Chicken egg antibodies for prophylaxis and therapy of infectious intestinal diseases. III. vivo tenacity test in piglets with artificial jejunal fistula. Zentralbl. Veterinarmed. B. 163-172.

Willats,W.G.T. (2002). Phage display: practicalities and prospects. Plant Mol Biol.*50*, 837-854.

Winter,G., Griffiths,A.D., Hawkins,R.E., and Hoogenboom,H.R. (1994). Making antibodies by phage display technology. Ann Rev Immunol. *12*, 433-455.

Winter,G. and Milstein,C. (1991). Man-made antibodies. Nature *349*, 293-299.

Worledge,K.L., Godiska,R., Barrett,T.A., and Kink,J.A. (2000). Oral administration of avian tumor necrosis factor antibodies effectively treats experimental colitis in rats. Dig Dis Sci. *45*, 2298-2305.

Wu,S.J., Luo,J., O'Neil,K.T., Kang,J., Lacy,E.R., Canziani,G., Baker,A., Huang,M., Tang,Q.M., and Raju,T.S. (2010). Structure-based engineering of a monoclonal antibody for improved solubility. Protein Eng Des Sel. *23(8)*:643-651.

Yau,K.Y.F., Lee,H., and Hall,J.C. (2003). Emerging trends in the synthesis and improvement of hapten-specific recombinant antibodies. Biotechnol Adv. *21*, 599-637.

Zhang,J., Tanha,J., Hirama,T., Khieu,N.H., To,R., Tong-Sevinc,H., Stone,E., Brisson,J.R., and Roger MacKenzie,C. (2004). Pentamerization of single-domain antibodies from phage libraries: a novel strategy for the rapid generation of high-avidity antibody reagents. J Mol Biol. *335*, 49-56.

Appendix I

```
630             MNKKNIAIAMSGLTVLASAAPVFAAT------TGTQGYTVVKNDWKKAVKQLQDGLKDNS
QCD             MNKKNIAIAMSGLTVLASAAPVFAAEDMSKVETGDQGYTVVQSKYKKAVEQLQKGLLDGS
                ************************       ** ******:..:****:***.** *.*

630             IGKITVSFNDGVVGEVAPKSANKKADRDAAAEKLYNLVNTQLDKLGDGDYVDFSVDYNLE
QCD             ITEIKIFFEG---TLASTIKVGAELSAEDASKLLFTQVDNKLDNLGDGDYVDFLISSPAE
                * :*.: *:.     .:. ... : . : *:: *:. *:.:**:********* :.   *

630             NKIITNQADAEAIVTKLNSLNEKTLIDIATKDTFGMVSKTQDSEGKNVAATKALKVKDVA
QCD             ----GDKVTTSKLVALKNLTGGTSAIKVATSSIIGEVENAGTPGAKNTAPSSAAVMSMSD
                     ::. :. :*:  *  . .: *.:**.. :* *.::  . .**.*.:.*  :.

630             TFGLKSGGSEDTGYVVEMKAGAVEDKYGKVGDSTAGIAINLPSTGLEYAGKGTTIDFNKT
QCD             VFDTAFTDSTETAVKLTIKDAMKTKKFGLVDGTTYSTGLQFADGKTEKIVKLGDSDTINL
                .*.    .* :*.  : :* .   .*:* *..:* . .::::..   *   *    *  :

630             LKVDVTGGSTPSAVAVSGFVTKDDTDLAKSGTINVRVINAKEESIDIDASSYTSAENLAK
QCD             AKELIITPASANDQAATIEFAKPTTQSGSPVITKLRILNAKEETIDIDASSSKTAQDLAK
                 *  :   ::..  *.:  .:*  *: ...   ::*::*****:******* .:*::***

630             RYVFDPDEISEAYKAIVALQNDGIESNLVQLVNGKYQVIFYPEGKRLETKS AN-DTIASQ
QCD             KYVFNKTDLNTLYRVLNGDEADTNR--LVEEVSGKYQVVLYPEGKRVTTKS AAKASIADE
                :***:  ::.  *:.: . : *  .  **: *.*****::******: ***.*   :**.:

630             DTPAKVVIKANKLKDLKDYVDDLKTYNNTYSNVVTVAGEDRIETAIELSSKYYNSDDKNA
QCD             NSPVKLTLKSDKKKDLKDYVDDLRTYNNGYSNAIEVAGEDRIETAIALSQKYYNSDDENA
                ::*.*:.:*::* **********:**** ***.: ********** **.*******:**

630             ITDKAVNDIVLVGSTSIVDGLVASPLASEKTAPLLLTSKDKLDSSVKSEIKRVMNLKSDT
QCD             IFRDSVDNVVLVGGNAIVDGLVASPLASEKKAPLLLTSKDKLDSSVKAEIKRVMNIKSTT
                *  .:*:::****..:**************.****************:*******:** *

630             GINTSKKVYLAGGVNSISKDVENELKNMGLKVTRLSGEDRYETSLAIADEIGLDNDKAFV
QCD             GINTSKKVYLAGGVNSISKEVENELKDMGLKVTRLAGDDRYETSLKIADEVGLDNDKAFV
                ******************:******:********:*:******* ****:*********

630             VGGTGLADAMSIAPVASQLK---------DGDATPIVVVDGKAKEISDDAKSFLGTSDVD
QCD             VGGTGLADAMSIAPVASQLRNANGKMDLADGDATPIVVVDGKAKTINDDVKDFLDDSQVD
                ******************:         *************** *.**.*.**. *:**

630             IIGGKNSVSKEIEESIDSATGKTPDRISGDDRQATNAEVLKE-----DDYFTDGEVVNYF
QCD             IIGGENSVSKDVENAIDDATGKSPDRYSGDDRQATNAKVIKESSYYQDNLNNDKKVVNFF
                ****:*****::*::**.****:*** **********:*:**     *:  .* :***:*

630             VAKDGSTKEDQLVDALAAAPIAGRFKE--------------------------SPAPII
QCD             VAKDGSTKEDQLVDALAAAPVAANFGVTLNSDGKPVDKDGKVLTGSDNDKNKLVSPAPIV
                ********************:*..*                           *****:

630             LATDTLSSDQNVAVSKAVPKDGGTNLVQVGKGIASSVINKMKDLLDM
QCD             LATDSLSSDQSVSISKVLDKDNGENLVQVGKGIATSVINKLKDLLSM
                ****:*****.*::**.: **.* **********:*****:****.*
```

Figure 27: Clustal W alignment of SLPs from strain QCD and CD630. Sequence identity between the two Low-MW subunits is low, however the High-MW subunits are highly conserved between the two strains. QCD belongs to PCR ribotype 027 strains, while CD630 belongs to PCR ribotype 012. The leader peptide that targets the SLPs to the cell wall is highlighted in yellow, while an arrow indicates the location of the highly conserved cleavage site of the SlpA precursor protein.

CONTRIBUTIONS OF COLLABORATORS

Thank you to Dr, Susan Logan and Annie Aubry for the technical and theoretical support in all live *C. difficile* work and antigen extractions.

Thank you to Dr. Mehdi Arbabi-Ghahroudi and his lab for constructing the immune llama phage-display library from which I isolated the immune clones.

Thank you to Dr. Roger MacKenzie, Henk van Fassen and Thanh-Dung Nguyen for conducting the SPR experiments.